

Surface Science

Room 120 - Session SS+AMS-MoM

Dynamics and Mechanisms in Heterogeneous Catalysis

Moderators: Prabhakar Kasala, Brookhaven National Laboratory, Arthur Utz, Tufts University

8:15am **SS+AMS-MoM-1 Accurate Dynamical Modelling of Vibrationally Enhanced N₂ Dissociation on Ru(0001) – Implications (Not Only) for Plasma Catalysis**, *F. van den Bosch, N. Gerrits, Jörg Meyer*, Leiden University, Netherlands

INVITED

Pioneering work of Mehta et al. [1] has quantified the efficiency of plasma-enhanced over conventional (temperature-driven) heterogeneous catalysis - nurturing hopes for a future more sustainable alternative that can be easily upscaled. The focus has been on ammonia synthesis and vibrationally excited states available in the plasma, because the dissociative chemisorption of N₂ molecules on a metal catalyst is usually the rate-limiting step. Prevalent micro-kinetic modeling based on transition state theory (TST) for the reaction rates needs to be extended by introducing vibrational-state-dependent rate constants. To do so, Mehta et al. have postulated that the computationally convenient Fridman-Macheret model often used for reactions in the gas phase [2] also works for surface reactions.

Using N₂ on Ru(0001) as a representative showcase, we scrutinize the effect of vibrational excitations of N₂ on its surface reactivity by using explicit molecular dynamics on an accurate potential energy surface using the quasi-classical trajectory method [3,4]. We compute the dissociative chemisorption probabilities as a function of the initial vibrational state ranging from 0 to 10 vibrational quanta. These calculations yield vibrational efficacies of about 1.8, i.e., vibrational excitations are more considerably more effective for promoting dissociative chemisorption reactions than equivalent amounts of translation energy. We compare our findings to TST-based models and carefully analyze why they cannot capture the vibrationally enhanced dissociation correctly. Finally, we discuss these findings in the context of thermal and plasma-enabled catalysis by critically investigating which molecules dominate the reactivity.

1. P. Mehta, P. Barboun, F. A. Herrera, J. Kim, P. Rumbach, D. B. Go, J. C. Hicks, and W. F. Schneider, Overcoming Ammonia Synthesis Scaling Relations with Plasma-Enabled Catalysis, *Nat. Catal.* 1, 269 (2018). DOI: 10.1038/s41929-018-0045-1
2. A. Fridman, *Plasma Chemistry*, Cambridge University Press, Cambridge, 2008.
3. K. Shakouri, J. Behler, J. Meyer, and G.-J. Kroes, Accurate Neural Network Description of Surface Phonons in Reactive Gas-Surface Dynamics: N₂ + Ru(0001), *J. Phys. Chem. Lett.* 8, 2131 (2017). DOI: 10.1021/acs.jpcllett.7b00784
4. P. Spiering, K. Shakouri, J. Behler, G.-J. Kroes, and J. Meyer, Orbital-Dependent Electronic Friction Significantly Affects the Description of Reactive Scattering of N₂ from Ru(0001), *J. Phys. Chem. Lett.* 10, 2957 (2019). DOI: 10.1021/acs.jpcllett.9b00523

8:45am **SS+AMS-MoM-3 SSD Morton S. Traum Award Finalist Talk: A Priori Designed NiAg Single-Atom Alloys for Selective Epoxidation Reactions**, *Elizabeth E. Hoppel¹*, Tufts University; *A. Jalil*, University of California at Santa Barbara; *S. Stratton*, Tulane University; *L. Cramer*, Tufts University; *P. Christopher*, University of California at Santa Barbara; *M. Montemore*, Tulane University; *E. Sykes*, Tufts University

Ethylene oxide, produced via the partial oxidation of ethylene, is among the largest volume chemicals produced by the chemical industry and has one of the largest carbon footprints. Using Ag catalysts, the reaction can achieve high selectivity ~90%, but only with a combination of promoters including Cl, Cs, and Re, and must be run at low conversions (< 15%) to avoid the total combustion of ethylene to carbon dioxide. Herein, we report a theory guided investigation demonstrating that the addition of low concentrations of Ni to Ag(111) lowers the barrier for O₂ dissociation and enables spillover of oxygen atoms to sites on the Ag surface. Temperature programmed desorption experiments quantify the facile dissociation, spillover and desorption of O₂ from NiAg(111) and demonstrate that, unlike all previous studies, Ni addition enables the population of the Ag(111) surface with atomic oxygen in near UHV pressure without having to atomize oxygen or introduce species like NO₂ or O₃. Furthermore, ambient pressure X-ray

photoelectron spectroscopy reveals that Ni not only aids in activation and spillover, but also stabilizes nucleophilic oxygen which is thought to be selective towards total oxidation. These results informed the synthesis and testing of supported catalysts which demonstrated that NiAg single-atom alloy nanoparticles produce ethylene oxide both with greater selectivity and conversion than Ag without the need for a co-flow of Cl and other promoters.

9:00am **SS+AMS-MoM-4 Effect of Surface Diffusion of Methoxy Intermediates on Methanol Decomposition on Pt/TiO₂(110)**, *C. Liu, B. Lu*, Hokkaido University, Japan; *H. Ariga-Miwa*, The University of Electro-Communications (UEC-Tokyo), Japan; *S. Ogura*, Tokyo Denki University, Japan; *K. Fukutani*, The University of Tokyo, Japan; *M. Gao, J. Hasegawa, K. Shimizu*, Hokkaido University, Japan; *K. Asakura*, Ritsumeikan University, Japan; *Satoru Takakusagi*, Hokkaido University, Japan

In oxide-supported metal catalysts, atomic-level understanding of dynamic behavior of intermediate adsorbates such as diffusion, spillover, and reverse spillover is crucial to unravel the origins of catalytic activity and product selectivity. Our previous *in situ* STM study on methanol adsorption process on a Pt/TiO₂(110) surface revealed that methoxy intermediates were formed on five-fold coordinated Ti⁴⁺ (Ti_{5c}) sites by dissociative adsorption of methanol on the Pt nanoparticles, followed by spillover to the TiO₂(110) substrate.^[1] They were mobile at room temperature. In this study, diffusion and thermal decomposition of the methoxy intermediates were examined by STM, density functional theory (DFT) calculation and temperature programmed desorption (TPD), in order to reveal how their diffusion affect activity and product selectivity in the methoxy decomposition on the Pt/TiO₂(110) surface.^[2] The TPD measurements showed that the methoxy intermediates were thermally decomposed at >350 K on the Pt sites to produce CO (dehydrogenation) and CH₄ (C-O bond scission) through their reverse spillover. We have found that activity and product selectivity for the methoxy decomposition was much dependent on the particle density, suggesting that it was controlled by diffusion of the methoxy intermediates. Decrease of the Pt nanoparticle density significantly enhanced the selectivity to CH₄, and thus we propose that Pt-TiO₂ interfacial sites are active for CH₄ formation while the other Pt sites for CO formation.

[1] S. Takakusagi, K. Fukui, R. Tero, K. Asakura, Y. Iwasawa, *Langmuir* 2010, 26, 16392.

[2] C. Liu, B. Lu, H. Ariga-Miwa, S. Ogura, T. Ozawa, K. Fukutani, M. Gao, J. Hasegawa, K. Shimizu, K. Asakura, S. Takakusagi, *J. Am. Chem. Soc.* 2023, 145, 19953.

9:15am **SS+AMS-MoM-5 Simultaneous Tracking of Ultrafast Surface and Gas-Phase Dynamics in Solid-Gas Interfacial Reactions**, *Keith Blackman, E. Segrest, G. Turner, K. Machamer, A. Gupta, M. Pathan*, University of Central Florida, Department of Physics; *N. Berriel*, University of Central Florida, Department of Material Science and Engineering; *P. Banerjee*, University of Central Florida, Department of Material Science and Engineering, Renewable Energy and Chemical Transformations Cluster (REACT); *M. Vaida*, University of Central Florida, Department of Physics, Renewable Energy and Chemical Transformations Cluster (REACT)

ABSTRACT

Real-time detection of intermediate species and final products at the surface and near-surface in interfacial solid-gas reactions is critical for an accurate understanding of heterogeneous reaction mechanisms. In this contribution, an experimental method that can simultaneously monitor the ultrafast dynamics at the surface and above the surface in photoinduced heterogeneous reactions is presented. The method relies on a combination of mass spectrometry and femtosecond pump-probe spectroscopy. As a model system, the photoinduced reaction of methyl iodide on and above a cerium oxide surface is investigated. The species that are simultaneously detected from the surface and gas-phase present distinct features in the mass spectra, such as a sharp peak followed by an adjacent broad shoulder. The sharp peak is attributed to the species detected from the surface while the broad shoulder is due to the detection of gas-phase species above the surface, as confirmed by multiple experiments. By monitoring the evolution of the sharp peak and broad shoulder as a function of the pump-probe time delay, transient signals are obtained that describe the ultrafast photoinduced reaction dynamics of methyl iodide on the surface and in gas-phase. Finally, SimION simulations are performed to confirm the origin of the ions produced on the surface and gas-phase.

¹ SSD Morton S. Traum Award Finalist

Monday Morning, November 4, 2024

9:30am **SS+AMS-MoM-6 In situ Photoemission of Ru(0001) Model Catalyst in Plasma-activated N₂-H₂ Mixtures, Roland Bliem**, Advanced Research Center for Nanolithography, Netherlands

In plasma-assisted catalysis, reactants are activated by a plasma discharge, resulting in vibrational excitation and the production of radicals and ions. Plasma catalysis with low-energy excitations has been reported to allow for remarkable efficiencies, under specific conditions even beyond the limits of thermal catalysis. More generally, the activation of strong molecular bonds in a plasma can soften the requirements on the operating conditions for important reactions, such as ammonia synthesis, and contribute options for their electrification and operation at small scales. While plasma-activation can facilitate certain reaction steps, the reaction pathway and product selectivity is still largely defined by the catalyst surface, making it key to catalyst design. However, at present the active state of catalyst surfaces in plasma is unknown, and *in situ* information on surfaces exposed to plasma is fully lacking.

Here, we follow the surface composition and chemistry of the Ru, one of the most active elements for conventional ammonia synthesis, *in situ* during exposure to plasma-activated N₂-H₂ mixtures using near-ambient pressure X-ray photoelectron spectroscopy (NAP-XPS). The activation of N₂ by a microwave discharge source results in extremely efficient sticking of nitrogen species to Ru(0001) and polycrystalline Ru surfaces, where they form nitrogen-metal bonds. The temperature-dependent stability of nitrogen species indicates the presence of at least two different configurations. The comparison of XPS spectra of plasma-exposed Ru to Ru nitride films grown using pulsed laser deposition suggests that the nitrogen species formed in plasma likely correspond to adsorbates on terraces and at extended defects. In the presence of hydrogen, the nitrogen peak reveals significant hydrogenation, and residual gas analysis shows the presence of NH₃ and N₂H_n. In a temperature-dependent study up to 300°C, we detect ammonia in the residual gas at all times, whereas the hydrogenated surface species in XPS spectra decrease with increasing temperature, indicating a shorter residence time or their decomposition.

9:45am **SS+AMS-MoM-7 Velocity Map Imaging of Desorbing Oxygen from sub-Surface States of Single Crystals**, A. Dorst, R. Dissanayake, Georg-August Universität, Göttingen, Germany; D. Killelea, Loyola University Chicago; Tim Schäfer, Georg-August Universität, Göttingen, Germany

We combine velocity map imaging (VMI) with temperature-programmed desorption (TPD) and molecular beam surface scattering experiments to record the angular-resolved velocity distributions of recombinatively-desorbing oxygen from single crystal surfaces. We assign the velocity distributions to desorption from specific surface and sub-surface states by matching the recorded distributions to the desorption temperature. These results provide insight into the recombinative desorption mechanisms and the availability of oxygen for surface-catalyzed reactions. We use concepts of detailed balance to analyze translational energy distributions of O₂ when shifted towards hyperthermal energies. These distribution indicate desorption from intermediate activated molecular chemisorption states.

10:30am **SS+AMS-MoM-10 Designing the Local Environment of Single Atom Catalysts for Product Selectivity: Theory Meets Experiment**, Talat Shahnaz Rahman, University of Central Florida

INVITED

Singly dispersed transition metal atoms on oxide surfaces, the so-called single atom catalyst (SAC) have recently been shown to attain chemical activity and selectivity for several technologically important reactions that surpass those of Pt single crystal surfaces, the prototype exemplary catalyst but with a large price tag. Apart from being cost-effective, single atom catalyst offer excellent opportunities for tuning their local environment and thereby their oxidation state, local coordination, and electronic structure. In this talk, I will present results of collaborative work with several experimental groups on singly-dispersed transition metal atoms anchored on metal oxide surfaces, with and without ligands, that have the potential to be cost-effective catalysts with high activity and product selectivity. Examples will include Pd and Pt atoms anchored on ZnO that form a bimetallic local environment consisting of one Pd and three Zn atoms with high catalytic activity for generation of H₂ through methanol partial oxidation (MPO) [1] and Pt atoms stabilized in specific fine-tuned local coordination environments that exhibit strikingly distinct catalytic behaviors in reactions as varied as CO oxidation and NH₃ oxidation [2]. I will also pay attention to the special role played by ligands (1,10-phenanthroline-5,6-dione (PDO)) in emergent catalytic properties of Pd single atoms stabilized on ceria surfaces [3]. I will also draw attention to some factors that control the emerging functionalities of the above systems in controlled confinement.

[1] Y. Tang, et al., Nano Lett. 20, 6255 (2020); T.B. Rawal, et al., ACS Catalysis 8, 5553-5569 (2018).

[2] W. Tan, et al., Nat Commun. 13, 7070 (2022)

[3] E. Wasim, N. Ud Din, D. Le, et al., J. Catalysis 413, 81 (2022)

* The work is supported by NSF grant CHE-1955343 and performed in collaboration with D. Le, N. U. Din, D. Austin, T. Rawal, T. Jiang, and the research groups of F. Tao (U of Kansas), F. Liu (UCF), S. Tait (Indiana U).

11:00am **SS+AMS-MoM-12 Stabilizing and Characterizing Single-Atom Catalysts: Rhodium on Titania**, Faith J Lewis, M. Eder, J. Hütner, D. Rath, J. Balajka, J. Pavelec, G. Parkinson, TU Wien, Austria

Single-atom catalysis (SAC) aims to minimize the amount of precious metals in catalysts while maintaining catalytic activity. SAC often uses oxide supports to stabilize individual transition metals as isolated active sites. A multi-technique surface science approach allows characterization of these sites to determine their coordination structure. In this work, rhodium adatoms, stabilized by carbon monoxide, were studied on a rutile titania (r-TiO₂(110)) surface.

In idealized SAC systems, metal atoms are assumed to stay isolated on oxide surfaces. In reality, this is not always the case. On titania, rhodium adatoms readily sinter into larger clusters above cryogenic temperatures. It has been suggested that adding ligands stabilizes single rhodium atoms on the surface; carbon monoxide has been proposed to form a geminal dicarbonyl (Rh(CO)₂) structure to stabilize the individual rhodium atoms on r-TiO₂(110).¹

The rhodium gem-dicarbonyl infrared (IR) stretch has been used to signify single rhodium atoms on titania surfaces since the turn of the century, but no scanning probe images have been published of this Rh(CO)₂/r-TiO₂(110) system. Using a newly integrated infrared reflection absorption spectroscopy (IRAS) system, a protocol for forming the Rh(CO)₂ species on r-TiO₂(110) in UHV was established. In this talk, I will present scanning tunneling microscopy (STM) and non-contact atomic force microscopy (nc-AFM) images of the rhodium gem-dicarbonyl system after annealing to various temperatures with complementary IRAS and X-ray photoelectron spectroscopy (XPS) data. The images show two distinct double-lobed species, one parallel to the [001] direction and one perpendicular, at a low coverage (0.005 ML). Contradictory to theoretical predictions,² the images show an asymmetry of the two lobes in both confirmations. Our results illustrate that the surface science approach provides unique information about single atom catalysts and is a prerequisite for their accurate theoretical description.

1. Frank, M.; Bäumer, M.; Kühnemuth, R.; Freund, H.-J., Metal Atoms and Particles on Oxide Supports: Probing Structure and Charge by Infrared Spectroscopy. *The Journal of Physical Chemistry B*, 8569-8576 (2001).

2. Tang, Y., Asokan, C., Xu, M. et al., Rh single atoms on TiO₂ dynamically respond to reaction conditions by adapting their site. *Nature Communications*, 4488 (2019).

11:15am **SS+AMS-MoM-13 In-Situ Observation of the Effects of Oxygen-Containing Compounds on MoS₂-Based Catalysts Using Near-Ambient Pressure Scanning Tunnelling Microscopy**, Kerry Hazeldine, M. Hedevang, Aarhus University, Denmark; L. Mohrhusen, Carl von Ossietzky University of Oldenburg, Germany; J. Vang Lauritsen, Aarhus University, Denmark

More than 20% of greenhouse gas emissions in the European Union are produced by the heavy transport and aviation sector. Pyrolysis oil derived from biomass is a promising replacement for fossil fuels for aviation and heavy transport applications and is one of the technologies being researched for the generation of green aviation fuel. Fast pyrolysis is a process of decomposing biomass into pyrolysis oil by rapidly heating it in an oxygen-free atmosphere. An advantage of pyrolysis oil derived from biomass is that it is compatible with the existing infrastructure that is used in the catalysis and distillation of jet fuels and diesel. However, the oxygen content in pyrolysis oil derived from biomass is unacceptably high (up to 50%) and can lead to corrosion and instability [1].

To reduce the oxygen content and produce useful and efficient hydrocarbons from the pyrolysis oil, a pre-treatment and hydrodeoxygenation (HDO) step is required to be added to the refining process. Molybdenum disulphide (MoS₂) has previously demonstrated its effectiveness as a catalyst in hydrodesulphurisation (HDS) and has further shown to be a promising candidate as a catalyst in HDO and is therefore the primary material of interest in this study [2].

To develop atomistic structure determination of the catalyst and elucidate to the reaction pathways for oxygen-containing molecules during HDO, model studies are required. In this study, the model system based on MoS₂ growth on Au(111), has been exposed to oxygen-containing molecules and characterised in-situ using the surface-sensitive techniques, near-ambient pressure scanning tunnelling microscopy (NAP-STM), and near-ambient pressure X-ray photoelectron spectroscopy (NAP-XPS). By using a gold substrate, the oxygen uptake can be evaluated without background from the oxide support. NAP-XPS shows evidence of O exchange on the sulphide phase, consistent with current theoretical models, whilst the corresponding NAP-STM shows structural changes to the particle shape and size of the sulphide phase. For example, preliminary work shows restructuring in the MoS₂ clusters when exposed to elevated pressures of methanol vapour. By using these complementary techniques, we can gain insight into both the chemical and physical changes of MoS₂ upon exposure to oxygen-containing compounds.

late transition metal nanoparticles across oxides streamlines development of optimal catalysts.

[1] Cao J, Zhang Y, Wang L, Zhang C, Zhou C. Unsupported MoS₂-Based Catalysts for Bio-Oil Hydrodeoxygenation: Recent Advances and Future Perspectives. *Front Chem.* 10, 928806 (2022).

[2] Salazar, N., Rangarajan, S., Rodríguez-Fernández, J. *et al.* Site-dependent reactivity of MoS₂ nanoparticles in hydrodesulfurization of thiophene. *Nat Commun.* 11, 4369 (2020).

11:30am **SS+AMS-MoM-14 Revealing Local Coordination of Ag Single Atom Catalyst Supported on CeO₂(110) and ZrO₂(-111), Syeda Sherazi, D. Le, K. Ye, S. Xie, F. Liu, T. Rahman, University of Central Florida**

Single atom catalyst (SAC) supported on metal oxide surfaces is a promising candidate for various reactions as it possesses high temperature stability and potentially high selectivity. Determining the local atomic coordination and geometric structure of the SAC is important for the understanding of its catalytic performance. In this work, we apply the ab initio thermodynamics approach to investigate the coordination environment of Ag SAC supported on CeO₂(110) and ZrO₂(-111), so chosen as accompanying experimental observations find the former to be a more viable support than the latter. We find that the Ag SAC structure in which Ag is embedded in the CeO₂ lattice with one surface oxygen vacancy nearby is the most favorable on the CeO₂(110) surface while the structure in which Ag embeds in the ZrO₂(-111) lattice without any oxygen vacancy nearby is the most favorable on the ZrO₂(-111) surface. Our results also show that it is easier to create oxygen vacancy near the Ag atom when the support is CeO₂(110) than ZrO₂(-111). We compare the trends in the energetics of NH₃ adsorption and dissociation on Ag SAC supported on CeO₂(110) with those on ZrO₂(-111) to compare with accompanying experimental observations that find the ceria-supported Ag SAC to exhibit a pronounced selectivity in ammonia oxidation. We will report experimental data to compare with our finding and comment on their implications for the catalytic performance of the Ag SAC.

Work is supported by National Science Foundation grant CHE-1955343.

11:45am **SS+AMS-MoM-15 Trends for Predicting Adhesion Energies of Catalytic Late Transition Metal Nanoparticles on Oxide Supports, Nida Janulaitis, The University of Washington; K. Zhao, C. Campbell, University of Washington**

Understanding the energetics of late transition metal nanoparticles dispersed on oxide-based catalyst support materials is important for the development of high-performance catalysts. Metal/support adhesion energies, which are used to estimate the metal chemical potential as a function of metal nanoparticle size, which in turn correlates with the surface reactivity and sintering kinetics of the metal nanoparticles. Single crystal adsorption calorimetry (SCAC) was used to directly measure Cu vapor adsorption energies and Cu chemical potential as a function of Cu coverage on the clean rutile-TiO₂(100) surface, while He⁺ low-energy ion scattering (LEIS) was used to measure the average size of the Cu nanoparticles. By fitting these data to a theoretical model, we extracted the adhesion energy of Cu nanoparticles on rutile-TiO₂(100). By comparing to earlier results for Ag, we find that the adhesion energies of metals on the rutile-TiO₂(100) surface correlate proportionally to the oxophilicity of the metal element. Similar proportional correlations for the adhesion energy of metals to MgO(100) and CeO₂(111) surfaces as a function metal oxophilicity have been previously published. Expanding upon these existing oxide adhesion energy trends with the new rutile-TiO₂(100) data clarifies the structure-function relationship between the physical properties of the oxide supports and their metal adhesion energetics. The ability to predict the adhesion energy, and thus the metal chemical potential versus size, of

Surface Science

Room 120 - Session SS+AMS-MoA

Surface Chemistry and Reactivity on Oxide Surfaces

Moderators: Ashleigh Baber, James Madison University, J. Anibal Boscoboinik, Center for Functional Nanomaterials, BNL

1:30pm SS+AMS-MoA-1 Dynamic Formation of Gem-Dicarbonyl on Rh Decorated Fe₃O₄(001), Jiří Pavelec, C. Wang, P. Sombut, L. Puntischer, M. Eder, Vienna University of Technology, Austria; Z. Jakub, CEITEC, Czechia; R. Bliem, Advanced Research Center for Nanolithography, Netherlands; M. Schmid, U. Diebold, Vienna University of Technology, Austria; C. Franchini, University of Vienna, Austria; M. Meier, G. Parkinson, Vienna University of Technology, Austria

Single atom catalysts (SACs) have the potential to reduce the amount of precious materials needed in catalytic reactions. Understanding and utilizing SACs requires studying the coordination of adatoms to their supports, as well as their coordination to reactants. This coordination can change during reactions, and intermediate dynamic steps may be invisible to conventional spectroscopy.

In this study [1], we employ scanning tunneling microscopy (STM) in combination with theory to investigate a model SAC: Rhodium decorated Fe₃O₄(001). Our results demonstrate that the formation of dicarbonyl on Rh₁ requires the initial presence of Rh₂ on the surface, a finding corroborated by detailed density functional theory (DFT) studies.

CO adsorption at Rh₁ sites at room temperature results exclusively in stable Rh₁CO monocarbonyls, as the Rh atom adapts its coordination to form a stable pseudo-square planar environment. Rh₁(CO)₂ gem-dicarbonyl species are also observed, but they form exclusively through the break up of Rh₂ dimers via an unstable Rh₂(CO)₃ intermediate. Identification of this intermediate step would be challenging without a multi-technique approach.

These results are compared to the Rh decorated TiO₂ model SAC using temperature-programmed desorption (TPD), infrared reflection absorption spectroscopy (IRAS) [2], nc-AFM, and X-ray photoelectron spectroscopy (XPS).

[1] Wang, C.; Sombut, P.; Puntischer, L.; Jakub, Z.; Meier, M.; Pavelec, J.; Bliem, R.; Schmid, M.; Diebold, U.; Franchini, C.; Parkinson, G. S., *Angewandte Chemie* **2024**, 63 (16).

[2] Rath D.; Mikerásek V., Wang C.; Eder M.; Schmid M.; Diebold U.; Parkinson G.S., Pavelec J. **2024**, *submitted*

1:45pm SS+AMS-MoA-2 Water-Gas Shift Reaction Mechanisms on Ligand Coordinated Pt Single Atom Catalyst: Insights from DFT & Microkinetics, Dave Austin, D. Le, T. Rahman, University of Central Florida

Hydrogen is a promising renewable and environmentally friendly fuel to meet future global energy needs. An important reaction to produce hydrogen is the water-gas shift (WGS) reaction, (CO+H₂O→CO₂+H₂; ΔH=-41.1 KJ/mol). Interest in the use of single-atom catalysts (SACs) for facilitating these reactions has grown. This project explores a new strategy that can create a metal-ligand coordinated SAC on metal oxide (Titanium oxide) support. 1,10-phenanthroline-5,6-dione (PDO), was chosen as the ligand for its oxidative potential for stabilizing metal cations in two bidentate sites. Our experimental collaborators Fereshteh Rezvani and Steve Tait from Indiana University were able to characterize the single-atom nature of the Pt with EXAFS, XPS, XRD, DRIFTS, and TEM. They evaluated for the WGS reaction, and it was discovered that Pt-ligand SAC supported on defective TiO₂ shows higher inherent catalytic activity than Pt NPs with significantly lower activation energy which is generally desirable for the redox mechanism.

First, the structure of the Pt-PDO molecule had to be determined, this is because the ligand has two bidentate sites. Experimental results that this complex has a ratio of 2:1 for the ligand to Pt, giving three different potential structures. After the molecule was determined, we had to understand the role of vacancies on the TiO₂ surface. The Pt-PDO complexes (all three configurations) were adsorbed onto to TiO₂ surface that was either clean, or had an oxygen, titanium, or oxygen and a titanium vacancy. We showed that the vacancies were important to activate the Pt-PDO complex, on the clean surface there is only van der Waals interaction between the surface and the complex. The electronic structure of these systems also shows the activation of the Pt atom from vacancies, as the Pt becomes more reactive and has its frontier orbitals pushed closer to the

Fermi level. The WGS reaction has two different proposed mechanisms. They are the Redox and the associative mechanisms. They differ by which point the reactants are adsorbed. These two mechanisms' pathways were simulated on the Pt-PDO complex and to understand the role of ligands the Redox mechanism was also studied on a single Pt atom. The DFT calculations confirmed that the redox mechanism has a lower energy barrier than the associative mechanism for Pt-ligand SAC. A microkinetic study was also performed to obtain the theoretical turnover frequency for all three reactions. The microkinetic study shows that the Redox mechanism has a higher turnover frequency than that of the associative and single Pt atom reactions.

2:00pm SS+AMS-MoA-3 Surface Chemistry and Catalysis of IrO₂(110), Jason Weaver, University of Florida; A. Asthagiri, Ohio State University; M. Kim, Yeungnam University, Republic of Korea; J. Jamir, C. Pope, University of Florida; J. Yun, Ohio State University; S. Ramasubramanian, University of Florida

INVITED

Developing more efficient catalytic processes to oxidize light-alkanes partially or completely is important for various applications, including power generation, exhaust gas remediation and chemical synthesis. In this talk, I will discuss investigations of alkane oxidation on the IrO₂(110) surface, and emphasize how mechanistic insights obtained from UHV surface science experiments and DFT calculations have been used to inform our understanding of rates and species coverages measured during alkane oxidation under catalytic conditions. I will discuss the development of a first-principles microkinetic model that accurately reproduces key aspects of the kinetics of methane oxidation on IrO₂(110) and identifies how different surface species, observed using operando spectroscopy, affect the catalytic kinetics. I will also discuss recent results which clarify how gaseous H₂O influences the catalytic oxidation of ethane on IrO₂(110) and the surface species that develop under reaction conditions. Our studies demonstrate how fundamental knowledge gained from surface science and DFT calculations can play a critical role in interpreting operando measurements and identifying the mechanisms of complex, catalytic reactions.

2:30pm SS+AMS-MoA-5 Room Temperature Activation of Methane and Its Dry Reforming by MgO Nanostructures Embedded in CuO_x on Cu(111), Areebin Islam, K. Reddy, Brookhaven National Laboratory; Y. Tian, Stony Brook University/Brookhaven National Laboratory; J. Rodriguez, Brookhaven National Laboratory

Natural gas, primarily methane, is valued for its versatility and potential in sustainable energy production through reforming or partial oxidation reactions. The investigation stems from the need for efficient technologies to utilize natural gas for sustainable syn gas or hydrogen production while simultaneously addressing carbon dioxide (CO₂) utilization and conversion challenges. MgO nanostructures show promise for methane activation due to their unique surface properties, while Cu-based catalysts are explored for selective methane oxidation at lower temperatures. This study investigates the growth and reactivity of MgO nanostructures on a Cu₂O/Cu(111) substrate, employing scanning tunneling microscopy (STM) and synchrotron-based ambient-pressure X-ray photoelectron spectroscopy (AP-XPS). Deposition of Mg atoms on the "29" structured copper oxide film induces oxygen transfer from the Cu₂O/Cu(111) substrate to the deposited Mg, forming MgO and CuO_x. Diverse morphologies are observed, including structured copper oxide films with embedded MgO clusters (1-3 Mg atoms) and randomly dispersed MgO nanoparticles. Reactivity studies reveal that MgO nanostructures smaller than 1 nm in width activate methane at room temperature, dissociating it into CH_x species. CO₂ dissociates into CO and C species instead of forming plain carbonates. The size and morphology of MgO nanostructures significantly influence their reactivity, enabling dry reforming of methane (MDR) by CO₂ into syn gas. Specifically, MgO nanostructures with a coverage of 0.04-0.11 ML activate methane at room temperature, leading to its dissociation into CH_x species. Additionally, smaller MgO clusters (0.2-0.5 nm in width, 0.4-0.6 Å in height) at lower coverages exhibit distinct reactivity towards CO₂, dissociating it into CO and C species. This investigation underscores the size- and morphology-dependent reactivity of MgO nanostructures, showcasing a behavior distinct from bulk MgO. The catalytic performance observed is attributed to the unique magnesium-copper interface, featuring multifunctional sites comprising magnesium cations, oxygen, and copper cations, which facilitate methane activation and drive the MDR processes forward at around 500K.

Monday Afternoon, November 4, 2024

2:45pm **SS+AMS-MoA-6 Mixed IrO₂/RuO₂(110) Thin Films: Distinct Surface Chemical Properties of the Single-Layer Oxides**, *Suriya Narayanan Ramasubramanian, C. Sudarshan, J. Shin, C. Lee*, University of Florida, Gainesville; *C. Plaisance*, Louisiana State University; *D. Hibbitts, J. Weaver*, University of Florida, Gainesville

Mixed metal-oxides of IrO₂ and RuO₂ have potential to serve as efficient catalysts for promoting the partial or complete oxidation of alkanes, due to the unusual ability of IrO₂ to activate light alkanes at low temperature as well as the possibility that the mixed oxides exhibit distinct surface chemical properties compared with the pure oxides. In this talk, I will discuss our recent studies of the growth and surface chemical properties of layered structures of IrO₂(110) and RuO₂(110) thin films as well as mixed IrO₂-RuO₂(110) films prepared in UHV. We find that single-layers (SL) of IrO₂(110) on RuO₂(110) and vice versa exhibit distinct binding properties toward adsorbed molecules compared with the corresponding multilayer (ML), bulk-like oxides. TPD shows that the binding of N₂ and O is stronger on SL-RuO₂(110) on ML-IrO₂(110) relative to ML-RuO₂(110), whereas these species bind more weakly on SL-IrO₂(110) on ML-RuO₂(110) relative to ML-IrO₂(110). These differences are especially pronounced for oxygen in that the binding energy of an adsorbed O-atom on top of a surface metal site increases in the order, SL-IrO₂ < ML-RuO₂ < ML-IrO₂ < SL-RuO₂, with the binding energy differing by ~50 kJ/mol between each single vs. multiple layer structure. I will discuss DFT calculations which show that these differences originate from a trans-ligand effect, wherein the bonding properties of surface metal atoms are strongly influenced by the bonding of sub-surface O-atoms to the second layer oxide. Lastly, I will discuss recent results showing that well-mixed Ir_xRu_yO₂(110) thin films can be generated in UHV and will discuss their surface chemical properties. The significant differences between the surface chemical properties of single vs. multiple layer oxide structures may have broad implications for understanding the catalytic behavior of mixed IrO₂/RuO₂ systems.

3:00pm **SS+AMS-MoA-7 Active Sites for Oxidation Reactions on Cu₂O Surfaces**, *Dario Stacchiola*, Brookhaven National Laboratory

Cu-based catalysts are active for partial and full oxidation reactions. Copper can be oxidized under moderate oxidant pressures and temperature to Cu₂O, and further to CuO under typical catalytic reaction conditions. We present here model systems using both copper oxide thin films and single crystals used to interrogate the effect of modifiers on the stability of exposed active Cu sites. *In situ* experiments allow the observation of dynamic processes and phases under reaction conditions.

References

- [1] "Oxidation of CO on a reconstructed Cu₂O surface", (submitted)
- [2] "Stabilization of Cu₂O through site-selective formation of a Co₂Cu hybrid single-atom catalyst", *Chem. Mat.* **34**,2313(2022)
- [3] "Potassium-Promoted Reduction of Cu₂O/Cu(111) by CO", *J. Phys. Chem. C* **123**, 8057–8066 (2019)
- [4] "Redox Properties of Cu₂O(100) and (111) Surfaces", *J. Phys. Chem. C* **122**, 28684–28691 (2018)

3:15pm **SS+AMS-MoA-8 Tracking Elementary Steps in Conversion of Carboxylic Acids on Single Crystalline and Nanofaceted TiO₂(101)**, *Xingyu Wang*, Pacific Northwest National Lab; *W. Debenedetti*, Los Alamos National Laboratory; *C. O'Connor*, Harvard University; *Z. Dohnalek, G. Kimmel*, Pacific Northwest National Lab

Ketonization of carboxylic acid used to be a method to produce acetone in industry. Recent interest has focused on this C-C coupling reaction due to its potential for upgrading biomass. The production of acetone from acetic acid was only observed in high pressure reactors on anatase nanoparticles. However, on anatase TiO₂(101) single crystals in ultra-high vacuum (UHV), acetone production from acetic acid has not been observed. This is an example of the material gap in surface science studies. The mechanism of ketonization is also under debate; the two most commonly proposed pathways are β-keto acid pathway and ketene pathway.

In this study, we introduced well-defined nanoparticles (NPs) with mostly (101) surfaces into a UHV chamber to elucidate the ketonization mechanism and bridge the material and pressure gaps in this system. A combined experimental approach of temperature programmed desorption (TPD), scanning tunneling microscopy (STM), X-ray photoelectron spectroscopy (XPS), and reflection absorption infrared spectroscopy (RAIRS) was used, along with theoretical studies. Our finding is that on single crystals, the ketene produced desorbs from the surface without encountering another acetate. In contrast, ketene desorbing from a given NP within a layer of NPs can subsequently react with an acetate on another

NP, leading to acetone production. To demonstrate this, we prepared three samples with varying thickness of anatase NP layers, with mostly (101) facets, in an UHV system. We then compared the reaction of acetic acid on these NP layers with its reaction on an anatase(101) single crystal. We found that the production of acetone starts from 10ML of acetic acid exposure, and the yield correlates with the depth of acetic acid absorption into the nanoparticle beds. Along with theoretical studies, we identified a mechanism through a key intermediate, α-enolate acetic acid, which forms through the reaction of gas phase ketene with surface-bound acetate species. Further studies, which involve dosing ketene through a homemade heated quartz tube ketene source onto an acetic acid pre-dosed single crystal surface, are currently underway to confirm this reaction mechanism.

3:30pm **SS+AMS-MoA-9 Developing First-principles Microkinetic Models for Selective Ethane Oxidation on Cl-substituted IrO₂(110)**, *Jungwon Yun*, The Ohio State University; *D. Bae, N. Park*, Yeungnam University, Republic of Korea; *J. Weaver*, University of Florida; *M. Kim*, Yeungnam University, Republic of Korea; *A. Asthagiri*, The Ohio State University

In this study, we investigated the role of Cl doping on ethylene selectivity for ethane oxidation on IrO₂(110) using a combination of density functional theory (DFT) and microkinetic modeling (MKM). Catalytic oxidative dehydrogenation (ODH) of ethane is an attractive route to produce value-added products such as ethylene. Our previous research demonstrated that stoichiometric IrO₂(110) exhibits significant potential for ethylene production at low temperature (~ 400 K) due to the low activation energy for initial C-H bond cleavage of light alkanes. Temperature programmed reaction spectroscopy (TPRS) experiments showed that surface HO groups promote ethylene selectivity in ethane ODH. Given Cl is isoelectronic to surface HO groups and has been experimentally shown to be able to substitute bridge O atoms on RuO₂(110) surfaces, we explored Cl substitution effects on ethylene selectivity on IrO₂(110). DFT calculations indicated that the presence of bridge Cl on the IrO₂(110) surface destabilizes adjacent adsorbed ethane and ethylene but has minimal impact on the reaction barriers of C₂H_x species with adjacent oxygen. This suggests that limited Cl substitution would still allow the IrO₂(110) surface to convert C₂H₆ to C₂H₄, but subsequently start to constrain further dehydrogenation and oxidation steps due to the lack of bridge O atoms. A DFT-based MKM was developed to understand the relationship between product yields (C₂H₆, C₂H₄, CO/CO_x) on degree of Cl substitution. The MKM modeled TPRS confirms that ethylene yield is increased by Cl substitution but eventually reaches a maximum where there is a drop due to the deactivation of the surface. This maximum in ethylene yield is dependent on initial C₂H₆ coverage since dehydrogenative oxidation steps produce surface HO groups that, when combined with bridge Cl, deactivate the surface. We will discuss ongoing work to extend the MKM simulations to reaction conditions where activity and selectivity are examined as a function of partial pressures of C₂H₆ and O₂ along with percent Cl substitution.

4:00pm **SS+AMS-MoA-11 Small Alcohol Reactivity Over TiO₂/Au(111) Inverse Model Catalysts**, *Ashleigh Baber*, James Madison University

Gold-based catalysts have received tremendous attention as supports and nanoparticles for heterogeneous catalysis, in part due to the ability of nanoscale Au to catalyze reactions at low temperatures in oxidative environments. Surface defects are known active sites for low temperature Au chemistry, so a full understanding of the interplay between intermolecular interactions and surface morphology is essential to an advanced understanding of catalytic behavior and efficiency. Our undergraduate research lab uses ultrahigh vacuum temperature programmed desorption (UHV-TPD) to investigate the fundamental interactions between small alcohols on Au(111) and the reactivity of TiO₂/Au(111) inverse model catalysts on small alcohol redox behavior. In a systematic study to better understand the adsorption and intermolecular behavior of small alcohols (C₁-C₄) on Au(111) defect sites, coverage studies of methanol, ethanol, 1-propanol, 1-butanol, 2-butanol, and isobutanol have been conducted on Au(111). These small alcohols molecularly adsorb on the Au(111) surface and high resolution experiments reveal distinct terrace, step edge, and kink adsorption features for each molecule. The desorption energy of small primary alcohols was shown to trend linearly with increasing C₁-C₄ carbon chain length, indicating that the H-bonded molecular packing of 1-butanol resembles that of methanol, ethanol, and 1-propanol, while isobutanol and 2-butanol deviate from the trend. These energy insights are particularly interesting when studying the redox behavior of small alcohols over TiO₂/Au(111). Depending on the surface preparation conditions, Au(111) supported TiO₂ nanoparticles react with

Monday Afternoon, November 4, 2024

small alcohols to form either reduced and oxidized products. The reactivity of the surface for ethanol oxidation was altered by controlling the oxidation state of TiO_x ($x < 2$) and coverage of TiO_2 . Low coverages of fully oxidized TiO_2 nanoparticles on Au(111) are active for the selective oxidation of ethanol to form acetaldehyde, but not all small alcohols behave similarly.

4:15pm **SS+AMS-MoA-12 Partial Chlorination of IrO_2 (110) for Selective Ethane Chemistry**, Connor Pope, University of Florida, Gainesville; J. Yun, Ohio State University; R. Reddy, J. Jamir, University of Florida, Gainesville; M. Kim, Yeungnam University, Republic of Korea; A. Asthagiri, Ohio State University; J. Weaver, University of Florida, Gainesville

Developing more efficient catalytic processes to convert ethane to ethylene is important for improving hydrocarbon-to-chemicals processing and transitioning to carbon-neutral technologies. Our prior work demonstrates that C_2H_6 dehydrogenation on the IrO_2 (110) surface produces C_2H_4 between ~350 and 450 K during temperature programmed reaction spectroscopy (TPRS), and that the C_2H_4 selectivity can be increased by pre-hydrogenating the oxide surface to deactivate a fraction of the surface oxygen sites. In this talk, I will discuss recent work in which we controllably replaced surface O-atoms of IrO_2 (110) with Cl-atoms through the oxidation of gaseous HCl in ultrahigh vacuum. We find that the stepwise adsorption of HCl on IrO_2 (110) with heating to 650 K causes H_2O desorption, and generates Cl atoms on bridging and on-top sites in about a 1:1 ratio, with the total Cl coverage saturating near 0.7 ML. Measurements using TPRS and XPS further demonstrate that the partitioning of Cl-atoms between bridging and on-top sites can be altered by exposing the surfaces to reducing vs. oxidizing conditions. Lastly, I will discuss how partial chlorination affects the surface reactivity toward CO and C_2H_6 , and produces a nearly two-fold increase in the selectivity of C_2H_6 dehydrogenation to C_2H_4 during TPRS. Our findings demonstrate the potential of controlled surface deactivation for improving the selectivity of IrO_2 (110) for partial alkane oxidation.

4:30pm **SS+AMS-MoA-13 Insights into CO_2 Hydrogenation on the InO_x/Cu (111) and InO_x/Au (111) Surfaces: Surface Electronic Structure and Reaction Mechanistic Studies**, Prabhakar Reddy Kasala, J. Rodriguez, Brookhaven National Laboratory

In CO_2 hydrogenation, In_2O_3 catalysts are known for their higher CH_3OH selectivity, primarily attributed to their oxygen vacancies. Subsequent studies explored depositing metals on In_2O_3 to enhance CO_2 conversion and oxygen vacancy formation.¹⁻² Besides metal supported on In_2O_3 -based catalysts, intermetallic In-M (M= Pd, Cu) compounds have also shown good performance for CO_2 hydrogenation to methanol synthesis.³⁻⁴ Despite extensive research on metal (M) supported In_2O_3 catalysts, the role of In-M alloy and M/ In_2O_3 interfaces in CO_2 activation and methanol selectivity remains unclear. Our surface electronic structural studies using APXPS reveal that during CO_2 hydrogenation, very low coverage (~0.035 ML) InO_x/Cu (111) undergoes structural changes at/above 500 K, forming a Cu-In intermetallic alloy at the surface. Further increase in Indium coverage (0.325 ML) results in InO_x/Cu (111) at the surface, while the interface remains an In-Cu alloy. Carbon 1s core level spectra of the InO_x/Cu (111) regions of the surface under 1 Torr of $\text{CO}_2 + \text{H}_2$ (1:3 ratio) show the formate (HCOO^*) and H_xCO^* species, with H_xCO having the higher concentration at 500 K in 0.035 ML, while the 0.325 ML Indium oxide has shown the carbonate (CO_3^*) at 300 K and decreased with an increase in temperature to 500 K. Our results clearly demonstrate the promotional effects of In_2O_3 for CO_2 hydrogenation. Furthermore, we extended our studies on InO_x/Au (111) and $\text{InO}_x/\text{TiO}_2$ (001) surfaces to understand the role of Oxide/Metal, Alloy, Oxide/Oxide roles in methanol selectivity. Our preliminary STM and XPS results on InO_x/Au (111) established the preparation of In/Au(111) and InO_x/Au (111) surfaces. We are making progress on indium-based catalysts for CO_2 hydrogenation to establish the role of possible alloys/intermetallic and metal-support interfaces in CO_2 activation and CO_2 hydrogenation to methanol under reaction conditions.

References:

1. Cao et. al., *ACS Catal.* 2021, 11, 1780-1786
2. Rui et. al., *ACS Catal.* 2020, 10, 11307-11317
3. Shi et. al., *J. Catal.* 2019, 379, 78-89
4. Chen et. al., *ACS Catal.* 2019, 9, 8785-8797

4:45pm **SS+AMS-MoA-14 Structural-Electronic Property Evolution of LiCoO_2 (001) Under Varied Oxygen Chemical Potentials**, Yuchen Niu, J. Reutt-Robey, University of Maryland College Park

Since its discovery as an intercalation Li-ion battery electrode in 1980, LiCoO_2 remains a popular cathode material for portable devices. Its surfaces also provide an unexplored opportunity to tune the structure and charge-

Monday Afternoon, November 4, 2024

transport properties for emergent electronic applications. In this study, we report on the evolution of LiCoO_2 (001) surfaces, specifically their structural and electronic property response to processing under low/high O_2 chemical potential extremes via scanning probe microscopy (SPM), low energy electron diffraction (LEED), X-ray photoelectron spectroscopy (XPS) and Raman spectroscopy.

Under a traditional UHV regimen at low O_2 chemical potentials, LiCoO_2 (100) persistently displays a diffused (1x1) LEED pattern after many cycles of Ar^+ sputtering- thermal annealing, suggestive of nanoscale disorder without major atomic surface reconstruction. UHV-STM imaging reveals the singular surface terminated by shallow grains of ~2 nm width, which coarsen to ~30 nm grains under prolonged processing. Atomically resolved images of local regions show ($\sqrt{7} \times \sqrt{7}$) R 19.1° ordering, which could be attributed to local Li ordering on Li-terminated layers. The electronic properties of this surface are further mapped with UHV scanning tunneling spectroscopy. Electronic band gaps derived from I-V spectroscopy are reported. This is corroborated by in situ XPS measurements of the surface chemical composition and valence band structures during the Ar^+ sputtering- thermal annealing cycles.

Under high O_2 chemical potentials (160~ 760 torr O_2), dramatic changes in surface structures are observed, indicating more efficient surface mass transport. In contrast to the nanograin features observed at low O_2 chemical potentials, high O_2 chemical potential treatments generate expansive atomically flat (100) terraces of ~ 1 μm width, step edges and quasi-hexagonal islands. Partial surface decomposition to Co_3O_4 due to Li loss is also observed.

2D Materials

Room 122 - Session 2D+AP+EM+QS+SS+TF-TuM

2D Materials: Synthesis and Processing

Moderators: **Jyoti Katoch**, Carnegie Mellon University, **Huamin Li**, University at Buffalo-SUNY

8:00am **2D+AP+EM+QS+SS+TF-TuM-1 Tailored Growth of Transition Metal Dichalcogenides Monolayers and Their Heterostructures, *Andrey Turchanin***, Friedrich Schiller University Jena, Germany **INVITED**

Two-dimensional materials (2D), their van der Waals and lateral heterostructures possess a manifold of unique electronic, optoelectronic and photonic properties which make them highly interesting for fundamental studies and technological applications. To realize this potential, their tailored growth as well as understanding of the role of their intrinsic defects and 2D-material/substrate interactions are decisive. In this talk, I will present an overview of our recent progress on the synthesis by chemical vapor deposition (CVD), material characterization and studying of fundamental electronic and photonic properties of 2D transition metal dichalcogenide (TMDs) including some applications in electronic and optoelectronic device as well as observing of new excitonic phenomena. A particular focus will be on the lateral heterostructures of TMD monolayers with atomically sharp boundaries and Janus TMDs.

References

- [1] A. George et al. *J. Phys. Mater.* **2**, 016001, 2019.
- [2] S. Shree et al. *2D Mater.* **7**, 015011, 2020.
- [3] I. Paradeisanos et al. *Nat. Commun.* **11**, 2391 (2020).
- [4] G. Q. Ngo et al., *Adv. Mater.* **32**, 2003826 (2020).
- [5] A. George et al. *npj 2D Mater. Appl.* **5**, 15 (2021).
- [6] S. B. Kalkan et al., *npj 2D Mater. Appl.* **5**, 92 (2021).
- [7] E. Najafidehaghani et al. *Adv. Funct. Mater.* **31**, 2101086 (2021).
- [8] Z. Gan et al. *Adv. Mater.* **34**, 2205226 (2022).
- [9] Z. Gan et al. *Small Methods* **6**, 2200300 (2022).
- [10] D. Beret et al., *npj 2D Mater. Appl.* **6**, 84 (2022).
- [11] G. Q. Ngo et al. *Nat. Photonics* **16** 769-776 (2022)
- [12] S.B. Kalkan, *Adv. Opt. Mater.* **11**, 2201653 (2023).
- [13] R. Rosati et al., *Nat. Commun.* **14**, 2438 (2023).
- [14] H. Lamsaadi et al., *Nat. Commun.* **14**, 5881 (2023).
- [15] J. Picker et al., *Nanoscale Adv.* **6**, 92-101 (2024).

8:30am **2D+AP+EM+QS+SS+TF-TuM-3 High-Coverage MoS₂ Growth by Two-Step Annealing Process, *Shinichi Tanabe, H. Miura***, Tokyo Electron Ltd., Japan; *N. Okada, T. Irisawa*, AIST, Japan; *Y. Huang, H. Warashina, A. Fukazawa, H. Maehara*, Tokyo Electron Ltd., Japan

Continuation of Moore's Law scaling requires thin channels in nanosheet field-effect transistor architecture. In this respect, transition-metal dichalcogenides (TMDs) are candidates for the channel material because TMDs are expected to show higher mobility than Si when thickness of the channel is extremely thin. Compatibility to Si nanosheet field-effect transistor fabrication process requires TMD/buffer multilayer film. To obtain such film, alternative preparation of TMD and buffer layers is necessary. Although high-quality TMD can be obtained on a buffer layer by transferring TMD from other substrates, development of a reliable transferring method is challenging. Thus, direct growth of a TMD on a buffer layer is preferable.

We report on a successful growth of high-coverage MoS₂ on SiO₂/Si substrate. The process starts with growing an initial film on SiO₂/Si substrate. Here, a continuous initial film can be easily grown by this process with high growth rate. Next, the initial film is sulfurized by a first annealing step followed by crystallization of the film by a second annealing step. The obtained film is a continuous layered film which was confirmed by cross-sectional TEM images. In addition, typical Raman spectra consisted of E_{2g} and A_{1g} peaks are observed in entire substrate which shows that MoS₂ is grown with high coverage. The difference of E_{2g} and A_{1g} peaks is about 21 cm⁻¹. These results indicate that the two-step annealing process is suitable for obtaining MoS₂ in large area.

8:45am **2D+AP+EM+QS+SS+TF-TuM-4 Anomalous Isotope Effect on the Optical Bandgap in a Monolayer Transition Metal Dichalcogenide Semiconductor, *Kai Xiao***, Center for Nanophase and Materials Sciences Oak Ridge National Laboratory; *Y. Yu*, School of Physics and Technology, Wuhan University, China; *V. Turkowski*, Department of Physics, University of Central Florida; *J. Hachtel*, Center for nanophase and Materials Sciences Oak Ridge National Laboratory; *A. Puzetzyk, A. Ievlev, C. Rouleau, D. Geohegan*, Center for Nanophase and Materials Sciences Oak Ridge National Laboratory

Isotope effects on optical properties of atomically thin 2D materials have rarely been studied to date due to significant challenges posed by sample-to-sample variations resulting from defects, strain, and substrate interactions, complicating the interpretation of optical spectroscopic results. Here, we report a novel two-step chemical vapor deposition method to synthesize isotopic lateral junctions of MoS₂, comprising monolayer single crystals with distinct isotopic regions. This method allowed the minimization of shifts in photoluminescence due to synthetic heterogeneities necessary to confirm the intrinsic isotope effect on the optical band gap of 2D materials. Raman measurements and temperature-dependent photoluminescence spectra revealed an unusual 13 (± 7) meV redshift as the Mo isotope mass increased in monolayer MoS₂. This shift is distinct from the trend observed in conventional semiconductors and quantum wells (Si, GaAs, diamond, hBN, etc.). Our experimental characterization, along with time-dependent density-functional theory (TDDFT) and many-body second-order perturbation theory, disclosed that this anomalous shift in the optical band gap in 2D MoS₂ resulted from significant changes in the exciton binding energy induced by strong exciton-phonon scattering. This study provides fundamental insights into understanding the effect of exciton-phonon scattering on the optoelectronic properties of atomically thin 2D materials.

Synthesis science was supported by the U.S. Dept. of Energy, Office of Science, Materials Science and Engineering Division. This work was performed at the Center for Nanophase Materials Sciences, which is a DOE Office of Science User Facility.

9:00am **2D+AP+EM+QS+SS+TF-TuM-5 CVD Growth and Characterization of High-Quality Janus SeMoS and SeWS Monolayers, *Julian Picker***, Friedrich Schiller University Jena, Germany; *M. Ghorbani-Asl*, Helmholtz Zentrum Dresden-Rossendorf, Germany; *M. Schaal, O. Meißner, F. Otto, M. Gruenewald, C. Neumann, A. George*, Friedrich Schiller University Jena, Germany; *S. Kretschmer*, Helmholtz Zentrum Dresden-Rossendorf, Germany; *T. Fritz*, Friedrich Schiller University Jena, Germany; *A. Krashennnikov*, Helmholtz Zentrum Dresden-Rossendorf, Germany; *A. Turchanin*, Friedrich Schiller University Jena, Germany

Structural symmetry breaking of two dimensional (2D) materials leads to novel physical phenomena. For 2D transition metal dichalcogenides (TMDs) such symmetry breaking can be achieved by exchange of one chalcogen layer with another one. The resulting, so-called Janus TMD structure exhibits an intrinsic dipole moment due to the different electronegativity values of the top and bottom chalcogen layers. Since Janus TMDs do not exist as bulk crystals, they cannot be obtained by exfoliation and need to be synthesized. Recently, we developed a route to grow Janus SeMoS monolayers (MLs) by chemical vapor deposition (CVD). [1] In this approach MoSe₂ monolayers are firstly grown on Au foils and then sulfurized to exchange the bottom selenium layer with sulfur atoms. The formation of high-quality Janus SeMoS MLs and the growth mechanism are proven by Raman and X-ray photoelectron spectroscopy (XPS), photoluminescence measurements, transmission electron microscopy and density functional theory (DFT). Here we present an investigation down to the atomic scale of Janus SeMoS MLs grown on Au(111). From low-energy electron diffraction (LEED) and scanning tunneling microscopy (STM) measurements we determine experimentally the lattice parameters of Janus SeMoS for the first time. The obtained results are in good agreement with the respective DFT calculation. Based on the angle-resolved ultraviolet photoelectron spectroscopy (ARUPS) study, we also obtain the spin-orbit splitting value of the valence band at the K point. Moreover, applying the same approach, we grow and characterize Janus SeWS MLs and provide a comparative analysis with the Janus SeMoS system.

- [1] Z. Gan, I. Paradeisanos, A. Estrada-Real, J. Picker, C. Neumann, A. Turchanin et al., *Chemical Vapor Deposition of High-Optical-Quality Large-Area Monolayer Janus Transition Metal Dichalcogenides*, *Adv. Mater.* **34**, 2205226 (2022).

Tuesday Morning, November 5, 2024

9:15am **2D+AP+EM+QS+SS+TF-TuM-6 Location-Selective CVD Synthesis of Circular MoS₂ Flakes with Ultrahigh Field-Effect Mobility**, *Chu-Te Chen, A. Cabanillas, A. Ahmed, A. Butler, Y. Fu, H. Hui, A. Chakravarty, H. Zeng*, University at Buffalo-SUNY; *A. Yadav*, Applied Materials, Inc.; *H. Li*, University at Buffalo-SUNY; *K. Wong*, Applied Materials, Inc.; *F. Yao*, University at Buffalo-SUNY

Two-dimensional (2D) semiconducting transition metal dichalcogenides (TMDs) have been considered as promising channel material candidates for future nanoelectronics. The device performance has been significantly improved over the years due to the advancements in understanding of TMD materials, device design, and fabrication process. Despite the early success in demonstrating proof-of-concept devices, scalable and single-crystal growth of TMD films on suitable substrates remains a formidable roadblock to the development of commercially viable TMD-based nanoelectronics. To mitigate this problem, we exploit a controlled growth of high-quality TMD layers at desired locations and demonstrate excellent and consistent electronic properties in transistor device architectures. Taking MoS₂ as an example, we develop a precursor-seeded growth strategy for the direct and site-specific synthesis on SiO₂ substrates using chemical vapor deposition (CVD). By employing electron-beam lithography to pattern seed layers, precise nucleation and growth at designated positions are achieved. Through systematic exploration of CVD synthesis parameters, ordered arrays of circular MoS₂ flakes are successfully grown with the MoO₃ seeds serving as the nucleation sites. A comprehensive suite of microscopic/spectroscopic characterizations along with electrical measurements is utilized to analyze the microstructural and transport properties of the as-grown MoS₂ flakes. The tri-layer circular MoS₂ arrays possess an adjustable and uniform size and exhibit a consistent field-effect mobility up to ~20 cm²/V·s with Bi/Au electrode contacts. These findings showcase a technological breakthrough to 2D material synthesis and hold great promise for future integration of 2D materials in the next generation nanoelectronics.

9:30am **2D+AP+EM+QS+SS+TF-TuM-7 Optoelectronic Properties of Exfoliated and CVD Grown TMD Heterostructures**, *Elycia Wright, K. Johnson, S. Coye, M. Senevirathna, M. Williams*, Clark Atlanta University

Transition metal dichalcogenides (TMDs) have attracted significant attention due to their distinctive electronic band structures, which result in intriguing optoelectronic and magnetic properties such as direct bandgap in the visible-infrared range, large exciton binding energies and the presence of two intrinsic valley-contrasting quantities—the Berry curvature and the orbital magnetic moment. Researchers have recently shown interest in studying heterostructures made from different TMD materials. The idea is to combine these materials to create synergistic effects, which can result in even more exciting properties than those found in individual TMDs. For instance, MoS₂/WS₂ heterostructure can exhibit novel and enhanced optoelectronic performances, including bipolar doping and photovoltaic properties. TMD-based heterostructures may open many possibilities for discovering new physics and developing novel applications. While the science of TMDs and TMD-based heterostructures has made significant strides over the past decade, the field has not yet matured. Numerous challenges, particularly in realizing TMD-based practical applications, remain unresolved. This underscores the importance of our collective efforts in pushing the boundaries of this field.

Exfoliation is a common method for assembling TMD heterostructures, but it has limitations in producing TMD heterostructures on a large scale. The chemical vapor deposition (CVD) method can be used to grow TMD heterostructures on a large scale, which is required in massive device production. However, there are numerous challenges in growing high-quality TMD heterostructures with large areas by CVD, which need to be solved before TMD-based practical applications can be achieved. Our research will focus on the growth of heterostructures (MoS₂/WS₂) on various substrates (such as sapphire and SiO₂/Si) using chemical vapor deposition (CVD). We will explore different mechanisms to achieve large area heterostructures and compare the resulting optoelectronic properties with exfoliated heterostructures. The properties will be characterized using Raman and Fourier Transform infra-red (FTIR) spectroscopy and confocal laser optical microscopy.

9:45am **2D+AP+EM+QS+SS+TF-TuM-8 Pulsed Laser Deposited Amorphous Boron Nitride for 2D Materials Encapsulation**, *Daniel T. Yimam, S. Harris, A. Puzetky, I. Vlasiouk, G. Eres, K. Xiao, D. Geohegan*, Oak Ridge National Laboratory, USA

Recent advancements in 2D materials have opened new avenues in optoelectronics and microelectronics. However, their integration is

hindered by challenges related to materials stability and degradation. Realizing the full potential of 2D materials requires synthesizing and functionalizing an encapsulation layer with desired properties. Recently amorphous boron nitride (aBN) has attracted attention as an ideal low-k material suitable for 2D electronics due to its effectiveness as a protective encapsulation layer. Unlike hexagonal boron nitride (h-BN), which requires high temperatures for deposition and poses challenges for large-area synthesis and integration, aBN can be deposited at significantly lower temperatures. This property makes aBN highly attractive and compatible for back-end-of-line (BEOL) processes in the semiconductor industry.

In this work, we demonstrate that pulsed laser deposition (PLD) enables the deposition of aBN with precise kinetic energy control of precursors, facilitating direct deposition onto 2D materials without significant defect formation. Various in situ plume diagnostics and monitoring tools during deposition were utilized to identify optimal deposition conditions, ensuring ideal kinetic energy ranges and accurate thickness control. This enhances the aBN as an effective encapsulation and barrier against 2D materials thermal degradation, while improving photoluminescence of encapsulated 2D materials. We believe our work significantly impacts future microelectronics by providing low thermal budget method for encapsulating 2D materials and understanding strain and defect evolution. Our work not only advances the practical applications of 2D materials but also paves the way for in situ experimental analysis and diagnostics in the field of material science.

This work was supported by the U.S. DOE, Office of Science, Materials Sciences and Engineering Division and the Center for Nanophase Materials Sciences, which is a DOE Office of Science User Facility.

Keywords: Pulsed Laser Deposition, Amorphous Boron Nitride, 2D Materials, Encapsulation, In Situ Diagnostics.

11:00am **2D+AP+EM+QS+SS+TF-TuM-13 Topotaxy for Compositional Variations of Transition Metal Dichalcogenides**, *Matthias Batzill*, University of South Florida

Topotaxy is a kind of solid-state reaction in which the product crystal is crystallographically related to the initial crystal. In 2D materials the initial crystal could be a single sheet or a few layers that are being reacted with same or dissimilar elements to produce novel 2D materials that may not exist in the bulk. Here we investigate such topotactical reactions for transition metal dichalcogenides (TMDs) by reacting them with vapor deposited transition metals. This can result in phase transformations of known layered materials, such as PtTe₂ + Pt => Pt₂Te₂ [1], new phases such as mirror twin grain boundary networks in MoSe₂ or MoTe₂ [2], or covalently linking bi-layer TMDs by intercalants of the same or different TMs [3]. The studies are performed on MBE grown TMDs and are further modified by post-growth reaction with TM. The resulting structures are characterized by surface probes, such as STM, photoemission, and LEED. In general, the open structure of many 2D materials make them ideal for topotaxy and provide an approach for modifying their composition and induce new properties. Moreover, it allows to locally modify an extended 2D sheet and thus produce in-plane heterojunctions between 'original' and modified 2D domains in a first step to create in-plane device structures.

[1] P.M. Coelho, H.P. Komsa, H. Coy Diaz, Y. Ma, A.V. Krasheninnikov, M. Batzill.

Post-Synthesis Modifications of Two-Dimensional MoSe₂ or MoTe₂ by Incorporation of Excess Metal Atoms into the Crystal Structure.

ACS Nano 12, 3975-3984 (2018)

[2] K. Lasek, J. Li, M. Ghorbani-Asl, S. Khatun, O. Alanwoko, V. Pathirage, A.V. Krasheninnikov, M. Batzill.

Formation of In-Plane Semiconductor–Metal Contacts in 2D Platinum Telluride by Converting PtTe₂ to Pt₂Te₂.

Nano Letters 22, 9571-9577 (2022)

[3] V. Pathirage, S. Khatun, S. Lisenkov, K. Lasek, J. Li, S. Kolekar, M. Valdivares, P. Gargiani, Y. Xin, I. Ponomareva, M. Batzill.

2D Materials by Design: Intercalation of Cr or Mn between two VSe₂ van der Waals Layers.

Nano Letters 23, 9579-9586 (2023)

11:15am **2D+AP+EM+QS+SS+TF-TuM-14 Solid State Reaction Epitaxy to Create van der Waals Heterostructures between Topological Insulators and Transition Metal Chalcogenides**, *Salma Khatun, O. Alanwoko, V. Pathirage, M. Batzill*, University of South Florida

Van der Waals (vdW) heterostructures have emerged as a promising avenue for exploring various quantum phenomena. However, the formation of these heterostructures directly is complicated, as individual materials could have different growth temperatures, and alloying can occur at the interface. We present an alternative process akin to a solid-state reaction to modify the surface layer of quantum materials and introduce new properties. Specifically, we used vapor-deposited transition metals (TMs), Cr and Mn, with the goal to react with Bi_2Se_3 and transform the surface layer into XBi_2Se_4 ($X = \text{Cr, Mn}$). Our results demonstrate that the TMs have a high selenium affinity that drives Se diffusion toward the TM. We found that when a monolayer of Cr is evaporated, the surface Bi_2Se_3 is reduced to Bi_2 -layer, and a stable (pseudo) 2D $\text{Cr}_{1+x}\text{Se}_2$ layer is formed, whereas MnBi_2Se_4 phase is formed with a mild annealing for monolayer amount of Mn deposition.^[1] However, this phase only occurs for a precise amount of initial Mn deposition. Sub-monolayer amounts dissolve into the bulk, and multilayers form stable MnSe adlayers. Our study highlights the delicate energy balance between adlayers and desired surface-modified layers that govern the interface reactions.^[1] The success of obtaining the MnBi_2Se_4 septuple layer manifests a promising approach for engineering other multicomponent vdW materials by surface reactions.

REFERENCE

[1] S. Khatun, O. Alanwoko, V. Pathirage, C. C. de Oliveira, R. M. Tromer, P. A. S. Autreto, D. S. Galvao, and M. Batzill, *Adv. Funct. Mater.* **2024**, 2315112

11:30am **2D+AP+EM+QS+SS+TF-TuM-15 AVS National Student Award Finalist Talk: Quasi-Van Der Waals Epitaxial Growth of Thin γ' -GaSe Films**, *Mingyu Yu*¹, University of Delaware; *S. Law*, Pennsylvania State University

As an advanced two-dimensional (2D) layered semiconductor, GaSe has various appealing properties, such as rare intrinsic p-type conductivity, nonlinear optical behavior, high transparency in 650-1800nm, and a shift from an indirect-bandgap single-layer film to a direct-bandgap bulk material. These features make GaSe rich in potential in quantum photonic devices, field-effect transistors, photodetectors, etc. GaSe has a hexagonal crystal structure composed of Se-Ga-Ga-Se quadruple layers (QLs). Each QL is bonded by weak van der Waals (vdW) forces, enabling multiple polymorphs: ϵ -(2H), β -(2R), δ -(4H), and γ -(3R). They have identical non-centrosymmetric QL with a D_{3h} space group. Besides the four extensively explored polymorphs, a new polymorph, γ' -(3-R) GaSe, was proposed for the first time in 2018. γ' -GaSe is unique for its centrosymmetric D_{3d} QL (Fig. S1), for which γ' -GaSe is predicted to show intriguing properties compared to other polymorphs. However, there are few existing reports on the observation of γ' -GaSe due to its less-favorable formation energy. Moreover, the wafer-scale production of pure GaSe single crystal thin films remains challenging because of the coexistence of stable multiphases and polymorphs.

We developed a quasi-vdW epitaxial growth method to obtain high-quality pure γ' -GaSe nanometer-thick films on GaAs(111)B at a wafer scale. It results in GaSe thin films exhibiting a smooth surface with a root-mean-square roughness as low as 7.2 Å (Fig. S2a) and a strong epitaxial relationship with the substrate (Fig. S2b). More interestingly, we observed a pure γ' -polymorph using scanning transmission electron microscopy (Fig. S2c,d). Through density-functional theory analysis (Fig. S3), γ' -GaSe can be stabilized by Ga vacancies since its formation enthalpy tends to become lower than that of other polymorphs when Ga vacancies increase. We also observed that, unlike other GaSe polymorphs, γ' -GaSe is inactive in room-temperature photoluminescence tests. This may be related to its centrosymmetric QL structure, which we are exploring further. Meanwhile, we systematically studied the growth window for GaSe with high structural quality and identified that GaAs(111)B is more suitable than c-sapphire as a substrate for GaSe growth. Overall, this study advances the wafer-scale production of γ' -GaSe films, and elucidates a method for direct epitaxial growth of hybrid 2D/3D heterostructures with atomically sharp interfaces, facilitating the development of heterogeneous integration. In the future, we will focus on developing the properties and applications of γ' -GaSe, and delving into the understanding of the epitaxial growth mechanism.

¹ AVS National Student Award Finalist

11:45am **2D+AP+EM+QS+SS+TF-TuM-16 Investigation of Dry Transfer of Epitaxial Graphene from SiC(0001)**, *Jenifer Hajzuz, D. Pennachio, S. Mack, R. Myers-Ward*, U.S. Naval Research Laboratory

Transfer of high-quality graphene from its growth substrate to substrates of technological interest can be necessary to enable its use in certain applications, however it remains challenging to achieve large-area transfer of graphene that is clean and intact. This work utilizes a dry transfer technique in which an adhesive metal stressor film is used to exfoliate epitaxial graphene (EG) from SiC(0001) [1]. In this method, the strain energy in the metal film must be high enough to allow for uniform exfoliation, but low enough such that self-exfoliation of graphene does not occur.

We investigate the dry transfer of monolayer EG (MEG) and hydrogen-intercalated, quasi-freestanding bilayer graphene (QFBEG) grown by sublimation of Si from nominally on-axis 6H-SiC(0001) in a CVD reactor in Ar ambient. A magnetron sputtered Ni stressor layer is used to exfoliate EG and transfer to GaAs, glass, and SiO_2/Si substrates. The Ar pressure during sputtering is found to impact the stress, film density, and roughness of the Ni film, as determined from wafer curvature and X-ray reflectivity (XRR) measurements. By using appropriate sputtering conditions, the Ni/graphene film exfoliates from the entire area of the SiC substrate with use of thermal release tape. Atomic force microscopy (AFM), scanning electron microscopy, Raman spectroscopy, x-ray photoelectron spectroscopy (XPS), and Nomarski microscopy are used to characterize the graphene. The Ni 2p peak was not detected in XPS of the transferred graphene after removal of the Ni film by etching in acid. Additionally, XPS revealed minimal oxide present at the graphene-GaAs interface, consistent with previous reports for this dry transfer method [2].

Raman spectroscopy mapping showed that predominately monolayer graphene is transferred from MEG, while predominately bilayer graphene is transferred from QFBEG. Raman spectroscopy of the SiC substrate after MEG exfoliation shows the $6\sqrt{3}$ buffer layer that forms during growth on SiC(0001) remains on the SiC substrate. Consequently, if there are regions of exposed $6\sqrt{3}$ buffer layer in the as-grown MEG on SiC, AFM shows that there are corresponding gaps in the transferred graphene film where the areas of exposed buffer layer do not transfer. The $6\sqrt{3}$ buffer layer is not present in QFBEG due to the hydrogen-intercalation process. It is found that the same Ni sputtering conditions that led to uniform exfoliation and transfer of MEG result in micron-scale tears in the Ni/QFBEG film. By lowering the strain energy in the sputtered Ni film, these tears can be reduced or eliminated.

[1] Kim, J., *et al.*, *Science*, 342, 833 (2013).

[2] Kim, H., *et al.*, *ACS Nano*, 15, 10587 (2021).

Surface Science

Room 120 - Session SS+CA+LS-TuM

Electrochemical Transformations on Surfaces

Moderators: *Florencia C. Calaza*, Instituto de Desarrollo Tecnológico para la Industria Química, Argentina, *Zhuanghe Ren*, University of Central Florida

8:00am **SS+CA+LS-TuM-1 Beyond Static Models: Chemical Dynamics in Energy Conversion Electrocatalysts**, *Beatriz Roldan Cuenya*, Fritz-Haber-Institut der Max-Planck-Gesellschaft, Germany

INVITED

Environmentally friendly technologies for green energy generation and storage in the form of chemical bonds are being urgently sought in order to minimize the future consequences of climate change. The latter includes developing more efficient and durable materials for green H_2 production from water splitting as well as for the re-utilization of CO_2 via its electrocatalytic reduction into value-added chemicals and fuels. Nonetheless, in order to tailor the performance of such energy conversion catalysts, fundamental insight must be gained on their evolving structure and surface composition under reaction conditions.

This talk will illustrate how morphologically and chemically well-defined pre-catalysts experience drastic modifications under operation. Examples for the electrocatalytic reduction of CO_2 as well as the oxygen evolution reaction in water splitting will be given. The model pre-catalysts studied range from size and shape-controlled nanoparticles (Co_3O_4 , $\text{Fe}/\text{Co}_3\text{O}_4$, Fe/NiO , Cu_2O , $\text{ZnO}/\text{Cu}_2\text{O}$, $\text{Au}/\text{Cu}_2\text{O}$), thin films (NiOx , CoFe_2O_4 , Co_3O_4 , Fe_3O_4) to single crystals (differently-oriented Cu surfaces). The need of a synergistic multi-technique *operando* microscopy, spectroscopy and diffraction approach will be evidenced in order to follow the active state formation of complex catalytic materials. Correlations between the

Tuesday Morning, November 5, 2024

dynamically evolving structure and composition of the catalysts and their activity, selectivity and durability will be featured.

8:30am SS+CA+LS-TuM-3 Sulfur-Doped Carbon Support Boosts CO₂RR Activity of Ag Electrocatalysts, Xingyi Deng, D. Alfonso, T. Nguyen-Phan, D. Kauffman, National Energy Technology Laboratory

In this work, we show that the activity of Ag electrocatalysts for electrochemical CO₂ to CO conversion is improved when supported on sulfur-doped (S-doped) carbon materials. S-doped carbon support was created by treating the heavily sputtered, highly oriented pyrolytic graphite (HOPG) in H₂S at elevated temperatures, as confirmed by the S 2p X-ray photoelectron spectroscopy (XPS) peak. Scanning tunneling microscopy (STM) images indicated that Ag nanoparticles supported on S-doped HOPG had similar size distributions as those supported on sulfur-free (S-free) HOPG. While both catalysts reached >90% CO Faradaic efficiency (FE_{CO}) at E = -1.3 V vs. the reversible hydrogen electrode (RHE) in the CO₂ reduction reaction (CO₂RR), Ag catalysts supported on S-doped HOPG demonstrated 70% higher CO turnover frequency (TOF_{CO} = 3.4 CO/atom_{Ag}/s) than those supported on S-free HOPG (TOF_{CO} = 2.0 CO/atom_{Ag}/s). Preliminary calculations based on density functional theory (DFT) indicated a more favorable energetic pathway of CO₂-to-CO at the C-S-Ag interface, tentatively consistent with experiments. These results hint at a new approach to design active and selective electrocatalysts for CO₂ conversion.

8:45am SS+CA+LS-TuM-4 Non-Metal Cations for Enhancing CO₂ Electroreduction on Bismuth Electrode, Theodoros Panagiotakopoulos, K. Shi, D. Le, X. Feng, University of Central Florida; T. Rahman, University of Central Florida

In exploring the effectiveness of non-metal cations in CO₂ electroreduction, we have carried out a comparative examination of the mechanisms for CO₂ electroreduction to formate (HCOO⁻) and CO on the Bi(111) electrode in the presence of cations, Na⁺ and NH₄⁺, using grand canonical density functional theory. Our results reveal that the reduction of CO₂ to formate is driven by the direct hydrogenation of aqueous CO₂ with a hydrogen atom adsorbed on the electrode (H*), i.e., CO₂(aq) + H* → HCOO⁻. The activation barrier for this process is found to be small, less than 100 meV, in the presence of both cations. Furthermore, our results show that the adsorbed intermediate COOH* is formed via a proton shuttling process, i.e., H* moves from the Bi(111) electrode to a H₂O molecule and one of its H atoms is then transferred to a CO₂*. The activation energy barrier for this step was determined to be 0.77 eV and 0.75 eV in the presence of Na⁺ and NH₄⁺, respectively. CO is formed via the dissociation of COOH* species with an activation energy barrier of 0.62 eV and 0.01 eV in the presence of Na⁺ and NH₄⁺, respectively. These findings lead to two important conclusions: 1) the non-metal cation NH₄⁺ can be equally effective as the alkali metal cation Na⁺ in promoting the CO₂ electroreduction to formate; 2) NH₄⁺ is actually more effective than Na⁺ in promoting the CO₂ electroreduction to CO on the Bi(111) electrode, in excellent agreement with experimental observations [1].

[1]K. Shi, D. Le, T. Panagiotakopoulos, T. S. Rahman, and X. Feng, Effect of Quaternary Ammonium Cations on CO₂ Electroreduction (Submitted, 2024).

This work is supported in part by the U.S. Department of Energy under grant DE-SC0024083.

9:00am SS+CA+LS-TuM-5 AVS National Student Award Finalist Talk/SSD Morton S. Traum Award Finalist Talk: How do Cations Promote CO₂ Reduction at the Electrode-Electrolyte Interface, Kaige Shi^{1,2}, D. Le, T. Panagiotakopoulos, T. Rahman, X. Feng, University of Central Florida

Electrochemical CO₂ reduction reaction (CO₂RR) can enable a promising path towards sustainable fuel production and closing the carbon cycle. Despite the reports of numerous electrocatalysts, the mechanism of CO₂RR at the electrode-electrolyte interface remains to be elucidated, particularly on the role of electrolyte cations in the reaction. While most studies of CO₂RR focused on alkali metal cations, we investigate CO₂RR using quaternary ammonium cations, which provide unique tunability in size, shape, and charge distribution to elucidate the cation effect. For the CO₂RR on a Bi catalyst that produces both CO and formate, we find that the cations are essential for both products. Furthermore, we observe a significant impact of the cation identity and concentration on CO production but a minor one on formate production. Our computational studies reveal that cations are required to stabilize adsorbed *CO₂ on Bi surface via electrostatic interaction, and the quaternary ammonium cations

have a more profound effect on the CO₂ adsorption characteristics and CO₂RR activity than metal cations. The adsorbed *CO₂ is an essential step for CO production, but not necessary for formate production due to the pathway with direct reaction of aqueous CO₂ with surface *H species. Based on the understanding, we employ the substitute ammonium cations to enhance CO₂ electrolysis in a gas-diffusion-electrode (GDE) flow cell, which achieves multi-fold improvement of the activity for CO₂RR to CO on Bi and other metal catalysts, as compared to that using alkali metal cations. Our work elucidates the critical effect of cations on the CO₂RR at the electrode-electrolyte interface and demonstrates a strategy to enhance electrocatalysis by optimizing electrolyte composition. This work is supported by the U.S. Department of Energy, Office of Science, Office of Basic Energy Sciences Catalysis Science program under Award Number DE-SC0024083.

9:15am SS+CA+LS-TuM-6 Atomistic Simulations on the Triple-Phase Boundary in Proton-Exchange Membrane Fuel Cells, J. Jimenez, G. Soldano, E. Franceschini, Facultad de Ciencias Químicas UNC, Argentina; Marcelo Mariscal, Universidad Nacional de Córdoba, Argentina INVITED

In this work, we use molecular dynamics simulations and electrochemical experiments on a Nafion/Pt/C system. We perform a systematic analysis, at an atomistic level, to evaluate the effect of several fundamental factors and their intercorrelation in the ECSA (electrochemical surface area) of the catalysts. Besides, we evaluate the diffusion and structuring processes of water at different system interfaces. Overall, this investigation allows us to rationalize how the catalyst utilization is affected, which is an important step in establishing the relationship between the environment and the effectiveness and durability of the PEMFC system. It is important to consider that when experimentally analyzing the changes originating from the different experimental parameters in the operation of a fuel cell, only the average effect of the catalyst, flow field and membrane as a whole can be measured, and it is not possible to separate the corresponding contributions, even less from a region as complex as the TPB. Thus, computational studies provide the appropriate tools for studying each of the parameters separately and in sufficient detail to understand the effects found experimentally.

Proton Exchange Membrane Fuel Cells (PEMFCs), are a well-developed technology aimed at providing cleaner and more sustainable energy solutions. They offer a promising alternative to traditional fossil fuel systems that produce harmful emissions. However, the success of these cells depends greatly on the Three-Phase Boundary (TPB), a critical region composed by the ionomer (liquid, usually Nafion), catalyst (solid, usually platinum) and fuel (H₂ gaseous) interact and is the most important region in a fuel cell, as it is where the electrochemical reaction occurs with the adsorption of the fuel (or oxygen) on the catalyst surface, electron transfer to form H⁺ and subsequent conduction of the generated ions to the ionomer for transport across the membrane. This is because experimentally only a few very general parameters, such as temperature, humidity or fuel flow rate, can be modified, and each of these parameters affects all components of the fuel cell and not just the three-phase region so it is impossible to separate the contributions corresponding to the three-phase boundary from the effects occurring, for example, in the membrane or from the kinetic effects in catalysis. Therefore, understanding, characterizing, and optimizing the variety of factors that affect the TPB content in fuel cells provide excellent opportunities for performance enhancement.

9:45am SS+CA+LS-TuM-8 Mechanism of Activity Decrease in Orr on Nitrogen-Doped Carbon Catalysts Based on Acid-Base Equilibrium, Kenji Hayashida, R. Shimizu, Tsukuba University, Japan; J. Nakamura, M. Isegawa, Kyushu University, Japan; K. Takeyasu, Hokkaido University, Japan

Fuel cells, which use the energy carrier hydrogen directly as a fuel, are important devices for achieving carbon neutrality. However, current fuel cell catalysts use a large amount of platinum, therefore a fuel cell catalyst that can replace platinum in the future is essential. A plausible candidate is nitrogen-doped carbon catalysts, which are durable and abundantly available. However, their activity is very low in acidic media, a practical condition, and this is the biggest challenge to overcome. In this study, we focused on the acid-base equilibrium of pyridinic nitrogen (pyri-N), the active site of nitrogen-doped carbon-based catalysts, to elucidate the reaction mechanism and clarify the mechanism of reduced activity in acidic media. Using a model catalyst with pyri-N-containing molecules adsorbed on a carbon support, we observed the change in electronic state upon immersion in electrolyte and application of potential, and analyzed the kinetics of the activities. It was found that the pyri-N, which is the active site, becomes protonated and hydration-stabilized in the acidic electrolyte,

¹ AVS National Student Award Finalist

² SSD Morton S. Traum Award Finalist

Tuesday Morning, November 5, 2024

resulting in a decrease in activity. In particular, kinetic analysis showed that the 2 or 2+2 electron pathway via H_2O_2 proceeds independently of the acid-base equilibrium. X-ray photoelectron spectroscopy revealed that the potential for the formation of pyri-NH, associated with oxygen adsorption, an important reaction intermediate, is 0.4 V lower in acidic than in basic conditions. This is due to the formation of pyri-NH⁺, in which pyri-N is protonated by acid-base equilibrium and its stabilization by hydration lowers the pyri-NH formation potential, resulting in lower activity in acidic conditions. Therefore, to improve catalytic activity in acidic conditions, it is important to increase the redox potential of this pyri-NH formation. A possible guideline is to decrease the pK_a and impart hydrophobicity.

11:00am **SS+CA+LS-TuM-13 Particle Size Effect of Ru Nanocatalyst for Nitrate Electroreduction**, *Zhen Meng, K. Shi, Z. Ren, X. Feng*, University of Central Florida

Electrochemical nitrate reduction reaction (NO_3RR) shows great promise for the recycling of nitrate from wastewater sources for the denitrification of wastewater and sustainable NH_3 production. Among various catalytic materials, Ru shows a high activity and selectivity for the NO_3RR to NH_3 , while the effect of Ru atomic structure and active sites on the NO_3RR activity and selectivity remains ambiguous. Here, we prepare size-controlled Ru nanoparticles ranging from 2.2 to 7.1 nm and investigate the dependence of the NO_3RR on the Ru particle size. The activity (current density) decreases along with the increase of Ru particle size, mainly due to the more Ru surface area for the smaller particles, given the same Ru loading. In contrast, the specific (Ru-surface-area-normalized) activity for the NO_3RR exhibits a volcano-shaped dependence on the particle size, with 4.9-nm Ru nanoparticles showing the highest activity, which should reflect their intrinsic activity and active sites. On the other hand, the specific activity for the competing hydrogen evolution reaction (HER) increases with the particle size, so that an optimal selectivity for NO_3RR to NH_3 is also reached on the 4.9-nm Ru nanoparticles. Looking into the size-dependent ratio of Ru surface sites, we find that the superior activity of 4.9-nm Ru nanoparticles correlates with the surface population of the D_5 step site, which favors the adsorption of NO_3RR reaction intermediate as compared to other surface sites. This work is supported by the National Science Foundation (NSF) Chemical Catalysis Program under Grant No. 1943732.

11:15am **SS+CA+LS-TuM-14 Probing Solvation with Liquid Jet Photoelectron Spectroscopy**, *Jared Bruce, S. Faussett, R. Woods*, University of Nevada, Las Vegas; *K. Zhang*, MIT; *A. Haines, F. Furche*, University of California Irvine; *R. Seidel*, Helmholtz Zentrum Berlin, Germany; *B. Winter*, Fritz-Haber-Institut der Max-Planck-Gesellschaft, Germany; *J. Hemminger*, University of California Irvine

The local chemical structure around solutes in aqueous solution is challenging to characterize on a molecular scale given the amount of hydrogen bonding interactions that occur in solution. Liquid jet photoelectron spectroscopy (LJ-XPS) can be a critical tool providing valuable chemical information both near the surface and in the bulk of the solution.

In this talk I will discuss how a combination of liquid jet photoelectron spectroscopy and electronic structure calculations were used to investigate the local chemical solvation of two systems – Fe^{2+} and acetic acid aqueous solutions. Each system has specific interfacial behavior that was investigated with liquid jet photoelectron spectroscopy. Fe showed coordination events with small anions like Cl^- alter the relative concentration of both species near the interface, whereas acetic acid shows alterations to its local solvation environment as a function of both the proximity to the interface and the pH of the bulk solution. Each will be discussed in detail and recent work from the lab at UNLV will be highlighted.

Tuesday Afternoon, November 5, 2024

2D Materials

Room 122 - Session 2D+LS+NS+SS-TuA

Electronics Properties

Moderators: Masa Ishigami, University of Central Florida, Slavomir Nemsak, Advanced Light Source, Lawrence Berkeley National Laboratory

2:15pm **2D+LS+NS+SS-TuA-1 NanoARPES for the Study of 2D Materials, Aaron Bostwick**, Advanced Light Source, Lawrence Berkeley National Laboratory **INVITED**

Angle-resolved photoemission spectroscopy (ARPES) is the premier technique for the determination of the electronic bandstructure of solids, and has found wide application for many classes of materials, such as oxides, semiconductors, metals, and low-dimensional materials and surfaces. Among the important topics it addresses are the underlying many-body interactions that determine the ground and excited state functionalities of all materials. Recently the development of nanoARPES using microfocused x-ray beams has opened ARPES to a wider class of samples and enabled the measurement of 2D devices *in-situ* with applied electric fields, currents, strain and femtosecond laser pulses to the samples. In this talk I will give an introduction to the ARPES technique, the MAESTRO facility and share some of our recent work on the bandstructure and many-body interactions in 2D heterostructures of chalcogenides, graphene, and boron nitride and light induced metastable phases in 1T-TaS₂.

2:45pm **2D+LS+NS+SS-TuA-3 Observation of Interlayer Plasmon Polaron in Graphene/WS₂ Heterostructures, S. Ulstrup**, Aarhus University, Denmark; *Y. Veld*, Radboud University, Netherlands; *J. Miwa*, Aarhus University, Denmark; *K. McCreary*, *J. Robinson*, *B. Jonker*, Naval Research Laboratory; *S. Singh*, Carnegie Mellon University, USA; *R. Koch*, *E. Rotenberg*, *A. Bostwick*, *C. Jozwiak*, Advanced Light Source, Lawrence Berkeley National Laboratory; *M. Rosner*, Radboud University, Netherlands; *Jyoti Katoch*, Carnegie Mellon University, USA

Van der Waals heterostructures offer us exciting opportunity to create materials with novel properties and exotic phenomena such as superconductivity, bound quasiparticles, topological states as well as magnetic phases. In this talk, I will present our work on directly visualizing the electronic structure of graphene/WS₂/hBN heterostructure using micro-focused angle-resolved photoemission spectroscopy (microARPES). Upon electron doping via potassium deposition, we observe the formation of quasiparticle interlayer plasmon polarons in graphene/WS₂ heterostructure due to many-body interactions. I will discuss that such low-energy quasiparticle excitation is important to consider as they can have huge implications on the electronic and optical properties of heterostructures based on 2D transition metal dichalcogenides.

3:00pm **2D+LS+NS+SS-TuA-4 Harnessing the Synergy of X-ray Photoelectron Spectroscopy (XPS) and Argon Cluster Etching for Profound Analysis of MoS₂ and Graphene, Jonathan Counsell**, Kratos Analytical Limited, UK; *C. Maffitt*, *D. Surman*, Kratos Analytical Inc.; *L. Soomary*, *K. Zahra*, Kratos Analytical Limited, UK

Understanding the intricate properties of two-dimensional (2D) materials such as MoS₂ and graphene is pivotal for advancing their applications across diverse fields. However, achieving comprehensive characterization at the nanoscale requires advanced analytical techniques. This study explores the synergistic potential of X-ray Photoelectron Spectroscopy (XPS) coupled with Gas Cluster Ion Source (GCIS) etching and depth profiling to delve deeper into the structural and electronic intricacies of MoS₂ and graphene.

By integrating XPS with GCIS etching, we not only discern the elemental composition, chemical bonding, and electronic states of these materials with exceptional precision but also unravel their depth-dependent characteristics. The incorporation of GCIS etching facilitates controlled removal of surface layers, enabling depth profiling to uncover buried interfaces, defects, and contamination effects that influence spectral results.

The combined approach allows for the characterization of MoS₂-graphene heterostructures, providing insights into interfacial interactions and electronic coupling mechanisms. Through systematic analysis, we demonstrate the complementary advantages of XPS and GCIS etching in elucidating the structural and electronic complexities of 2D materials.

The integration of GCIS etching with XPS not only enhances the depth resolution and sensitivity of the analysis but also offers a deeper understanding of the nanoscale landscape of MoS₂, graphene, and their heterostructures. This multidimensional approach accelerates the

development of tailored devices and applications based on 2D materials, propelling advancements in nanotechnology and beyond.

4:00pm **2D+LS+NS+SS-TuA-8 Manipulation of Chiral Interface States in a Moiré Quantum Anomalous Hall Insulator, Tiancong Zhu**, Purdue University **INVITED**

Quantum anomalous Hall (QAH) effect reflects the interplay between magnetism and non-trivial topology characterized by integer Chern numbers, which is expressed by chiral edge states that carry dissipationless current along sample boundaries. The recent discovery of QAH effect in van der Waals moiré heterostructures provides new opportunities in studying this exotic two-dimensional state of matter. Specifically, magnetism in these moiré QAH systems is induced by orbital motion of electrons, which allows full electrical control of the magnetic and the corresponding topological state. In this talk, I will discuss our recent scanning tunneling microscopy and spectroscopy (STM/STS) measurements on twisted monolayer-bilayer graphene (tMBLG), where QAH effect with gate-switchable Chern numbers have been observed previously in transport measurement. First I will discuss local scanning tunneling spectroscopy measurements on the correlated insulating states at $\nu = 2$ and $\nu = 3$ electrons per moiré unit cell, where the $\nu = 3$ state shows a total Chern number of ± 2 . Under a small magnetic field, the sign of Chern number at the $\nu = 3$ states can be switched by changing the local carrier concentration with gating, which is a result of competition between bulk and edge orbital magnetization of the QAH state.¹ The observation of a gate-switchable Chern number provides us an opportunity to directly visualize the chiral edge state in a moiré QAH insulator for the first time, which I will show through gate-dependent STS measurement and dI/dV mappings.² I will also demonstrate the capability to manipulate the spatial location and chirality of the QAH edge state through controlling the local carrier concentration with the STM tip.

¹ C. Zhang, T. Zhu et al., Nature Communications, 14, 3595 (2023)

² C. Zhang, T. Zhu et al., Nature Physics (2024)

4:30pm **2D+LS+NS+SS-TuA-10 Scanning Tunneling Microscopy and Spectroscopy of Single Layer NiTe₂ on Au, Stephanie Lough**, University of Central Florida; *M. Ishigami*, University of Central Florida

Previous angle-resolved photoemission studies [1, 2] have shown that NiTe₂ is a type II Dirac material that possesses a Dirac point very close to the Fermi level. In addition, the material has a topological surface state which can be valley spin-polarized. A recent study [3] has shown that this state can be exploited to develop Josephson diodes with potential applications as memory devices which can be coupled to qubits. There has been a significant interest [3-5] in studying properties of single layer NiTe₂ due to its strong interlayer coupling in bulk via Te p_z orbitals.

In this talk, we will discuss the properties of single layer NiTe₂ on Au generated by gold-assisted exfoliation measured using low temperature scanning tunneling microscopy and spectroscopy. We find that this interface possesses rectangular lattice with periodicities that are different from bulk NiTe₂ or Au (111) by over 30%. Tunneling spectra reveals strong coupling between NiTe₂ and Au (111). We compare these results recent theoretical calculations [6] on strained NiTe₂ and its impact on topological surface states.

1. Ghosh, S., et al., *Observation of bulk states and spin-polarized topological surface states in transition metal dichalcogenide Dirac semimetal candidate NiTe₂*. Physical Review B, 2019. **100**.

2. Mukherjee, S., et al., *Fermi-crossing Type-II Dirac fermions and topological surface states in NiTe*. Scientific Reports, 2020. **10**(1).

3. Pal, B., et al., *Josephson diode effect from Cooper pair momentum in a topological semimetal*. Nature Physics, 2022. **18**(10): p. 1228-+.

4. Zhao, B., et al., *Synthetic Control of Two-Dimensional NiTe Single Crystals with Highly Uniform Thickness Distributions*. Journal of the American Chemical Society, 2018. **140**(43): p. 14217-14223.

5. Zheng, F.P., et al., *Emergent superconductivity in two-dimensional NiTe crystals*. Physical Review B, 2020. **101**(10).

6. Ferreira, P.P., et al., *Strain engineering the topological type-II Dirac semimetal NiTe*. Physical Review B, 2021. **103**(12).

4:45pm **2D+LS+NS+SS-TuA-11 Nanoscale heterogeneities at Transition Metal Dichalcogenide-Au Interfaces, Taisuke Ohta, A. Boehm, A. Kim, C. Spataru, K. Thuermer, J. Sugar**, Sandia National Laboratories; *J. Fonseca Vega*, *J. Robinson*, Naval Research Laboratory

Two-dimensional geometry renders unique screening properties in transition metal dichalcogenides (TMDs). Consequently, the electronic

Tuesday Afternoon, November 5, 2024

properties of TMDs are susceptible to extrinsic factors (*e.g.*, substrate, strains, and charge transfer), and display spatial nonuniformities. Thus, material combinations (*i.e.*, TMD, dielectrics, and metals) and their nuanced interactions need to be considered when designing TMD-based devices. Of particular importance are the interfaces with metallic contacts. Uncovering the origin of heterogeneities at TMD-metal interfaces and establishing strategies to control TMD-metal interfaces could enable engineering pathways for future applications. We show that the electronic structures of exfoliated WS₂-Au interfaces exhibit pronounced heterogeneity arising from the microstructure of the supporting metal. These electronic structure variations indicate spatially nonuniform doping levels and Schottky barrier height across the junction. Through examination using photoelectron emission microscopy, we reveal key differences in the work function and occupied states. With *ab initio* calculation, electron backscatter diffraction, and scanning tunneling microscopy, our measurements show distinct variations in excess of 100meV due to the crystal facets of Au. Additionally, when multilayer WS₂ and Au(111) facets are azimuthally aligned, strong interactions induce mechanical slippage of the interfacing WS₂ layer, with respect to the rest of the WS₂ layers, resulting in local stacking variations with an occupied state energy shift of 20-50meV. Finally, we employed oxygen plasma treatment of Au to fabricate homogenous TMD-Au interfaces while also tuning the electronic properties of the TMDs. Our findings illustrate that the electronic properties of TMDs are greatly impacted by the interface interactions at energy and length scales pertinent to electronics and optoelectronics.

The work at Sandia National Laboratories (SNL) was supported by LDRD program and the US Department of Energy (DOE), Office of Basic Energy Sciences, Division of Materials Sciences and Engineering (BES 20-017574). The work at the US Naval Research Laboratory was funded by the Office of Naval Research. SNL is a multi-mission laboratory managed and operated by National Technology and Engineering Solutions of Sandia, LLC, a wholly-owned subsidiary of Honeywell International, Inc., for the US DOE's National Nuclear Security Administration under contract DE-NA0003525. This paper describes objective technical results and analysis. Any subjective views or opinions that might be expressed in the paper do not necessarily represent the views of the US DOE or the US Government.

5:00pm **2D+LS+NS+SS-TuA-12 Xenon Trapping in Silica Nanocages Supported on Metal Powder, Laiba Bilal**, SBU; *A. Boscoboinik*, Brookhaven National Laboratory

Trapping of Xenon gas atoms in silica nanocages supported on metal powders (Ru and Co) is investigated by lab-based ambient pressure X-ray photoelectron spectroscopy (AP-XPS). Xenon, being a noble gas, has very low reactivity¹. This makes it useful for applications where chemical reactions are unwanted. The first use for Xenon was in flash lamps used in photography², and it is still used for this purpose today. It has wide applications, from its use in the cells of plasma television as a propellant in spacecraft that use ion propulsion³ to its various applications in the medical industry⁴.

Xenon occurs in slight traces within Earth, 1 part in 10 million by volume of dry air². Like several other noble gases, xenon is present in meteorites and manufactured on a small scale by the fractional distillation of liquid air. However, Xe's concentration in the earth's crust and the atmosphere are much lower than predicted, which is also known as the "missing Xenon paradox"⁵.

The Discovery of an effective way to trap and separate Xenon from other gases can have significant advantages. The presence of Xenon in nuclear fuel rods was partially responsible for the Chernobyl accident⁶. Consequently, the nuclear energy industry is also trying to imprint a way to control the release of Xe, produced during the nuclear fission of uranium. Characteristics of chemical interactions between Xe and metal surfaces have been observed and explained, also several low-energy electron diffraction studies at cryogenic temperatures have experimentally demonstrated an on-top site adsorption preference for Xe adatoms on metal surfaces⁷.

Prior studies on 2D silicate bilayers grown on metal supports at Brookhaven National Lab showed that these structures could irreversibly trap all noble gases larger than Ne⁸ at room temperature. The noble gas atoms were trapped within hexagonal prism-shaped silicate nanocages-like structures and could then be released by heating the materials to different temperatures, *i.e.*, Ar: 348 K, Kr: 498 K, Xe: 673 K, Rn: 775 K^{8,9}. Figure 1A illustrates the potential energy diagram for a noble gas atom getting trapped in a silica nanocage. It can be seen that the activated physisorption

mechanism that traps noble gas atoms has a high desorption energy barrier (E_{des}).

Figure 1B shows a silicate bilayer structure (side and top views), while Figure 1C shows a hexagonal prism nanocage, the building block of the bilayer structure.⁸ Since synthesizing such silicate bilayers is very expensive and time-consuming¹⁰ for practical purposes, my project focuses on developing and testing scalable silicate nanocage⁹ materials to trap noble gases, with especial focus on Xenon.

Surface Science

Room 120 - Session SS+CA+LS-TuA

Electrochemistry and Photocatalysis

Moderators: Jared Bruce, University of Nevada Las Vegas, Taku Suzuki, NIMS (National Institute for Materials Science), Japan

2:15pm **SS+CA+LS-TuA-1 Surface Sensitive Studies of the Electrolyte-Electrode Interface, Edvin Lundgren**, Lund University, Sweden **INVITED**

The electrified electrode electrolyte interface is notoriously difficult to study during electrochemical (EC) reactions. Most traditional surface science techniques are disqualified due to the use of electrons, on the other hand, several new in-situ experimental methods have been developed recently. Examples are Electro Chemical X-ray Photoelectron Spectroscopy (ECXPS), Scanning Tunneling Microscopy (STM), Atomic Force Microscopy (AFM), High Energy Surface X-Ray Diffraction (HESXRD) [4] and EC-IRAS [5].

In the first part of the talk, the corrosion of an industrial Ni base Ni-Cr-Mo alloy will be addressed. A comprehensive investigation combining several synchrotron-based techniques are used to study the surface region of a Ni-Cr-Mo alloy in NaCl solutions in situ during electrochemical polarization. X-Ray Reflectivity (XRR) and ECXPS were used to investigate the thickness and chemistry of the passive film. Grazing Incidence X-ray Diffraction (GIXRD) was used to determine the change in the metal lattice underneath the passive film. X-Ray Fluorescence (XRF) was used to quantify the dissolution of alloying elements. X-ray Absorption Near Edge Structure (XANES) was used to determine the chemical state of the dissolved species in the electrolyte. Combining these techniques allowed us to study the corrosion process, detect the passivity breakdown in situ, and correlate it to the onset of the Oxygen Evolution Reaction (OER) [6].

In the second part, an alternative approach to study the development of a model electro catalyst surface is presented. By using a combination of Grazing Incidence X-ray Absorption Spectroscopy (GIXAS) [7], 2D Surface Optical Reflectance (2D-SOR) [8] and Cyclic Voltammetry (CV) and a Au(111) electrode model surface, direct surface information during real-time CV can be obtained.

[1] S. Axnanda et al, *Sci. Rep.* **5** (2016) 9788.

[2] A. A. Gewirth, B. K. Niece, *Chem. Rev.* **97** (1997) 1129.

[3] K. Itaya, *Prog. Surf. Sci.* **58** (1998) 121.

[4] M. Ruge et al, *J. Electrochem. Soc.* **164** (2017) 608.

[5] T. Iwasita, F. C. Nart, *Prog. Surf. Sci.* **55** (1997) 271.

[6] A. Larsson et al, *Adv. Mat.* (2023) 230462.

[7] H. Abe, Y. Niwa, M. A. Kimura, *Phys. Chem. Chem. Phys.* **22** (2020) 24974.

[8] S. Pfaff et al, *ACS Appl. Mater. Interfaces* **13** (2021) 19530.

2:45pm **SS+CA+LS-TuA-3 Operando Studies of CO₂, CO and N₂ Catalytic Hydrogenation Reactions Investigated with Ambient Pressure XPS, Peter Amann**, Scienta Omicron, Germany

Some of the most essential catalytic reactions for our energy society is to reduce CO₂ to hydrocarbons and alcohols to be used as fuels and base chemical for the chemical industry. Furthermore, the catalytic reduction of N₂ to ammonia has been considered as one of the most important discoveries during the 20th century to produce fertilizers for a growing population. Despite an enormous effort in studying these catalytic reactions we are still lacking experimental information about the chemical state of the catalytic surface and the adsorbates existing as the reaction is turning over. X-ray photoelectron spectroscopy (XPS) is a powerful surface sensitive technique that can provide almost all essential chemical information and it has been developed to operate also in a few mbar of pressure with great success for probing oxidation catalytic reactions. Unfortunately, this pressure regime is too low for the hydrogenation reactions to turn over.

Tuesday Afternoon, November 5, 2024

Here we will present how Fischer-Tropsch, methanol and ammonia synthesis reactions on single crystal metal surfaces have been probed during operando conditions in the pressure range 100 mbar-1 bar using a specially engineered XPS system built at Stockholm University (1) and permanently located at the PETRA III synchrotron in Hamburg. The instrument is commercially available at Scienta Omicron (BAR XPS) and can vary the incidence angle of the X-rays allowing it to be either surface or bulk sensitive. Examples will be presented about the chemical state of Zn in Cu-Zn methanol (2) and of Fe in Fischer-Tropsch (3,4) and ammonia synthesis reactions (5) as well as the various adsorbates at different pressures and temperatures.

- (1) P. Amann et al. Rev. Sci. Instrum. **90**, 103102 (2019)
- (2) P. Amann et al. Science **376**, 603-608 (2022)
- (3) D. Degerman et al. J. Phys. Chem. C **128**, 13, 5542-5552 (2024)
- (4) M. Shipilin et al. ACS Catalysis **12**, 7609-7621 (2022)
- (5) C.M. Goodwin et al. Nature, **625**, 282-286 (2024)

3:00pm **SS+CA+LS-TuA-4 Understanding the Intrinsic Activity and Selectivity of Cu for Ammonia Electrosynthesis from Nitrate**, *Zhuanghe Ren, K. Shi, Z. Meng, X. Feng*, University of Central Florida

Electrocatalysis play a central role in the development of renewable energy technologies towards a sustainable future, such as the recycling of nitrate from wastewater sources. The concentration of nitrate (NO_3^-) in ground water, rivers, and lakes has been increasing due to the excessive use of agricultural fertilizers and the discharge of industrial wastewater, which has caused severe environmental problems such as eutrophication. Electrochemical reduction of nitrate to ammonia has emerged as a promising route for the recycling of nitrate from wastewater and sustainable ammonia production when powered by renewable electricity. Here I present our recent study of Cu catalyst for nitrate electroreduction, with a focus on its intrinsic activity and selectivity. Using polycrystalline Cu foils for benchmarking, we elucidated the impact of often overlooked factors on nitrate reduction, including Cu facet exposure, nitrate concentration, and electrode surface area. We find that an electropolished Cu foil exhibits a higher activity and selectivity for nitrate reduction to ammonia than a wet-etched Cu foil, benefiting from a greater exposure of Cu(100) facets that are more favorable for the reaction. While the NH_3 selectivity shows no apparent dependence on the nitrate concentration, it increases with Cu electrode area, which is attributed to a promoted conversion of intermediately produced NO_2^- to NH_3 on a larger electrode. Based on the understandings, we developed a modified Cu foil electrode with increased Cu(100) facets and surface area, which enhanced the NO_3^- RR activity by ~50% with a NH_3 Faradaic efficiency of 91% at -0.2 V vs RHE.

This work is supported by the National Science Foundation (NSF) Chemical Catalysis Program under Grant No. 1943732.

References:

- (1) Ren, Z.; Shi, K.; Feng, X. Elucidating the intrinsic activity and selectivity of Cu for nitrate electroreduction. *ACS Energy Lett.* **2023**, *8*, 3658-3665.

3:15pm **SS+CA+LS-TuA-5 Insights Into Photocatalytic Reduction Activities of Different Well-Defined Single Bulk Crystal TiO_2 Surfaces in Liquid**, *Olawale Ayode, W. Lu, H. Zhu, Z. Zhang*, Baylor University

Understanding the activity of TiO_2 photocatalysts is crucial for designing and optimizing efficient photocatalysts, requiring a fundamental understanding of the photooxidation and photoreduction activities of different TiO_2 crystal facets. Although photoreduction activities on several TiO_2 crystal facets have been extensively studied in reactor or ultra-high vacuum environments, studies of well-defined TiO_2 crystal facets in a liquid environment are still lacking. In this study, the photocatalytic reduction activities of resazurin (RZ) were investigated using well-defined bulk single-crystal anatase (001), anatase (101), rutile (001), and rutile (110) facets. The experiment used a liquid cell containing RZ solution and TiO_2 crystal. A lab-built Raman microscope monitored the photoluminescence (PL) spectra of RZ under UV irradiation. We observed an increase in peak intensity at 583 nm and a decrease at 630 nm in the PL spectra of the solution on the TiO_2 crystal facets upon UV illumination, suggesting a conversion from RZ to its product, resorufin (RS). Given that both RZ and RS have distinctive peaks, we used their ratios to estimate their concentrations. This enabled us to assess the conversion rate and reaction rate of the crystals. Our results show that rutile had significantly higher conversion rates and faster reaction rates than anatase for RZ reduction. Rutile (110) had conversion rates about four times greater, and rutile (001) about three times greater than anatase. Rutile (110) reaction rates were about 1.5 times faster than rutile (001) and

significantly faster than anatase (101) & (001). Further evaluation of the photoreactivity was conducted using pseudo-order kinetics to determine the rate constant. The significant difference observed in rates between the rutile and anatase phases highlights the successful migration of electrons to the surface of the rutile crystal compared to the anatase surface, emphasizing the importance of crystal structure. The difference observed between rutile (001) and rutile (110) (as well as anatase facets 001 and 101) shows the effect of surface structure on photocatalytic activity. To advance the development of effective TiO_2 -based photoreduction materials, we explored plasmon-assisted photoreactions. We have studied the impact of Au nanoparticles on the reactivity of the aforementioned TiO_2 facets. This study will involve modulating hot electron generation and increasing electric fields to better understand their effects on photoreactivity.

4:00pm **SS+CA+LS-TuA-8 Selectivity Control by Ionic Liquid Layers: From Surface Science to the Electrified Interface**, *Joerg Libuda*, Friedrich-Alexander-Universitaet Erlangen-Nuernberg, Germany **INVITED**

Recently, the concept of "Supported Catalysts with Ionic Liquid Layer" (SCILL) has attracted much attention in heterogeneous catalysis and electrocatalysis. In the SCILL concept, a heterogeneous catalyst is impregnated with a thin layer of ionic liquid (IL) that serves as a catalytic modifier. In this presentation, we will give an overview of selected surface science and electrochemical surface studies on the origin of this selectivity control.

In the surface science studies, we investigated the growth, wetting behavior, structure formation and thermal behavior of various ILs on a wide range of model catalysts (Pt, Pd and Au single crystal surfaces and supported nanoparticles) using scanning tunneling microscopy (STM), atomic force microscopy (AFM) and infrared reflection absorption spectroscopy (IRAS). We were able to show that most ILs form a strongly interacting wetting layer with a high degree of intrinsic structural flexibility. Depending on the conditions, 2D glassy or different crystalline wetting layers are formed, in which the molecular orientation is dynamic and allows the embedding of reactants and thus the modification of the reaction environment.

In our electrochemical surface science studies, we investigated the interaction of selected imidazolium-based ILs with reactive and non-reactive single-crystal electrodes (Au, Pt). Using electrochemical IRAS (EC-IRRAS), we monitored the potential-dependent adsorption of IL ions on the electrode and used electrochemical STM (EC-STM) to investigate the effects of the ILs on the electrode structure. We used the selective oxidation and reduction of hydrocarbon oxygenates as test reactions. For the selective electrooxidation of 2,3-butanediol (a very structure-sensitive reaction at Pt electrodes), we were able to show that small additions of specific ILs (e.g. $[\text{C}_2\text{C}_2\text{Im}][\text{OTf}]$) have a large effect on selectivity (e.g. on C-C bond cleavage and selectivity towards the two partial oxidation products acetoin and diacetyl). We attribute these effects to the possible adsorption of the IL anions on the Pt surfaces.

Our results rationalize the origin of selectivity control by IL coatings in heterogeneous catalysis and demonstrate the potential of ILs for selectivity control in electrocatalysis.

- [1] R. Eschenbacher et al., J. Chem. Phys. Lett. **12**, 10079 (2021)
- [2] T. Yang et al., Angew. Chem. Int. Ed. **61**, e202202957 (2022)
- [3] M. Kastenmeier et al., J. Phys. Chem. C **127**, 22975 (2023)
- [4] H. Bühlmeier et al., Chem. Eur. J., in press (2024), DOI10.1002/chem.202301328
- [5] Y. Yang et al., J. Phys. Chem. C, accepted for publication (2024)

4:30pm **SS+CA+LS-TuA-10 Area Selective Atomic Layer Deposition for Spatial Control of Reaction Selectivity on Model Photocatalysts**, *Wilson McNeary*, National Renewable Energy Laboratory; *W. Stinson*, Columbia University; *W. Zang, M. Waqar, X. Pan*, University of California Irvine; *D. Esposito*, Columbia University; *K. Hurst*, National Renewable Energy Laboratory

Photocatalytic water splitting holds great potential in the pursuit of the U.S. Department of Energy's Hydrogen Shot initiative to bring the cost of H_2 to \$1/kg by 2031. A key challenge in the development of photocatalysts is increasing their overall solar-to-hydrogen efficiency by enhancing charge separation yields and redox selectivity. In this work, we use area selective ALD of oxide films (e.g., TiO_2 and SiO_2) to develop tunable interphase layers for selective oxidation and reduction reactions on a single substrate. This presentation details initial synthesis and characterization of monometallic Pt- and Au-based planar thin film electrodes in which Au regions were deactivated towards ALD growth through self-assembled thiol monolayers.

Tuesday Afternoon, November 5, 2024

The efficacy of thiols in suppressing ALD growth was assessed through ellipsometry, X-ray photoelectron spectroscopy (XPS), and cyclic voltammetry. A patterned planar sample comprised of interdigitated arrays of Au and Pt, used as a surrogate for a photocatalyst particle containing two different co-catalysts, was exposed to ALD growth and removal of the inhibitor species. Area selectivity of the ALD coatings on the patterned substrates was evaluated through cross-sectional scanning transmission electron microscopy with energy dispersive X-ray spectroscopy (STEM-EDS). Scanning electrochemical microscopy (SECM) was then used to probe the local activity of different regions of the patterned surface towards the hydrogen evolution reaction (HER) and iron oxidation and correlated with the ionic and e⁻ blocking effects of the area selective ALD coating. We will also detail the application of these findings to the ongoing development of 3D, particle-based photocatalysts

4:45pm SS+CA+LS-TuA-11 Titanium-Based Catalysts for CO₂ Activation: Experimental Modelling of Hybrid (Photo-)Catalysts, N. Kruse, J. Klimek, C. Groothuis, Lars Mohrhusen, University of Oldenburg, Germany

Conversion of greenhouse gases and especially CO₂ into useful hydrocarbons via a low-cost route is among the major challenges of the current energy transition. For this purpose, photocatalysis may be a relevant technology, as sunlight is a free and unlimited energy source, and photoreactions usually do not require high temperatures. Oxide-based photocatalysts usually consist of a semiconducting oxide support with nanostructured (noble) metal particles.¹ Unfortunately, these metals are often expensive and have limited lifetimes due to for example sintering, coking or poisoning with carbon monoxide. Thus, for several reasons, it is attractive to develop strategies to replace noble metal in such systems.²

Titanium is one of the few elements, that are attractive in terms of its natural availability and considering various economic and ecological aspects. Titanium dioxide (TiO₂) for example offers a broad platform, as e.g. defects such as Ti³⁺ interstitials can boost the photocatalytic activity towards oxygen containing molecules.^{3,4} TiO₂ also readily forms hybrid systems with other oxides (e.g. WO₃ clusters)⁴ or sulfides such as MoS₂.⁵ Thus, we investigate titanium-based hybrid photocatalytic systems using well-defined model catalysts under ultrahigh-vacuum conditions.

Herein, we present selected results from well-defined model catalysts en route to the desired Ti-based hybrid materials, for example, nanostructured combinations of TiS₂ and TiO₂. TiS₂ has a broad light absorbance throughout the visible range, is easily reduceable and widely inert to CO poisoning, rendering it an attractive material. Our multi-method approach involves combinations of spectroscopy (esp. photoelectron spectroscopy (XPS)), microscopy (scanning tunneling microscopy (STM)) and reactivity studies (temperature-programmed desorption (TPD)). As one example, nanoparticles of TiS₂ as a classic 2D TMDC can be fabricated and studied on various substrates to derive an atomic-level understanding of structure-reactivity relationships.

References

- [1] Linsebigler, Lu, Yates: Chem. Rev. **95**, 735-758 (1995).
- [2] Shen et al. Solar RRL **4**, 1900546 (2020).
- [3] Mohrhusen, Al-Shamery Catal. Lett. **153**, 321-337 (2023).
- [4] Mohrhusen, Kräuter, Al-Shamery PCCP **21**, 12148-12157 (2021).
- [5] Kibsgaard et al., J. Catal. **263** 98-103 (2009).

5:00pm SS+CA+LS-TuA-12 Tracking the Ultrafast Dynamics of a Photoinduced Reaction at the Surface of a Reactive Semiconductor: CH₃I Photoinduced Reaction on TiO₂ (110) Surface, A. Gupta, University of Central Florida; T. Wang, University of Washington; K. Blackman, C. Smith, University of Central Florida; X. Li, University of Washington; Mihai E. Vaida, University of Central Florida

The detection of intermediate species during surface photoinduced reactions and the correlation of their dynamics with the properties of the surface is crucial to fully understand and control heterogeneous reactions. In this study, a technique that combines time-of-flight mass spectrometry with laser spectroscopy and fast surface preparation with molecules is employed to investigate the mechanism of photoinduced CH₃I reactions on a TiO₂(110) surface through the direct detection of intermediate species and final products. On a freshly prepared TiO₂(110) surface, the photoinduced reaction dynamics of CH₃I follows similar trends observed on other metal oxide surfaces.^{1,2} Specifically, the pump laser pulse at 266 nm excites the CH₃I molecule into the dissociative A-band, which leads to the formation of CH₃ and I intermediates that can further react to form I₂ and reform the CH₃I molecule. Subsequently, the probe laser pulse ionizes the

intermediate and final products, which are detected by a mass spectrometer as a function of the pump-probe time delay. The minimum dissociation time of CH₃I obtained by monitoring the CH₃⁺ fragment, which is 110 fs, and the fast rise of the CH₃⁺ signal, indicates that CH₃I is adsorbed on pristine TiO₂(110) with I atom facing the surface. A fraction of the I atoms produced on a freshly prepared TiO₂(110) are trapped on the surface. On this TiO₂(110) surface decorated with I atoms, the CH₃ fragment can react with CH₃I to form CH₃ICH₃, which leads to a completely different dynamics at the surface due to a change into the pump-probe schema. The evolution dynamics of CH₃⁺ and CH₃I⁺ after the CH₃ICH₃ photoexcitation will be discussed and compared with results obtained for CH₃I dosed on a freshly prepared TiO₂(110) surface.

1. M. A. K. Pathan, A. Gupta and M. E. Vaida, *J. Phys. Chem. Lett.*, **2022**, **13**, 9759-9765.
2. M. E. Vaida and T. M. Bernhardt, in *Ultrafast Phenomena in Molecular Sciences: Femtosecond Physics and Chemistry*, eds. R. de Nalda and L. Bañares, Springer International Publishing, Cham2014, pp. 231-261.

5:15pm SS+CA+LS-TuA-13 Kinetic Theory of Mixed-Potential-Driven Catalysis and the Experimental Proof, M. Yan, N. Namari, R. Arsyad, H. Suzuki, University of Tsukuba, Japan; J. Nakamura, Kyushu University, Japan; Kotaro Takeyasu, Hokkaido University, Japan

It has recently been suggested that thermal heterogeneous catalysis can also involve electrochemical processes, resulting in selectivity that is markedly different from that of conventional thermal catalysis. If the catalyst is conductive and a suitable electrolyte is present nearby, anodic and cathodic half-reactions may occur simultaneously on a single catalyst surface, forming a mixed potential. This reaction is characterized by the anode and cathode being exposed to the same reactant, unlike conventional fuel cells where different reactants are supplied to each electrode. Interestingly, mixed potentials have been reported to be involved in reactions with gas molecules, such as the formation of H₂O₂ and the oxidation of alcohol. These reports suggest that electrochemical processes play a role in controlling catalytic activity and selectivity without external energy. Catalysts based on mixed potentials are a promising new category of catalysts for both basic research and industrial applications, but the principles that determine their activity and selectivity are not yet fully understood.

We first report the theoretical framework of mixed-potential-driven catalysis, including exchange currents, as a parameter of catalytic activity. The mixed potential and partitioning of the overpotential were determined from the exchange current by applying the Butler–Volmer equation at a steady state far from equilibrium [1].

To prove the theoretical framework, we measured the short-circuit current in a model reaction system without applying an external potential to demonstrate electron transfer for enzyme-like glucose oxidation. Specifically, glucose oxidation includes paired electrochemical anodic glucose oxidation and cathodic oxygen reduction, as evidenced by the consistency between the predicted and measured mixed potentials in identical reaction environments. Therefore, it can be categorized as a mixed-potential-driven catalysis. We further demonstrated that the Gibbs free energy drop, as the total driving force, was partitioned into overpotentials to promote each half-reaction in the mixed-potential-driven catalysis. This driving force partitioning, which is controlled by catalytic activity, is a powerful tool for guiding the design of mixed-potential-driven catalytic systems [2].

[1] M. Yan, N. A. P. Namari, J. Nakamura, K. Takeyasu, *Commun. Chem.* **7**, 69 (2024).

[2] M. Yan, R. Arsyad, N. A. P. Namari, H. Suzuki, K. Takeyasu, *ChemCatChem*, accepted (2024).

Surface Science

Room 120 - Session SS+2D+AMS-WeM

On-Surface Synthesis: Atomic and Molecular Ensambling on Surfaces

Moderators: Irene Groot, Leiden University, The Netherlands, Nan Jiang, University of Illinois - Chicago

8:00am **SS+2D+AMS-WeM-1 On-surface Synthesis of Porous Graphene Nanoribbons**, T. Qin, Junfa Zhu, University of Science and Technology of China **INVITED**

The low-dimensional porous graphene nanomaterials might have intriguing electronic properties and open exciting possibilities in the field of functional materials. By using rationally designed precursor molecules, on-surface synthesis approach has emerged as a powerful platform for the synthesis of porous low-dimensional graphene-based nanostructures with atomic precision. In this presentation, we report our recent work on the synthesis of porous graphene nanoribbon and nanosheet on different metal surfaces. We have successfully synthesized the one-dimensional graphene nanoribbons (GNRs) containing periodic [14]annulene pores on Ag(111) and the two-dimensional graphene nanosheets containing periodic [30]annulene pores on Au(111), originating from a same precursor. Two distinct reaction pathways on the two surfaces were regulated by different thermodynamic and kinetic mechanisms. With the combination of the scanning tunneling microscopy, synchrotron radiation photoemission spectroscopy and density functional theory (DFT) calculations, we identified the reaction products, intermediates precisely, and obtained insights into the reaction mechanism. On Ag(111), the formation of porous GNR is a thermodynamically favored pathway, by going through a flexible and reversible organometallic intermediate state. In contrast, on Au(111), because the debromination process is the rate-limiting step for the covalent coupling reaction and the generated covalent structures are irreversible, giving rise to the hierarchical formation of covalent chains and 2D porous nanosheet. The reaction mechanisms were confirmed by a series of control experiments, and the appropriate thermodynamic and kinetic parameters for optimizing the reaction pathways were proposed. Furthermore, DFT calculations revealed the influence of surface confinement on the band structures of these two nonplanar pores embed carbon materials, which enhances the conjugation of π -electrons thus shrinking the band gap.

8:30am **SS+2D+AMS-WeM-3 Tailoring Pt-Based Organometallic Nanomesh on Ag(111): A Model System for "Host-Guest" Chemistry**, V. Carreño-Díaz, A. Ceccatto, E. Ferreira, Abner de Siervo, University of Campinas (UNICAMP), Brazil

On-surface synthesis has been extensively used to produce complex functional nanostructures, such as Metal-Organic Frameworks (MOFs). MOFs are composed of highly ordered molecular structures, where metal adatoms act as connecting nodes, generating porous structures that exhibit a long-range order, offering a favorable environment for the adsorption and reaction of molecules in confined spaces, the so-called "host-guest" chemistry [2]. In the present work, we have studied the formation of bidimensional porous networks with hexagonal geometry (nanomesh) resulting from the combination of two molecular precursors: 1,3,5-tris[4-(pyridin-4-yl)-[1,1'-biphenyl]]benzene (TPyPPB) and dichloro-(1,10-phenanthroline)-platinum(II) (Cl_2PhPt), deposited on the surface of Ag(111). Our results reveal that when the TPyPPB molecules are deposited on the Ag(111) surface, they adopt a porous arrangement with triangular packing mediated by hydrogen bonds [3]. On the other hand, in the presence of the Cl_2PhPt molecule, the chemical interactions between both molecules change upon annealing at 400K, which leads to various ordering patterns before stabilizing in a network with hexagonal geometry. After dehalogenation, the Cl_2PhPt molecule is transformed into a new complex, PhPt, maintaining the Pt atom in its structure. The Cl atoms dissociated from the Cl_2PhPt precursor decorate the periphery of TPyPPB molecules. PhPt molecules can interconnect TPyPPB molecules through metallic coordination between the Pt atom and the N from the pyridyl group (N–Pt–N). The present investigation is based on room temperature scanning-tunneling microscopy (STM) measurements. This experimental approach allows us to explore the properties and structure of these materials at the atomic and molecular levels, opening new perspectives on the design and properties of MOFs.

Acknowledgments:

This work was financially supported by FAPESP (2022/12929-3), CNPq, and CAPES from Brazil.

1. Barth, J., Costantini, G. & Kern, K. Engineering atomic and molecular nanostructures at surfaces. *Nature* 437, 671–679 (2005).

2. Marta Viciano-Chumillas, et al. "Metal-Organic Frameworks as Chemical Nanoreactors: Synthesis and Stabilization of Catalytically Active Metal Species in Confined Spaces". *Accounts of Chemical Research* 53 (2020) 520–531.

3. Alisson C. dos Santos, Vanessa Carreño-Díaz, et al. "On-Surface Design of Two-Dimensional Networks through Nonmetal Atoms" (under preparation).

8:45am **SS+2D+AMS-WeM-4 Modulating the Reactivity of "Single-Atom Catalyst" Sites Within 2D Metal-Organic Frameworks by Small Structural Distortions**, Zdenek Jakub, CEITEC - Central European Institute of Technology, Czechia; J. Planer, D. Hruza, A. Shahsavar, P. Prochazka, J. Cechal, CEITEC, Czechia

Detailed atomic-scale understanding is a crucial prerequisite for rational design of next-generation single-atom catalysts (SACs). However, the sub-ångström precision needed for systematic studies is difficult to achieve on working SACs. We present a 2D metal-organic system featuring Fe- N_4 single-atom sites,^{1,2} in which the height of the atomically-defined structure is modulated by the 0.4 Å corrugation of the inert graphene/Ir(111) support. We show that the support corrugation significantly affects the system reactivity, as the sites above the support "valleys" bind TCNQ (tetracyanoquinodimethane) much stronger than the sites above the "hills".³ The experimental temperature stability of TCNQ varies by more than 60 °C on these seemingly identical sites. We expect that similarly strong effects of sub-ångström structural distortions will likely take place whenever large molecules interact with neighboring "single-atom catalyst" sites or when multiple reactants co-adsorb on such sites.

References

[1] Z. Jakub, A. Shahsavar, et al., *JACS*, **146**, 3471–3482 (2024)

[2] Z. Jakub, A. Kurowská, et al., *Nanoscale*, **14**, 9507-9515 (2022)

[3] Z. Jakub, J. Planer, et al., in preparation

9:00am **SS+2D+AMS-WeM-5 On-Surface Synthesis of Polycyclic Heteroatom-Substituted Nanocarbon Materials**, Willi Auwärter, Technical University of Munich, Germany **INVITED**

On-surface synthesis protocols provide elegant routes to individual molecular complexes, oligomers, and other nanocarbon materials on metal supports [1]. The resulting structural, physical, and chemical properties can be controlled by heteroatom-substitution.

In this talk, I will present an overview of our activities employing temperature-induced reactions on coveage metal supports in an ultrahigh vacuum environment, affording specific porphyrinoids and BN-substituted nanocarbon materials. On the one hand, routes to unsubstituted, square-type porphyrin tetramers [2] and peripherally O-doped porphyrins are addressed. On the other hand, dehydrogenation processes of borazine [3] and BN-functionalized carbon scaffolds will be discussed, in view of the synthesis and potential transfer of two-dimensional BNC materials.

[1] Grill, L.; Hecht S. *Nat. Chem.* **2020**, *12*, 115.

[2] Corral Rascon, E. *et al. J. Am. Chem. Soc.* **2023**, *145*, 967.

[3] Weiss, T. *et al.*, *Adv. Mat. Interfaces* **2024**, *11*, 2300774

9:30am **SS+2D+AMS-WeM-7 Atomic-Scale Investigation of the Highly Enantiospecific Decomposition of Tartaric Acid on Chiral Cu Surfaces**, Avery Daniels, C. Sykes, Tufts University

Enantioselectivity is the quintessential form of structure-sensitive surface chemistry, as differences in reactivity arise solely from the lack of mirror symmetry of the surface. Studying enantioselectivity on chiral surfaces provides insight into the design of enantioselective heterogeneous catalysts, which are important in pharmaceutical, agrochemical, and other industries. To determine the optimum surface facet for a given chemical reaction, it is essential to study the reaction on a wide variety of surface facets. Given the serial nature of surface science experiments on single crystals, high-throughput methods to study multiple facets at the same time would circumvent this issue. We have designed surface structure spread single crystals (S4Cs) that expose a vast variety of different surface facets on a single sample. Interestingly, a large portion of these facets are also chiral and therefore the use of S4Cs is ideal for studying for enantioselective surface chemistry. Tartaric acid decomposition on chiral Cu surfaces is known to be highly enantiospecific. With spatially resolved X-ray photoelectron spectroscopy (XPS), we have previously investigated the

Wednesday Morning, November 6, 2024

decomposition of tartaric acid on a Cu(110) ± 14o S4C where surfaces vicinal to Cu(14,17,2) were found to be the most enantiospecific. We have now combined these XPS results with scanning tunneling microscopy (STM) imaging to unveil the atomic-scale origins of the highly enantiospecific decomposition of tartaric acid on chiral Cu surfaces. We found extensive enantiospecific surface restructuring of surfaces vicinal to Cu(110) leading to the formation of facets vicinal to Cu(14,17,2). This reconstruction of the surface depends on both the TA enantiomer and the chirality of the surface itself, and is therefore enantiospecific. These results provide valuable insight into the origins of structure sensitivity for enantioselective reactions and demonstrate the efficacy of S4Cs in performing high-throughput surface science investigations.

9:45am **SS+2D+AMS-WeM-8 Competition between Hydrogen Bonding and van der Waals Interactions During Binary Self-Assembled Monolayer Formation**, *Rachael Farber, L. Penland, H. Hirushan, N. Dissanayake*, University of Kansas

Binary self-assembled monolayers (SAMs) comprised of polar and nonpolar molecules, such as 3-Mercaptopropionic Acid (MPA) and 1-Decanethiol (DT), offer the ability to carefully tune the interfacial properties of Au surfaces. The formation of molecularly precise binary SAMs through the displacement of one molecule with another *via* solution phase processing requires fine control over the structure and composition of the initial SAM. While DT has been extensively characterized using ultra-high vacuum (UHV) surface science techniques, the structural properties of MPA SAMs are less well understood. The relationship between solution phase processing procedures of MPA and island vacancy density, domain size, film uniformity, and the subsequent displacement behavior when exposed to DT, has not been established.

In this work, the effects of solution phase incubation temperature and time on MPA SAM formation and subsequent DT displacement behavior were determined using UHV scanning tunneling microscopy. Three MPA incubation procedures were studied: 3 hr MPA incubation at 35 °C (**MPA-1**), 3 hr MPA incubation at 25 °C (**MPA-2**), and 24 hr MPA incubation at 25 °C (**MPA-3**). While **MPA-1** and **MPA-2** both showed the characteristic MPA lattice, **MPA-1** had fewer domain boundaries and vacancy islands compared to **MPA-2**. **MPA-3**, which had the fewest domain boundaries and vacancy islands, showed regions of an MPA bilayer species across the surface. To determine the consequences of defect density and the presence of an MPA bilayer on DT displacement, **MPA-1**, **MPA-2**, and **MPA-3** were subsequently placed in a 2 μM DT solution for 20 min, 60 min, 3 hr, and 24 hr. **MPA-1** and **MPA-2** had comparable rates of DT displacement, with the formation of a high-density DT film across the surface within 3 hr. **MPA-3** had markedly slower DT displacement. Following a 24 hr incubation of **MPA-3** in the DT solution, small regions of the low-coverage, lying down phase (β) and 2-D gas phase (α) of DT were found across the surface. Only after a 48 hr incubation of **MPA-3** in DT did the high-density DT phase form. These results highlight the significance of the bonding interactions of the initial SAM on displacement kinetics during the formation of binary SAMs.

11:00am **SS+2D+AMS-WeM-13 Learning More with Less: High-Throughput Screening of Molecular Layer Deposition Processes**, *David Bergsman*, University of Washington **INVITED**

Because of its ability to deposit organic, inorganic, and hybrid ultrathin films with sub-nanometer thickness and compositional control, molecular layer deposition (MLD) has seen growing interest for use in technologies where precise interfacial control is essential, such as in semiconductor processing, membrane separations, and catalysis. However, development of these technologies is inhibited by the relatively slow process times for MLD vs atomic layer deposition and the large number of combinations of inorganic & organic reactants available to MLD.

This presentation will highlight the intrinsic advantages of accelerating MLD process development, both for technology development and for fundamental research. First, previous work in MLD process development will be highlighted, focusing on areas where comparisons between processes yielded fundamental insight into film growth phenomena. Then, an approach for rapidly screening new materials deposited by MLD using a custom-built, high-throughput, multiplexing MLD-style reactor will be discussed. In such a system, multiple reaction chambers are connected to shared reactants and pumping lines, allowing for the elimination of redundant reactor components and reducing capital costs compared to an equivalent number of independent systems. Finally, an example of how this approach can be applied to future technologies, such as EUV photolithography, will be given, demonstrating how materials made using

these parallel systems can be screened for their properties of interest and be used to obtain process-structure-property relationships.

11:30am **SS+2D+AMS-WeM-15 Organic Molecular Architectures Synthesized on Si(001) by Means of Selective Click Reactions**, *T. Glaser, J. Peters, Justus Liebig University Giessen, Germany; D. Scharf, U. Koert, Philipps University Marburg, Germany; Michael Dürr, Justus Liebig University Giessen, Germany*

The concept of molecular layer deposition on solid surfaces is promising for the synthesis of layers with well-controlled physical and physicochemical properties. Molecules with two functional groups are suitable building blocks for covalent layer-by-layer synthesis. However, with symmetric bifunctional organic molecules, i.e., with two identical functional groups at one molecule, side reactions which hinder the well-controlled layer-by-layer growth, e.g., by chain termination, may occur.

Here we solve this problem using a combination of two selective and orthogonal click reactions for controlled covalent layer-by-layer growth on Si(001). In order to do so, we combine ultrahigh-vacuum- (UHV)-based functionalization of the Si(001) surface with solution-based click chemistry for the attachment of the further layers. The starting point is the Si(001) substrate which is functionalized via selective adsorption of the bifunctional ethynylcyclopropylcyclooctyne (ECCO) molecule under UHV conditions [1]. This first-layer sample is then transferred into solution [2] in order to perform the subsequent layer-by-layer synthesis using the two orthogonal click chemistry reaction steps in an alternating fashion: First, a diazide is coupled in acetonitrile via a copper-catalyzed azide-alkyne click reaction; second, a layer of ECCO molecules is coupled via a catalyst-free, strain-promoted azide-alkyne click reaction. Without contact to ambient conditions, the samples are analyzed by means of X-ray photoelectron spectroscopy in UHV after each reaction step in solution; the N 1s spectra clearly indicated in the first step the selective click reaction of the primary azido group of the diazide molecule, whereas the tertiary azido group stayed intact. In the second step, this tertiary azido group was reacted selectively with the strained triple bond of the ECCO molecule in solution, forming a third layer of organic molecules on Si(001) with the terminal triple bond of ECCO available for further reactions according to this cyclic reaction scheme. Alternating application of the two orthogonal reaction steps then led to a well-controlled layer-by-layer growth up to 11 layers [3]; it opens the possibility for the controlled synthesis of layers with physical or physicochemical properties that alternate on the molecular scale.

[1] C. Länger, J. Heep, P. Nikodemiak, T. Bohamud, P. Kirsten, U. Höfer, U. Koert, and M. Dürr, *J. Phys.: Condens. Matter* 31, 34001 (2019).

[2] T. Glaser, J. Meinecke, C. Länger, J. Heep, U. Koert, and M. Dürr, *J. Phys. Chem. C* 125, 4021 (2021).

[3] T. Glaser, J. A. Peters, D. Scharf, U. Koert, and M. Dürr, *Chem. Mater.* 36, 561 (2024).

11:45am **SS+2D+AMS-WeM-16 Confinement Effects at Surfaces**, *J. Anibal Boscoboinik*, Brookhaven National Laboratory

Nanosized spaces at surfaces offer an interesting playground to understand the effect of confinement in chemistry and physics. Two examples will be described in this talk. In the first one, the water formation from hydrogen and oxygen is studied on a metal surface both in its bare state and also covered with a two-dimensional porous silicate. A change in reaction pathway is observed due to confinement effects. In the second example, nanosized silicate cages supported on a metal are shown to trap single atoms of noble gases through a new ionization-facilitated trapping mechanism. In this case, the gas phase species are first ionized. These ions can then enter the nanocages, at which point they get neutralized by an electron donated by the adjacent metal, resulting a neutral species that are kinetically trapped inside the confined space.

12:00pm **SS+2D+AMS-WeM-17 Facilitating CO₂ Capture Enabled by Weak Intermolecular Interactions Among CO₂, Water and PEEK-Ionene Membrane**, *Jennifer Yao, L. Strange, J. Dhas, PNNL; S. Ravula, J. Bara, University of Alabama; D. Heldebrant, Z. Zhu, PNNL*

Poly (ether ether ketone) (PEEK)-ionene membranes have shown significant potential for direct CO₂ capture due to their high selectivity, durability, and efficiency.¹ Despite their promise, the mechanisms of CO₂ transport through these membranes and the impact of water vapor on its CO₂ capture and diffusion remain poorly understood. Time-of-flight secondary ion mass spectrometry (ToF-SIMS) can detect and distinguish the characteristic molecular ions,^{2,3} making it an ideal tool for studying complex intermolecular interactions of the CO₂, water and the membrane. In this study, a combination of isotopic labeling and SIMS provides a unique

Wednesday Morning, November 6, 2024

method to track small molecules in organic matrixes at nanoscale. We investigated the interactions of PEEK-ionene membranes with $^{13}\text{CO}_2$ and D_2O using cryo ToF-SIMS. ToF-SIMS 3D imaging provided chemical mapping of the distribution of these species from the surface down to several micrometers into the membrane. The cryo ToF-SIMS data did not show any significant enhancement of the $^{13}\text{C}/^{12}\text{C}$ ratio, implying weak CO_2 -membrane interactions and CO_2 vaporization even at $-130\text{ }^\circ\text{C}$ in vacuum condition. In contrast, cryo ToF-SIMS revealed a relatively uniform distribution of D_2O within the heavy water-loaded membrane. This suggests that water-membrane interactions are stronger than CO_2 -membrane interactions. Additionally, the presence of D_2O in the membrane did not enhance $^{13}\text{CO}_2$ retention, indicating weak CO_2 - D_2O interactions and minimal impact of water vapor on CO_2 diffusion within membrane. For comparison, ToF-SIMS data demonstrated that $^{13}\text{CO}_2$ readily reacts with a basic Na_2CO_3 solution to form $\text{NaH}^{13}\text{CO}_3$, highlighting the potential for modifying CO_2 -membrane interactions via functional group modifications. Specifically, introducing basic functional groups may enhance CO_2 -membrane interactions, whereas acidic modifications may reduce them.

References:

1. K. O'Harra, I. Kammakakam, P. Shinde, C. Giri, Y. Tuan, E. M. Jackson and J. E. Bara, ACS Applied Polymer Materials, 2022, 4, 8365-8376.
2. L. E. Strange, S. Ravula, Z. Zhu, J. E. Bara, P. Chen, D. J. Heldebrant and J. Yao, Surface Science Spectra, 2024, 31.
3. L. E. Strange, D. J. Heldebrant, S. Ravula, P. Chen, Z. Zhu, J. E. Bara and J. Yao, Surface Science Spectra, 2024, 31.

Surface Science

Room 120 - Session SS+2D+AMS-WeA

Defects Nanoarchitecture and Complex Systems

Moderators: Dario Stacchiola, Brookhaven National Laboratory, Zhenrong Zhang, Baylor University

2:15pm SS+2D+AMS-WeA-1 Exploring ZIF-8 Vibrational Spectra with Its IR Peak Assignments and Defect Signal Characterization, Mueed Ahmad, Stony Brook University/Brookhaven National Laboratory; **R. Patel,** University of Minnesota; **D. T. Lee,** Stony Brook University/Brookhaven National Laboratory; **P. Corkery, A. Kraetz,** Johns Hopkins University; **P. Prerna,** University of Minnesota; **S. Tenney, D. Nykpanchuk, X. Tong,** Brookhaven National Laboratory; **J. Siepmann,** University of Minnesota; **M. Tsapatsis,** Johns Hopkins University; **J. Boscoboinik,** Stony Brook University/Brookhaven National Laboratory

Surface chemistry is critical in elucidating the functional properties of Zeolitic Imidazolate Framework-8 (ZIF-8), a versatile material with applications in gas separation, sensing, catalysis, and lithography. Comprising zinc that is tetrahedrally coordinated with 2-methylimidazolate (2mlm) linker, ZIF-8 is synthesized through various methodologies to modulate its crystalline characteristics and integration into nanocomposites including powder, film and membranes.

Despite efforts to achieve defect-free ZIF-8 structures, deviations in structure may occur due to the presence of defects such as vacancies in 2mlm ligands, zinc vacancies, and physically adsorbed 2mlm molecules within pores, substantially impacting its performance and stability. Infrared reflection absorption (IRRA) spectroscopy is employed to probe these defects, although interpretations of IR spectra vary across studies. Our investigation employs experimental IR spectroscopy alongside first-principles molecular dynamics (FPMD) simulations to scrutinize ZIF-8's vibrational spectra, with a specific focus on defect-induced signals. X-ray Photoelectron Spectroscopy (XPS) is utilized to probe the surface composition of the material up to a depth of 10 nanometers.

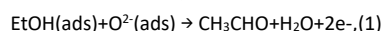
We have highlighted the prevalence of defects in the synthesis of ZIF-8 films/membranes, which are critical in gas separation applications. Notably, we observed the formation of SiO_x as a notable defect, stemming from exposure to silicon grease in vacuum reactors. This phenomenon is pertinent to materials synthesized under vacuum conditions, as vacuum grease residues may persist over time.

Through the resolution of conflicting interpretations of IR spectra and the identification of defect signals, our objective is to gain a comprehensive understanding to enhance the quality control and design of ZIF-8-based materials for diverse applications.

2:30pm SS+2D+AMS-WeA-2 Molecular Sensing ZnO Surfaces Studied by Operando Low-Energy Ion Beam Analysis, Taku Suzuki, Y. Adachi, T. Ogaki, I. Sakaguchi, National Institute for Materials Science, Japan

1. Introduction

The basic mechanism of the resistive gas sensing has been established; it is essentially a redox reaction of the surface mediated by the negatively charged oxygen adsorbate. For example, the sensing of ethanol (EtOH) with the ionosorbed oxygen of O²⁻ is written as,



where (ads) denotes an adsorbate. It is reasonable to assume that the gas sensing properties differ between crystallographic atomic planes. Indeed, the crystal plane dependent gas sensing response has been studied by many research groups in the last decade for EtOH sensing by ZnO, which is one of the most intensively studied target gas – sensing material combinations. The specific knowledge of the crystal plane dependence of gas sensing is useful for the development of sensing materials.

The ZnO crystal plane dependence of the gas sensing properties has typically been studied using a nanocrystal. However, the effect resulting from the contact between the particles has hindered straightforward interpretation. To overcome this problem, the ZnO crystal plane dependence of the EtOH sensing was investigated using an analytical approach in the present study, namely low-energy ion scattering spectroscopy (LEIS) combined with the pulsed jet technique.

2. Method: LEIS combined with pulsed jet

We applied a newly developed He⁺ LEIS combined with the pulsed jet technique to analyze the surface structure of ZnO during the EtOH sensing.

In this novel technique, the free gas jet is periodically blown onto the sample surface to simulate the gas sensing surface in a vacuum as one under the realistic working condition, while the background pressure is kept low enough for the operation of He⁺ LEIS.

The sample was ZnO single crystals with an atomically flat mirror-polished surface. Four dominant low-index surfaces, which are Zn-terminated (0001) (c+), O-terminated (0001) (c-), (10-10) (m), and (11-20) (a), were used to evaluate the crystal orientation dependent gas sensing properties.

References

- [1] N. Saito et al., Chemical Sensors 39(2023)108. (Japanese)
- [2] T. Suzuki et al., Surfaces and Interfaces 35(2022)102371.
- [3] T. Suzuki et al., Appl.Surf.Sci.538(2021)148102.

2:45pm SS+2D+AMS-WeA-3 Finding Surface Defects in Electronic Materials, Sujitra Pookpanratana, National Institute of Standards and Technology

INVITED

All electronic materials contain a wide range of defects ranging in length scales from point defects to micrometer (or sub-millimeter) scale features. Some defects can be beneficial, benign, or detrimental to the functionality of the material. It's critical to identify and locate defects, and determine their impact in the host material. Here, I will highlight the identification of defects and their impact in 2D graphene-based systems and wide bandgap semiconductors using photoemission electron microscopy (PEEM). PEEM is a nanoscale, surface-sensitive, full-field imaging technique based on the photoelectric effect. PEEM provides real space imaging of surfaces with enhanced contrast mechanism based on topographic and electronic properties, and measurement of electronic properties. In the first example, we image epitaxial graphene (EG) topography in real space and measure the electronic structure of monolayer EG regions with micrometer-scale angle resolved photoemission (μ -ARPES). We detect characteristic electronic features of graphene such as the Dirac points and the π -band, and the electronic flat band at region with different contrast [1]. Through Raman spectroscopy on the same regions that were analyzed by PEEM, and we estimated a significant amount of compressive strain ($\sim 1.2\%$) coinciding with the flat band region [1]. In the second example, we highlight the full-field PEEM capability by following the de- and re-intercalation of 2D Ag within EG under heating conditions. For the 2D Ag system, we find Ag clusters initially diffuse to the top EG surface and finally re-intercalate through defects with the Ag intercalation front to be $0.5 \text{ nm s}^{-1} \pm 0.2 \text{ nm s}^{-1}$ [2]. The EG defects serve as intercalation "doors." Lastly, we will show extended surface defects propagating through epitaxy GaN and β -Ga₂O₃ which also induce the presence of bandgap states.

- [1] F. Niefind, H. G. Bell, T. Mai, A. W. Hight Walker, R. E. Elmquist, S. Pookpanratana, J. Appl. Phys. 131, 015303 (2022).
- [2] F. Niefind, Q. Mao, N. Nayir, M. Kowalik, J. J. Ahn, A. Winchester, C. Dong, R. A. Maniyara, J. Robinson, A. van Duin, and S. Pookpanratana, Small 20, 2306554 (2024).

3:15pm SS+2D+AMS-WeA-5 SSD Morton S. Traum Award Finalist Talk: Silver Iodide – Surface Structure and Ice Nucleation Investigated by Noncontact AFM, Johanna Hütner¹, D. Kugler, Vienna University of Technology, Austria; **F. Sabath,** Bielefeld University, Germany; **M. Schmid,** Vienna University of Technology, Austria; **A. Kühnle,** Bielefeld University, Germany; **U. Diebold, J. Balajka,** Vienna University of Technology, Austria

Silver iodide (AgI) is used as a cloud seeding material due to its ability to nucleate ice efficiently, which is explained by the good lattice match between AgI and hexagonal ice. The basal (0001) cleavage plane of AgI deviates from the lattice of hexagonal ice by as little as 2.5%. However, AgI consists of stacked planes of positively charged Ag⁺ alternating with negatively charged I⁻. Cleaving a AgI crystal along the (0001) plane thus exposes Ag⁺ and I⁻ terminated surfaces. Both terminations are polar and inherently unstable.

We present atomically resolved noncontact atomic force microscopy (NC-AFM) images that show how AgI(0001) surfaces compensate for this non-zero electric dipole perpendicular to the surface. Both Ag and I terminated surfaces form reconstructions, whose structure affects their ice nucleating abilities. NC-AFM images of UHV cleaved surfaces exposed to water vapor reveal that ice forms an epitaxial layer only on the Ag terminated surface, whereas on the I termination ice forms three-dimensional clusters.

These atomic-level observations could enhance our understanding of ice formation processes in the atmosphere.

¹ SSD Morton S. Traum Award Finalist

Wednesday Afternoon, November 6, 2024

3:30pm **SS+2D+AMS-WeA-6 SSD Morton S. Traum Award Finalist Talk: Reversible Non-Metal to Metal Transition and Effective Debye Temperatures of Highly Crystalline NiFe₂O₄ Thin Films, Arjun Subedi¹, D. Yang, X. Xu, P. Dowben, University of Nebraska-Lincoln, USA**

The surface of NiFe₂O₄ thin film undergoes a conductivity change with temperature. X-ray photoelectron spectroscopy (XPS) of NiFe₂O₄ thin film at room temperature showed large binding energy shifts in Ni 2p_{3/2}, Fe 2p_{3/2}, and O 1s core levels, due to photovoltaic surface charging indicating that prepared NiFe₂O₄ thin film was dielectric or non-metallic at room temperature. The core level binding energy shifts, due to photovoltaic surface charging, were found to be around 5 eV for each of the core levels at room temperature. The core level binding energy shifts decreased when the thin film was annealed in vacuum. The XPS core level binding energy shifts from the expected values became negligible at an elevated temperature of 410 K and beyond. This suggests that NiFe₂O₄ thin film became metallic at the temperature of 410 K and beyond. When the sample cooled down to room temperature, the sample reversibly became more dielectric, showing again the same core level binding energy shifts of 5 eV. Such reversible phase change of the thin film was further supported by the reversible Fermi edge shift with temperature. Low energy electron diffraction (LEED) images, taken for the NiFe₂O₄ thin film surface, showed that the surface was highly crystalline throughout the reversible temperature controlled non-metal to metal transition. The XPS spectra of Ni 2p_{3/2}, Fe 2p_{3/2}, and O 1s core levels taken at different temperatures showed that the changes in core level binding energies followed a proposed Arrhenius-type model with temperature. The effective bulk Debye temperatures of 629.10 ± 58.22 K and 787.03 ± 52.81 K were estimated using temperature dependent intensities of Fe 2p_{3/2} and Ni 2p_{3/2} XPS spectra respectively indicative of different sites for Fe and Ni. The effective surface Debye temperature of 249.7 ± 11.1 K was estimated using temperature dependent intensities of LEED. Lower effective Debye temperature was observed for surface, as expected. The phase transition, the estimates of the effective Debye temperatures, and the model applied to the core level binding changes with temperature altogether shed light on the fundamental properties of the material with temperature.

4:15pm **SS+2D+AMS-WeA-9 In situ Structure Study of a MnOx-Na₂WO₄/SiO₂ Catalyst for OCM under Na₂WO₄ Melting Conditions, Yong Yang, ShanghaiTech University, China; D. Wang, E. Vovk, ShanghaiTech.edu.cn, China; Y. Liu, J. Lang, ShanghaiTech University, China**
MnO_x-Na₂WO₄/SiO₂ catalyst exhibited notable C₂ selectivity/yield in the oxidative coupling of methane (OCM), a promised green chemistry reaction^{1,2}. Nevertheless, the reaction mechanism of this catalyst remains a subject of contention, particularly regarding the role of Na₂WO₄ in the activation^{3,4}. In this study, *in situ* characterizations of a TiO₂-modified MnO_x-Na₂WO₄/SiO₂ catalyst, are conducted by XRD and XPS correlating to the OCM reaction condition, focusing on the simultaneous phase transition of catalyst components within its activation temperature zone. The online MS along with XPS/XRD coupled activity study confirm that transition from Mn³⁺ to Mn²⁺ stands as a pivotal factor influencing the reactivity. *In situ* XRD further revealed that in this narrow temperature window there is a particular three-step Na₂WO₄ phase change, ending as molten salt, right before the substantial Mn³⁺ to Mn²⁺ transfer initiated. In addition, the rarely observed Na₂WO₄ behavior as molten salt is obtained by *in situ* XPS with rapid spectra collected during an on-stage heating process. A sensitive self-reduction of the tungsten upon heating to melting point is found. These comprehensive *in situ* catalyst characterizations, covering the extensive structure-activity relationship from solid state to partial molten salt condition, providing an interlocking pathway for the reactive oxygen species transferring at high temperature. The results provide new important insight into the complex MnO_x-Na₂WO₄/SiO₂ catalyst as a key to understand the activation mechanism of NaWmSi catalyst in OCM.

[1] Lunsford JH, Catalytic conversion of methane to more useful chemicals and fuels: a challenge for the 21st century. *Catalysis today* 63 (2000) 165-174;

[2] Lunsford JH The Catalytic Oxidative Coupling of Methane. *Angewandte Chemie International Edition in English* 34 (1995) 970-980;

[3] Si J, Zhao G, Sun W, Liu J, Guan C, Yang Y, Shi XR, Lu Y Oxidative Coupling of Methane: Examining the Inactivity of the MnO_x-Na₂WO₄/SiO₂ Catalyst at Low Temperature. *Angewandte Chemie International Edition* 61 (2022) e202117201

[4] Fang X, Li S, Gu J, Yang D Preparation and characterization of W-Mn catalyst for oxidative coupling of methane. *J Mol Catal* 6 (1992) 255-261

4:30pm **SS+2D+AMS-WeA-10 Characterization of Nanoplastics Samples, T. Roorda, M. Brohet, S. Campos Jara, Irene Groot, Leiden University, Netherlands**

Plastic particles in the ocean have become a contaminant of emerging concern due to their damage to humans and marine animals. Of all plastic production, which is increasing still, it has been shown that more than 99% of plastic waste which ends up in the oceans cannot be accounted for. The belief is that all of this plastic degrades to a nano-sized scale which is extremely hard to detect. In order to understand the fate of nanoplastics in aquatic environments, we must have a better understanding of the degradation mechanisms at an atomic and chemical level. In this project, we have developed procedures to evaporate powdered materials and deposit them onto a prepared surface. The deposition of nanoplastics is confirmed by mass spectrometry, Auger electron spectroscopy, and X-ray photoelectron spectroscopy. Using atomic force microscopy combined with scanning tunneling microscopy, the deposited plastics are investigated.

We also investigate plastics samples after several degradation mechanisms, such as oxygenation, hydrogenation, UV exposure, and thermal annealing. After degradation, the plastics samples are studied in ultra-high vacuum with atomic force microscopy combined with scanning tunneling microscopy and with X-ray photoelectron spectroscopy.

4:45pm **SS+2D+AMS-WeA-11 Oxidation of NiCr and NiCrMo- Unraveling the Role of Mo with XPEEM Studies, Keithen Orson, D. Jessup, University of Virginia; W. Blades, Juniata College; J. Sadowski, Brookhaven National Laboratory; Y. Niu, A. Zakharov, Lund University, Sweden; P. Reinke, University of Virginia**

Nickel-chromium based superalloys combine good mechanical strength with excellent resistance to corrosion over a wide range of conditions. Passivity stems primarily from a thin layer of chromium oxides and hydroxides and increasing Cr content above a threshold of 11-15wt% results in a protective passive layer. Adding minor alloying elements like Mo has an outsized impact on corrosion resistance, but there is debate in literature over the mechanism of this action. To investigate the interplay of Cr concentration and Mo alloying, the early-stage oxidation (0-65 Langmuir of O₂) of Ni₂₂Cr, Ni₅Cr, and Ni₂₂Cr₆Mo were studied on a clean metal surface and moderate temperatures (450-500 °C). The oxidation was studied *in-situ* using x-ray photoelectron microscopy (XPEEM), which yields x-ray absorption hyperspectral images at 0, 5, 20, and 65 L of exposure, and a timeseries observing the oxide evolution from 0 to 65L at a single photon energy representative of Cr₂O₃. XPEEM valence band spectra, and conventional XPS study of the same samples complement the experiment. To analyze the ~10⁷ spectra produced by hyperspectral imaging, several data dimensionality reduction techniques including principal component analysis and non-negative matrix analysis were used to gain insight into the oxide evolution, the species present, and their spatial distribution. The amounts of each species present in the hyperspectral images were quantified using cosine similarity. Oxidation of Ni₂₂Cr produces islands of Cr₂O₃ along with a surface oxide, while on Ni₅Cr larger, sparser islands are observed. For both binary alloys the oxide grows in a layer-plus-island morphology. The oxide island chemistry of Ni₅Cr appears to include some NiO as well as Cr₂O₃. Ni₂₂Cr₆Mo, on the other hand, does not nucleate oxide islands visible with XPEEM but instead forms a continuous oxide layer whose thickness increases over time. This is commensurate with a layer-by-layer growth mode which is a significant advantage for protective function. This observation has implications for Mo's protective mechanism in the passive film, suggesting that Mo may be protecting from localized breakdown by altering the morphology of the oxide to produce a more uniformly protective oxide layer.

5:00pm **SS+2D+AMS-WeA-12 An Investigation of Local Distortions on High Entropy Alloy Surfaces, Lauren Kim, University of Wyoming; P. Sharma, Lehigh University; G. Balasubramanian, Lehigh University; T. Chien, University of Wyoming**

High entropy alloys (HEAs) are a widely studied family of materials that typically contain five or more elements. There are many combinations of elements that can create HEAs, and material properties can be tuned simply by changing elemental compositions. These properties of HEAs result in numerous applications, such as catalysis, energy storage, and aerospace engineering refractory materials. Severe-lattice-distortion is identified as one of the four core effects impacting the physical properties in HEAs. In this work, we demonstrate atomic resolution images of the surface of a CrMnFeCoNi HEA (Cantor alloy) using scanning tunneling

Wednesday Afternoon, November 6, 2024

microscopy (STM). This data allows us to determine lattice local distortions unambiguously. Additionally, we report our findings on the types of local defects on the surface, such as grain boundaries, phase changes, and amorphization, and how these defects can impact local distortions of the crystals nearby.

5:15pm **SS+2D+AMS-WeA-13 Grain Boundary and Twin Boundary Solute Segregations in Nanocrystalline Al-Mg Alloy**, *Xuanyu Sheng, z. Shang, A. Shang*, Purdue University, China; *H. Wang, X. Zhang*, Purdue University

Chemical segregations at grain boundaries (GBs) have been broadly investigated in Al alloys. However, there are limited experimental evidence demonstrating the dependence of solute segregation on GB characteristics. Here, we quantified solute segregation at GBs in nanocrystalline Al-1Mg (at.%) alloy by combining energy-dispersive X-ray spectroscopy, high-resolution scanning transmission electron microscopy and automated crystallographic indexing and orientation mapping. The dependence of solute segregation on the grain boundary misorientation angle is analyzed. Due to their higher excess free volume, high angle grain boundaries contain more Mg solutes than the low angle grain boundaries. Furthermore, coherent twin boundaries (CTBs) exhibit low solute segregation. However, incoherent twin boundaries (ITBs) display greater solute concentration. The different solute segregation behavior between CTBs and ITBs originates from their grain boundary structure. The solute segregation behavior reported here may shed light on the GB engineering of Al alloys.

5:30pm **SS+2D+AMS-WeA-14 Charge Ordering Phase Transition in Bilayer Sn on Si(111)**, *Nathan Guisinger, M. Chan*, Argonne National Laboratory; *C. Lilley*, University of Illinois - Chicago

The atomic-scale investigation of the “bilayer” reconstruction of Sn on heavily doped n-type Si(111) was performed with scanning tunneling microscopy. When cooled to 55K, the bilayer reconstruction undergoes both a structural and electronic transition. Structurally, the dimer units of the bilayer shift to form a herringbone pattern with a rhombohedral ordering. The electronic structure transitions into a very uniform square lattice with similar dimensions to the structural dimers. There are distinct differences between the structural and electronic spacing that resolves itself when counting multiple periods. This ordering is like behavior observed in materials that exhibit charge density waves. Furthermore, STS point spectra show a transition from a small gap to a large insulating gap at low temperature that is consistent with a transition to a Mott insulating ground state. The charge ordering coupled with the relaxation to a Mott insulating phase upon cooling the Sn bilayer presents unique physics when the dimensionality is reduced from the bulk.

5:45pm **SS+2D+AMS-WeA-15 SSD Morton S. Traum Award Finalist Talk: On-Surface Design of Highly-Ordered Two-Dimensional Networks Stabilized by Nonmetal Atoms**, *Alisson Ceccatto*¹, University of Campinas (UNICAMP), Brazil; *G. Campi*, Yachay Tech University, Ecuador; *V. Carreño, E. Ferreira*, University of Campinas (UNICAMP), Brazil; *N. Waleska-Wellnhofer, E. Freiberger, S. Jaekel*, Friedrich-Alexander-University Erlangen-Nürnberg (FAU), Germany; *C. Papp*, Freie Universität Berlin, Germany; *H. Steinrück*, Friedrich-Alexander-University Erlangen-Nürnberg (FAU), Germany; *D. Mowbray*, Yachay Tech University, Ecuador; *A. de Siervo*, University of Campinas (UNICAMP), Brazil

Supramolecular nanoarchitectures have been widely explored to precisely design low-dimensional materials at atomic and molecular levels [1]. Such control is mainly based on bottom-up fabrication methods, e.g. on-surface synthesis, by combining molecular building blocks and atoms to engineer novel nanomaterials [2]. Particularly, the self-assembled monolayers (SAMs) of organic molecules present the potential for applications in nanoelectronics due to their reversible non-covalent interactions [3]. Such intermolecular interactions allow the fabrication of almost defect-free supramolecular nanostructures. Typically, the geometry of these nanoarchitectures can be controlled by the insertion of metal and non-metal atoms in the reaction process. To date, the adatom-mediated SAM fabrication concentrates on the use of metal adatoms, especially d metals (Cu, Co, Au, and Fe) [4]. Herein, by combining scanning tunneling microscopy (STM) measurements and density functional theory (DFT) calculations, we report the 2D self-assembled of 1,3,5-tris[4-(pyridin-4-yl)-[1,1'-biphenyl]]benzene (TPyPPB) molecules on Ag(111) in the presence of Cl adatoms. The adsorption of the TPyPPB molecules on the clean Ag(111) surface forms an almost defect-free porous SAM stabilized by hydrogen bonds, so-called triangular packing. Such packing can be explored as a host-guest material for atom/molecular confinement. However, in the presence

of Cl adatoms, the molecular arrangement changes dramatically. The molecular assembly changes its geometry, forming a non-porous SAM stabilized by H...Cl...H bonds. Such halogen-mediated SAM presents the advantage that the adatom used to stabilize the nanostructure has less influence on the electronic density compared to the typical metal adatoms.

Keywords: On-surface synthesis, STM, Self-assembly monolayer, Nanoporous networks.

Acknowledgments: This work was financially supported by FAPESP (2021/04411-1), FAPESP (2022/12929-3), CNPq, and CAPES (627946/2021-00).

References

1. Fan, Q. et al. *Accounts of Chemical Research* 48, 2484–2494 (2015).
2. Pawlak, R. et al. *Journal of the American Chemical Society* 142, 12568–12573 (2020)
3. Casalini, S. et al. *Chemical Society Reviews* 46, 40–71 (2017)
4. Shi, Z. et al. *Journal of the American Chemical Society* 133, 6150–6153 (2011)

¹ SSD Morton S. Traum Award Finalist

Surface Science

Room 120 - Session SS-ThM

Celebration of Robert J. Madix and his Contributions to Surface Science (INVITED SESSION)

Moderators: Dan Killelea, Loyola University Chicago, Jason Weaver, University of Florida, Linye Árnadóttir, Oregon State University

8:00am **SS-ThM-1 Selective Bimetallic Catalysts for Dehydrogenation of Liquid Organic Hydrogen Carriers**, Donna Chen, M. Qiao, University of South Carolina; A. Ahsen, Gebze Technical University, Turkey; F. Li, University of South Carolina

INVITED

Hydrogen is a promising source of clean and renewable energy, but a major challenge lies in its storage and transportation. The use of liquid organic hydrogen carriers (LOHC) allows hydrogen to be stored in organic molecules that are liquids at room temperature and therefore suitable for transportation through the existing infrastructure for petroleum. For example, the methycyclohexane (MCH)-toluene pair has been used for the catalytic cycle of hydrogenation to store hydrogen and dehydrogenation to release hydrogen. While inexpensive and efficient catalysts are already available for hydrogenation, there is still the need for the development of selective dehydrogenation catalysts that inhibit deactivation due to carbon fouling. In this work, bimetallic Pt-Sn alloy surfaces prepared by annealing Sn films on Pt(111) and vapor-deposited Pt-Sn clusters on a rutile TiO₂(110) support have been studied as model catalysts for MCH dehydrogenation, in which the addition of Sn is used to inhibit fouling on Pt. Compositions of the bimetallic clusters are characterized by temperature programmed desorption with CO as a probe molecule and by low energy ion scattering. The sizes and morphologies of the bimetallic clusters are determined by scanning tunneling microscopy. Bimetallic Pt-Sn can be grown via deposition of Pt on Sn or Sn on Pt, but the cluster surfaces are always rich in Sn due to the lower surface free energy of Sn compared with Pt. These model surfaces were then transferred into a flow reactor coupled directly to the UHV chamber for kinetic studies under realistic pressure conditions. The turnover frequency for MCH dehydrogenation on the Pt(111) surface is four times lower than for supported Pt clusters, and this behavior is attributed to the higher activity of undercoordinated sites that exist on the clusters. Similar studies are also being carried out for Ni-Cu bimetallic clusters on TiO₂, in which the presence of Cu is used to prevent fouling of the active Ni sites.

8:30am **SS-ThM-3 Infrared Spectroscopy Studies of Surface Chemical Reactions on Single Atom Alloys**, Michael Trenary, University of Illinois - Chicago

INVITED

Low coverages of catalytically active metals deposited onto the surfaces of less active host metals can form single atom alloys (SAAs), which often display unique catalytic properties. The catalytic properties of SAAs are ultimately determined by their surface structure. We have used reflection absorption infrared spectroscopy (RAIRS) and temperature programmed desorption (TPD) of adsorbed CO to probe the structure of Pd/Cu(111), Pt/Cu(111) and Pd/Ag(111) SAA surfaces. At certain values of the surface temperature and/or CO coverage, CO adsorbs only on Pd or Pt atoms and not on Cu or Ag sites. For low Pd and Pt coverages, only CO adsorbed at atop Pd or Pt sites is detected. At higher Pd or Pt coverages, CO adsorption at bridge sites is observed indicating that metal dimers or other aggregates have formed. Polarization dependent RAIRS was used to study selective hydrogenation reactions of acetylene, propyne, and 1,3-butadiene over a Pd/Cu(111) SAA surface. Reactants and products were monitored in the gas phase with s-polarized spectra, while p-polarized spectra were obtained to identify surface species present during the reaction. In each case, no hydrogenation occurred over the Cu(111) surface, but selective hydrogenation occurred over the Pd/Cu(111) SAA. Full hydrogenation to the saturated alkane did not occur. It is also found that coupling reactions occur to produce a carbonaceous layer on the surface, but that hydrogenation proceeds even in the presence of this layer.

9:00am **SS-ThM-5 Vibrationally Hot Precursors as Reactants in the Dissociative Chemisorption of Methane on Ir(111) and Ir(110)**, Arthur Utz, Tufts University

INVITED

Precursor-mediated reactions can potentially play a key role in the dissociative chemisorption of methane at the high temperatures (> 1000K) typical of steam-reforming reactors. At the average kinetic energies present, reactants can first physically adsorb to the surface as a precursor

prior to undergoing subsequent diffusion and reaction (or desorption)^{1,2}. High process temperatures also lead to significant populations of vibrationally excited gas-phase reagents and thermally excited lattice motion. This presentation will focus on the unique role that vibrational energy in the incident reactant and surface can play in activating these reactions.³

We use beam-surface scattering measurements coupled with infrared laser vibrational-state-selective excitation to prepare methane reactants with well-defined kinetic and vibrational energies. In this work, we study the role of methane's ν_3 antisymmetric C-H stretching vibration ($E_{\text{vib}} = 36$ kJ/mol). The prepared molecules impinge on the surface held at a fixed temperature (which dictates the extent of thermal lattice vibration), and we quantify reaction probability as a function of incident kinetic energy, vibrational state, and surface temperature.^{2,3} Independent control over these energetic coordinates allows us to unravel their contribution to reactivity. We chose to study the low-index Ir(111) and Ir(110)(1x2) surfaces because their minimum barrier height for dissociation is similar to, or slightly higher than the vibrational energy content of the laser-prepared molecules.

The experiments, when coupled with quasiclassical trajectory calculations, show that vibrational energy in a physisorbed precursor molecule survives long enough to promote reactivity with the same efficacy as reactivity occurring via a direct reaction mechanism. The calculations also point to the pivotal role of surface excitation in providing energetically accessible reaction paths for the physisorbed molecules.

1. J. F. Weaver, A. F. Carlsson, R. J. Madix, The adsorption and reaction of low molecular weight alkanes on metallic single crystal surfaces. *Surf. Sci. Rep.* **50**, 107-199 (2003).
2. E. Dombrowski, E. Peterson, D. DelSesto, A. Utz, Precursor-Mediated Reactivity of Vibrationally Hot Molecules: Methane Activation on Ir(111). *Catalysis Today* **244**, 10-18 (2015).
3. R. Moiraghi *et al.*, Nonthermalized Precursor-Mediated Dissociative Chemisorption at High Catalysis Temperatures. *J. Phys. Chem. Lett.* **11**, 2211-2218 (2020).
4. P. R. Shirhatti *et al.*, Observation of the adsorption and desorption of vibrationally excited molecules on a metal surface. *Nature Chemistry* **10**, 592-598 (2018).

9:30am **SS-ThM-7 Modeling of Reaction Mechanisms and Kinetics on Metal Surfaces and the Connection to Experimental Catalysis**, Linye Árnadóttir, Oregon State University/PNNL

INVITED

Chemical reactions on surfaces are of central importance for our understanding of catalytic activity in heterogeneous catalysis. Density functional theory calculations and microkinetic modeling are often used to determine reaction mechanisms and kinetics and to model changes in surface coverage and product distribution and for comparison with experiments. With fast-growing computational resources, theoretical studies for reaction mechanisms and microkinetic models have become more commonplace. Traditionally researchers approximate the vibrational frequencies of an adsorbate from an Hessian matrix calculated using a finite difference approach and then use the harmonic oscillator approximation to calculate all modes of motion in the partition function but some of Bob Madix's early work on preexponential factors^[1] motivated me and C.T. Campbell to propose the hindered translator/rotor model for the three modes of motion parallel to the surface, one for each of the two translations in the directions parallel to the surface and one for rotation about the axis perpendicular to the surface. These methods have since been modified and improved by other scientists and applied to microkinetic modeling by myself and others, inspired by Bob Madix work. Here we will discuss the implementation of these methods and recent DFT and microkinetic models for propane hydrogenation on Pt and Al₂O₃-decorated Pt surfaces and as well as complimentary temporal analysis of products (TAP) experiments by our collaborators at INL and ForgeNano, and the many ways Madix influenced our work and effort to bridge the gap between surface science and catalysis.

- [1] R.J. Madix, G. Ertl and K. Christmann, Preexponential factors for hydrogen desorption from single crystal metal surfaces, *Chemical Physics Letters*, **62**, 1, 1979

Thursday Morning, November 7, 2024

11:00am **SS-ThM-13 Crossing the Great Divide Again: Bridging Atomic-Scale Mechanistic Insight from Single-Crystals to Functional Catalysts Using Transient Flow and Spectroscopy.**, *C. O'Connor*, Harvard University; *E. High*, Tufts University; *T. Kim*, Korea Institute of Energy Research, Republic of Korea; **Christian Reece**, Harvard University **INVITED**

A key aspiration in the rationale design of catalysts is predictive performance (activity, selectivity, and stability) and surface properties (composition and structure) under realistic reaction conditions. This requires an atomic-scale understanding of catalyst reaction systems. Surface science studies on model catalytic systems are the “gold standard” for providing kinetic and mechanistic insight into heterogeneous catalysis. However, transferring this fundamental insight often measured on planar single crystals under ultra-high vacuum (UHV) conditions to applied catalytic reactors using technical catalytic materials at elevated temperatures and pressure can be challenging. Herein, we demonstrate our newly developed transient flow reactor to perform step transient experiments in a packed bed reactor at atmospheric pressure. We examine CO oxidation over palladium-based catalysts as a probe catalytic system to recreate the catalytic performance of planar Pd/Al₂O₃ in coincident molecular beams experiments under vacuum. We demonstrate that surface science derived kinetics can quantitatively model CO₂ production in our step transient experiments in an atmospheric pressure flow reactor. We establish a continuity of surface species under steady-state reaction conditions and sub-second evolution of surface species for step transient experiments using a custom low-volume Diffuse reflectance infrared Fourier transform spectroscopy (DRIFTS) reactor. This work demonstrates a unique ability to bridge the understanding of the state of the catalyst surface and reaction kinetics from vacuum conditions established using molecular beam experiments to ambient pressure conditions using a transient flow reactor and numerical simulations. Our technique provides a new regime for studying technical catalysts under applied reaction conditions.

11:30am **SS-ThM-15 Recent Games in the Surface Chemistry Stadium; Bob helped Build It, and They Came**, *Charles Sykes*, Tufts University **INVITED**

One cannot overstate Robert Madix's influence on the modern field of well-defined surface chemistry. His numerous contributions have brought a deep understanding of important chemical processes at surfaces. Inspired by Bob's works linking molecular scale processes and well-defined active sites with the rates and selectivity of real catalysts I have strived to collaborate broadly in order to achieve this level of understanding and control. Bob performed fundamental studies with the belief that one day they will inform the design of catalysts. In this talk I will argue we have reached that point and I will discuss a new class of heterogeneous catalysts called *Single-Atom Alloys* in which precious, reactive metals are utilized at the ultimate limit of efficiency.¹⁻⁶ These catalysts were discovered by combining atomic-scale scanning probes with more traditional approaches to study surface-catalyzed chemical reactions. This research provided links between atomic-scale surface structure and reactivity which are key to understanding and ultimately controlling important catalytic processes. In collaboration with Maria Flytzani-Stephanopoulos these concepts derived from our surface science and theoretical calculations have been used to design *Single-Atom Alloy* nanoparticle catalysts that are shown to perform industrially relevant reactions at realistic reaction conditions. For example, alloying elements like platinum and palladium with cheaper, less reactive host metals like copper enables 1) dramatic cost savings in catalyst manufacture, 2) more selective hydrogenation and dehydrogenation reactions, 3) reduced susceptibility to CO poisoning, and 4) higher resistance to deactivation by coking. I go on to describe very recent theory work by collaborators Stamatakis (Oxford University) and Michaelides (Cambridge University) that predicts reactivity trends for a wide range of *Single-Atom Alloy* combinations for important reaction steps like H-H, C-H, N-H, O-H, and CO₂ activation. Overall, I hope to highlight that this combined surface science, theoretical, and catalyst synthesis and testing approach (that Bob contributed so much to) provides a new and somewhat general method for the a priori design of new heterogeneous catalysts.

References:

- [1] Kyriakou et al. *Science* **335**, 1209 (2012).
- [2] Marcinkowski et al. *Nature Materials* **12**, 523 (2013).
- [3] Lucci et al. *Nature Communications* **6**, 8550 (2015).
- [4] Liu et al. *JACS* **138**, 6396 (2016).
- [5] Marcinkowski et al. *Nature Chemistry* **10**, 325 (2018).
- [6] Hannagan et al. *Science* **372**, 1444 (2021).

Surface Science

Room 120 - Session SS-ThA

Celebration of Robert J Madix and his Contributions to Surface Science & Reception

Moderators: Liney Árnadóttir, Oregon State University, Dan Killelea, Loyola University Chicago

2:15pm **SS-ThA-1 Alkane Activation and Oxidation on Solid Surfaces, Jason Weaver**, University of Florida **INVITED**

In this talk, I will discuss pioneering advances made in Bob Madix's group to understand the mechanisms for alkane activation on metal surfaces and how this knowledge has guided my group's studies of alkane chemistry on late transition-metal oxide surfaces. Madix's work was among the first to distinguish direct vs. trapping-mediated mechanisms for alkane activation on surfaces, and clarify dynamic factors that influence these reactions. My talk will provide an overview of Madix's key findings about alkane adsorption and activation determined from supersonic molecular beam studies and molecular dynamics simulations, including mechanisms for alkane adsorption and initial C-H cleavage, energy exchange processes in alkane trapping and dynamic effects in direct alkane dissociative chemisorption. I will lastly discuss how this fundamental knowledge has influenced my research on the surface chemistry of late transition-metal oxides, and enabled new discoveries.

2:45pm **SS-ThA-3 Thermodynamics and Kinetics of Elementary Reaction Steps on Late Transition Metal Catalysts: A Tribute to R. J. Madix, Charles T. Campbell**, University of Washington **INVITED**

I will review experimental and theoretical results from my own group concerning the thermodynamics and kinetics of elementary chemical reactions of importance in catalysis on late transition metal surfaces. I will focus on topics wherein my interest was inspired by work from Madix's group. These include: (1) the first proposed mechanism for methanol synthesis catalyzed by Cu, (2) measurements of pre-exponential factors and their interpretations through transition-state theory (TST), (3) measurements of the entropies of adsorbates and their trends, (4) using these together with elementary-step rate measurements and adsorbate energies to build microkinetic models for multi-step catalytic reactions, (5) a method for analyzing these that quantifies the extent to which the energy of each elementary-step transition state and intermediate controls the net rate, called the degree of rate control (DRC), and (6) interpreting kinetic isotope effects (KIEs) through DRC analysis. Work supported by NSF and DOE-OBES Chemical Sciences Division.

Surface Science

Room Central Exhibit Hall - Session SS-ThP

Surface Science Poster Session

SS-ThP-1 A Model Interstellar Medium Reactivity Study: Low Energy Electron Induced Chemistry of CH₃OH@H₂O, Ahmad Nawaz, M. Asscher, The Hebrew University of Jerusalem, Israel

The desorption kinetics for MeOH@H₂O sandwich films from Ru(0001) surfaces are investigated using temperature-programmed desorption (TPD) at ultrahigh vacuum, with a base pressure of 2×10^{-10} Torr and temperature 25K. The TPD spectra of all the prominent stable molecular products were well detected by an in-situ quadrupole mass spectrometer (QMS). However, variation of the QMS signals were observed to be lower at different exposure to the negative charges in different time interval. Further, the MeOH parent molecules decompose, upon exposure to electrons at energies of 100 eV and 6.4 eV. Molecules at m/z of 2, 28 and 44, assigned to H₂, CO and CO₂, were the most abundant products. The typical mass spectra of the parent molecules within the sandwich layer (16 ML) are shown in Figure 1. Here, the MeOH peaks appears at ~140K while the water desorption peak is at ~160K.

SS-ThP-2 Near Ambient Pressure XPS Indicates that the Relevant State of Silver under Ethylene Epoxidation Conditions is Mostly Metallic, Elizabeth E. Hoppel, Tufts University; P. Christopher, University of California at Santa Barbara; M. Montemore, Tulane University; E. Sykes, Tufts University

Epoxidation reactions are some of the highest value processes in the chemical industry; however, despite decades of research, the mechanism of ethylene epoxidation is still under debate. A central question in the field is the state of the industrial Ag catalyst under reaction conditions. Controversy remains about whether the active site for selective oxidation is metallic or oxidized and several in situ studies have reported the presence of both phases. We utilize near ambient pressure XPS under both purely oxidizing conditions and ethylene: oxygen ratios at a temperature that yields the same reactant chemical potentials as a typical flow reactor. Our XPS results reveal that electrophilic and nucleophilic oxygen formed on Ag(111) after exposure to pure oxygen at 433 K, with a O : surface Ag ratio of 0.11. However, when ethylene is introduced to the oxygen atmosphere at an industrially relevant 5:2 ratio, the nucleophilic oxygen is reacted away immediately, and the electrophilic oxygen coverage slightly increases which we attribute to the formation of carbonate which has the same binding energy as electrophilic oxygen. Most significantly, the O : surface Ag ratio decreases to 0.05, almost half of which is carbonate. These results indicate that the Ag(111) surface is mostly metallic under simulated reactor conditions meaning that Ag/oxide interfaces, at which the proposed oxametallacycle (OMC) intermediate is formed, must be considered in mechanistic epoxidation models.

SS-ThP-3 Surface Chemistry of Zirconium Borohydride on Zirconium Diboride (0001), M. Trenary, Ayoyele Ologun, University of Illinois - Chicago

Transition metal diborides are known to either have a metal-terminated or boron-terminated surface. While group-V MB₂ has boron-terminated surfaces, group-IV MB₂ has metal-terminated surfaces. ZrB₂, a group-IV metal-terminated diboride, is an extremely hard material with a high melting point of 3246 °C and can be grown conformally via chemical vapor deposition (CVD) using zirconium borohydride Zr-(BH₄)₄ as a precursor. Using reflection absorption infrared spectroscopy (RAIRS), we investigated the surface chemistry of ZrB₂ growth from Zr-(BH₄)₄ on a ZrB₂(0001) surface. Using low-energy electron diffraction and X-ray photoelectron spectroscopy (XPS), we demonstrate that ZrB₂ can have a boron-terminated surface in boron-rich conditions. The RAIR spectrum obtained after exposing the surface at 90 K to Zr-(BH₄)₄(g) matched that of the pure compound, indicating adsorption without decomposition. However, new surface intermediates were formed upon heating to 280 K, as shown by the presence of νB-Ht stretch (2569 cm⁻¹) and δH-B-H (1228 & 1057 cm⁻¹) peaks in the RAIR spectra. Decomposition of Zr(BH₄)₄ on ZrB₂(0001) surface at 1173 K revealed a $\sqrt{3} \times \sqrt{3}$ boron terminated surface, with a stoichiometry of ZrB_{2.60}. In contrast to the zirconium-terminated surface, the boron-terminated surface is resistant to oxidation.

SS-ThP-4 Selective Hydrogenation of 1,3-butadiene on a Pd/Cu (111) Single-Atom-Alloy, Mohammad Rahat Hossain, M. Trenary, University of Illinois at Chicago

Selective hydrogenation of 1,3-butadiene (BD) to 1-butene (1-B) is critical in refining alkene streams for high-quality polymer production. Typically, Pd and Pt are employed in hydrogenation reactions due to their nearly negligible barrier for H₂ activation. However, these catalysts are prone to coking and their high activity often reduces selectivity. Single-atom alloy (SAAs) catalysts are being developed to achieve high selectivity while retaining high activity. In an SAA, small amounts of an active metal, such as Pd or Pt, are doped into a less active host metal such as Cu. Previous work has shown that a Pd(111) surface exhibits superior selectivity for BD hydrogenation to 1-B compared to Pt(111),¹⁻⁴ suggesting that Pd/Cu(111) could be a suitable SAA model catalyst for this reaction. In this study, we investigated the adsorption and hydrogenation of 1,3-butadiene (BD) to 1-butene (1-B) over a Pd/Cu (111) SAA under ultrahigh vacuum (UHV) and ambient pressure conditions using reflection absorption infrared spectroscopy (RAIRS). Temperature programmed reaction spectroscopy (TPRS) in UHV showed that monolayer BD desorbs at 217 K, while 2nd-layer and multilayer BD desorb between 112 to 180 K. RAIRS detected gas-phase 1-B formation and BD consumption. In ambient pressure conditions, this reaction was found to be first-order (1.12±0.03) in H₂ and zero-order (-0.12±0.01) in BD, correlating to a turnover frequency of 36 s⁻¹ at 380 K. The activation energy was calculated to be 63.2 ± 2.8 kJ/mol from an Arrhenius plot of the temperature dependence of the rate constant. Complete conversion of BD was found with 84% selectivity towards 1-B, without butane production. No surface species were detected during the reaction. Post-reaction analysis using Auger electron spectroscopy (AES) revealed carbon deposition, indicating some dissociation during hydrogenation.

References:1.C.-M. Pradier, E. Margot, Y. Berthier and J. Oudar, Appl. Catal. 43 (1), 177-192 (1988).2.G. Tourillon, A. Cassuto, Y. Jugnet, J. Massardier and J. Bertolini, J. Chem. Soc., Faraday Trans. 92 (23), 4835-4841 (1996).3.T. Ouchai, J. Catal. 119 (2) (1989).4.J. Massardier, J. Bertolini, P. Ruiz and P. Delichere, J. Catal. 112 (1), 21-33 (1988).

SS-ThP-5 The Influence of Substrate Roughness and Long-Range Molecular Order on 3-Mercaptopropionic Acid Displacement by 1-Decanethiol, Lindsey Penland, H. Hetti Arachchige, N. Dissanayake, R. Farber, University of Kansas

Thiolate self-assembled monolayers (SAMs) are widely used for their ability to tune the interfacial properties of Au surfaces for applications such as nano-fabrication and bio-functionalization. This molecular control over interfacial properties can be further enhanced by introducing a second molecular species, resulting in a binary SAM. Binary SAMs offer an appealing route to control the molecular scale density of specific functional groups. One approach to forming binary SAMs is through the displacement of one molecule with another through solution phase deposition. The fabrication of molecularly precise binary SAMs requires precise control of the molecular interactions and substrate properties, such as surface roughness.

In this work, using ultra-high vacuum scanning tunneling microscopy (UHV-STM) and solution-phase preparation methods, the relationship between chain length, functional group, and substrate roughness on the displacement of 3-Mercaptopropionic Acid (MPA) by 1-Decanethiol (DT) was investigated. First, three categories of MPA substrates were prepared: **MPA-1**) well-ordered smooth surface formed during a 3 hr MPA incubation at 35 °C, **MPA-2**) disordered smooth surface formed during a 3 hr MPA incubation at 25 °C, and **MPA-3**) well-ordered rough surface formed during a 24 hr MPA incubation at 25 °C. Then, following the formation of **MPA-1**, **-2**, and **-3**, the substrates were sequentially placed in a 2 μM DT solution for 20 min, 60 min, 3 hr, and 24 hr. UHV-STM analysis of the MPA substrates showed that **MPA-1** and **MPA-2** had faster rates of displacement than **MPA-3** and resulted in a uniform high-density DT film across the surface. **MPA-3**, which started with a uniform MPA SAM and nanoscale roughness due to the formation of Au nano-islands across the substrate related to the longer MPA incubation time, had the slowest rate of displacement. Interestingly, the DT SAM that formed following displacement of the **MPA-3** sample was comprised of the low-coverage, lying down phase (β) and 2-D gas phase (α) of DT. Ongoing work is focused on understanding the relationship between substrate roughness and MPA ordering on the slower displacement rate and low-density DT phases observed for **MPA-3**.

SS-ThP-6 Visualizing on-surface Intramolecular C-C Coupling Reaction Using Scanning Tunneling Microscopy and Tip-Enhanced Raman Spectroscopy, *Soumyajit Rajak, N. Jiang*, University of Illinois, Chicago

Metal surface-supported physicochemical transformations provide additional degrees of freedom to tune the structural and electronic properties of molecular functional materials. To obtain a higher degree of control over the reaction outcome, submolecular scale characterization of the chemical intermediates and their local environment is required. Determining the real-space surface adsorbed configurations of molecules is challenging using ensemble-averaged surface science techniques. Again, probing the effect of the local environment of chemical species is challenging because the spatial resolution of conventional optical spectroscopic techniques is limited by the diffraction limit of light. Coupling light with plasmonic nano-objects creates highly localized surface plasmons (LSPs), which allows us to break the diffraction limit. Herein we present a combined topographical and chemical analysis of different surface-adsorbed configurations and surface-sensitive arrangements of a tetrabenzoporphyrin molecule and their chemical reactivity on a metal surface using angstrom-scale resolution scanning tunneling microscopy (STM) and ultra-high vacuum tip-enhanced Raman spectroscopy (UHV-TERS). Low temperature (77K) scanning tunneling microscopic images and localized surface plasmon resonance enhanced Raman signals reveal different adsorbate configurations of single molecule entities and their thermal reaction products with a fundamental view of adsorbate-substrate binding interactions. TERS uses the apex of the STM tip made of a plasmonic metal as a nano object to couple light to the near field. The Raman modes of the nanostructure underneath this tip are enhanced by the nano-confined surface plasmons which allows us to obtain chemical information with Angstrom scale spatial resolution. The atomic scale insights obtained into the local environment enable precise control over the fabrication of molecules with tailored optoelectronic properties.

SS-ThP-7 Click Chemistry on Functionalized Silicon Surfaces: UHV- and Solution-Based Strategies, *T. Glaser*, Justus Liebig University Giessen, Germany; *J. Meinecke*, Philipps University Marburg, Germany; *C. Langer, L. Freund*, Justus Liebig University Giessen, Germany; *U. Koert*, Philipps University Marburg, Germany; *Michael Durr*, Justus Liebig University Giessen, Germany

Click chemistry is a well-known and established reaction scheme in organic chemistry for the synthesis of well-defined organic molecular structures. The direct application of click chemistry reactions to selectively functionalized silicon surfaces could thus open the route to synthesizing new organic molecular architectures on these substrates, e.g., with tailored optical or physicochemical properties ("more than Moore"). However, click reactions such as the most prominent alkyne-azide coupling are performed in the presence of a catalyst dissolved in an adequate solvent. On the other hand, highly reactive surfaces such as the technologically most important Si(001) surface, are typically prepared and stored under UHV conditions in order to guarantee a high level of cleanliness and structural perfection. The direct application of solution-based click chemistry schemes to such vacuum processed surfaces thus seems as an experimental contradiction.

Here we show two different approaches to solve this problem: First, we demonstrate how to combine surface functionalization performed under UHV conditions with a solution-based alkyne-azide click reaction in order to build organic molecular architectures on functionalized semiconductor surfaces. The UHV-based functionalization of the Si(001) surface was realized via chemoselective adsorption of ethynyl cyclopropyl cyclooctyne (ECCO) from the gas phase [1]. The samples were directly transferred from UHV into the azide solution without contact to ambient conditions. The second organic layer was then coupled in acetonitrile solution via the copper-catalyzed alkyne-azide click reaction. Each reaction step was monitored by means of X-ray photoelectron spectroscopy in UHV; the N 1s spectra clearly indicated the click reaction of the azide group of the two test molecules employed, i.e., methyl-substituted benzylazide and azide substituted pyrene. Using optimized copper (I) catalysts, effective reaction yields of up to 75 % were obtained [2].

Second, a carefully tuned enoether/tetrazine cycloaddition was shown to be applicable even under UHV conditions and without catalyst [3]. We employed this reaction for coupling a tetrazine molecule to an enol ether group which was covalently attached on a Si(001) surface via cyclooctyne as a linker.

[1] C. Langer, J. Heep, P. Nikodemiak, T. Bohamud, P. Kirsten, U. Hofer, U. Koert, and M. Durr, *J. Phys.: Condens. Matter* 31, 34001 (2019).

[2] T. Glaser, J. Meinecke, C. Langer, J. Heep, U. Koert, and M. Durr, *J. Phys. Chem. C* 125, 4021 (2021).

[3] T. Glaser, J. Meinecke, L. Freund, C. Langer, J.-N. Luy, R. Tonner, U. Koert, and M. Durr, *Chem. Eur. J.* 27, 8082 (2021).

SS-ThP-8 Adsorption of Fluorinated β -Diketones on a Surface of ZnO Nanopowder: Dependence of Adsorbates on the Chemical Structure, *Sanuthmi Dunuwila, A. Teplyakov*, University of Delaware

This study investigates the surface modification of ZnO nanopowder using gas-phase fluorinated β -diketones, namely hexafluoro acetylacetone (hfach) and trifluoro acetylacetone (tfach), to elucidate their attachment chemistry.

Surface modification was investigated through *in-situ* infrared spectroscopy, X-ray photoelectron spectroscopy (XPS), and solid-state NMR analysis (ssNMR) to determine the dominant adsorbate on nanopowder surfaces. To supplement the experimental findings, density functional theory was employed to identify stable surface species of ZnO nanopowder.

This study examines how the binding behavior of β -diketones on the ZnO surface varies depending on the specific nature of the β -diketone molecule. The gas phase for both diketones investigated consisted of the mixture of enol and ketone forms, with enol being most dominant for hfach. Despite this observation, surface adsorption is dominated by the tetra- σ -bonded diketone, which is very different from the commonly accepted adsorption model for β -diketones on oxide surfaces. In the case of tfach, the adsorption is indeed dominated by the dissociated enolate form. These differences are apparently governed by the amphoteric nature of ZnO. When a more basic oxide material, MgO, is used, hfach does form enolate as a dominant adsorbate, as confirmed by ssNMR.

This work expands our understanding of the β -diketone adsorption on oxide materials that is used in a variety of applications, from surface sensitization to heterogeneous catalysis, and from material growth to etching.

SS-ThP-9 In-situ X-Ray Absorption Spectroscopy (XAS) study of CeO₂-based Catalysts for CO₂ Hydrogenation, *Irene Barba-Nieto*, Brookhaven National Laboratory, Spain; *J. Rodriguez*, Brookhaven National Laboratory

Carbon dioxide (CO₂) is the main gas responsible for the greenhouse effect in Earth's atmosphere, leading to higher global temperatures and climate change. To limit global warming to 1.5°C and reach net zero carbon dioxide emissions by 2050, it is necessary to advance in industrial processes that facilitate the generation of clean fuels from CO₂. One of the most promising strategies in this regard is the utilization of CO₂ and its transformation into valuable chemicals.

This study examines the effectiveness of two catalyst types, RuCeO₂ and RuCeO₂-TiO₂ systems, for converting CO₂ into methane. Results demonstrate that despite lower Ru content, TiO₂-containing systems exhibit significantly enhanced catalytic activity for CO₂ conversion to methane. To understand this fact, *in situ* X-ray absorption measurements have been carried out on the Ru K-edge and Ce L₃-edge analyzing their behavior under H₂, CO₂ and H₂+CO₂ between 30°C to 250°C. The Ru K-edge results indicate that the RuCeO₂ systems display a remarkable oxidation-reduction capacity, as evidenced by the reduction of the metal center in the presence of both H₂ and CO₂/H₂, along with its oxidation in CO₂ atmosphere. However, this behavior undergoes a drastic change in the TiO₂-containing catalyst, as a consequence of strong CeO₂-TiO₂ interactions, where the presence of hydrogen at 250°C leads to irreversible reduction of Ru.

The analysis of the Ce L₃-edge revealed that the RuCeO₂ systems predominantly exhibit Ce⁴⁺, which was observed to undergo partial reduction under both H₂ and H₂/CO₂ atmospheres, followed by its re-oxidation under CO₂. However, the RuCeO₂-TiO₂ catalysts demonstrate a substantially higher concentration of Ce³⁺ compared to the RuCeO₂ sample under all conditions (H₂, CO₂, H₂/CO₂), with the amount of Ce³⁺ further increasing under atmospheres with H₂ and H₂/CO₂.

Therefore, the XAS findings indicate that the presence of TiO₂ in the catalysts stabilizes the metallic state of Ru, which remains in this state during the methanation reaction. Moreover, TiO₂ promotes the formation of Ce³⁺, enhancing the catalysts' reactivity. This effect is attributed to TiO₂ facilitating an electronic transfer at the interface and perturbing the regular fluorite geometry of ceria, thus promoting the presence of Ce³⁺. A trend that is in agreement with previous studies for CeO₂/TiO₂(110) model systems. The presence of Ce³⁺ significantly impacts the catalytic properties of the sample, aiding in the oxidation-reduction of Ce and stabilizing Ru.

Consequently, the presence of reduced cerium plays a crucial role in determining the surface chemistry of the catalyst, crucial for efficiently converting CO₂ into methane.

SS-ThP-10 Insights from the Atomic Scale: Cobalt Sulfide Sheets on Au(111) and Initial Oxidation of Pt(111), D. Boden, M. Prabhu, M. Rost, I. Groot, Jörg Meyer, Leiden University, Netherlands

This poster highlights two recently published articles from a successful experiment-theory collaboration within the Leiden Institute of Chemistry:

1. Cobalt Sulfide Sheets on Au(111) [1] Transition metal dichalcogenides (TMDCs) are a type of two-dimensional (2D) material that has been widely investigated by both experimentalists and theoreticians because of their unique properties. In the case of cobalt sulfide, density functional theory (DFT) calculations on free-standing S-Co-S sheets suggest there are no stable 2D cobalt sulfide polymorphs, whereas experimental observations clearly show TMDC-like structures on Au(111). In this study, we resolve this disagreement by using a combination of experimental techniques and DFT calculations, considering the substrate explicitly. We find a 2D CoS(0001)-like sheet on Au(111) that delivers excellent agreement between theory and experiment. Uniquely this sheet exhibits a metallic character, contrary to most TMDCs, and exists due to the stabilizing interactions with the Au(111) substrate.
 2. Initial Oxidation of Pt(111) [2] In situ scanning tunneling microscopy experiments on the initial oxidation of Pt(111) found complex intermediary platinum surface oxides, consisting of spoke wheel and stripe structures [3]. The structure of the spoke wheels is poorly understood because of their size and complexity. Here we employ atomistic thermodynamics based on an established reactive force field to investigate the structure and stability of spoke wheels at the elevated temperature (>530 K) and pressure (1–4 bar) conditions of the in situ experiments. At those conditions, the thermodynamic stability of the structural model for the spoke wheel is similar to that of the stripes, while the degree of surface oxidation is much lower. The spoke wheel is found to be much more stable than partially formed stripes with a similar degree of oxidation. These results are consistent with experimental findings, where the spoke wheel is observed first, at slightly lower oxygen pressures. They thus provide a better understanding of the oxidation pathway for Pt(111)-based catalysts in the context of oxidative catalysis.
1. M. K. Prabhu, D. Boden, M. J. Rost, J. Meyer, and I. M. N. Groot, *J. Phys. Chem. Lett.* **11**, 9038 (2020).
 2. D. Boden, I. M. N. Groot, and J. Meyer, *J. Phys. Chem. C* **126**, 20020 (2022).
 3. M. A. van Spronsen, J. W. M. Frenken, and I. M. N. Groot, *Nat. Commun.* **8**, 1 (2017).

SS-ThP-11 Hard X-Ray Photoelectron Spectroscopy Reveals Fe Segregation in NiFe Electrodes During Oxygen Evolution Reaction, Filippo Longo, Chemical Energy Carriers and Vehicle Systems Laboratory, Empa, Swiss Federal Laboratories for Materials Science and Technology, Switzerland; P. Lloreda Jurado, J. Gil-Rostra, A. González-Elipse, F. Yubero, Nanotechnology on Surfaces and Plasma, Institute of Materials Science of Seville (CSIC-US), Seville, Spain; A. Borgschulte, Chemical Energy Carriers and Vehicle Systems Laboratory, Empa, Swiss Federal Laboratories for Materials Science and Technology, Switzerland

Alkaline water electrolysis represents one of the simplest methods employed to perform water splitting reaction [1]. This process is one of the most efficient ways of producing H₂ and O₂ at low cost and high purity [2]. The bottleneck of this reaction stems from the sluggish kinetics of the anodic reaction, i.e., the oxygen evolution reaction (OER), which consists of a four-electron transfer process [3]. The extraordinary performance of NiFe as electrocatalysts for the OER [4] is still a subject of debate. The changes that occur on the electrode surface during electrochemical reactions add another dimension of complexity, which hinders the rational design of electrodes for water splitting. Particularly for binary alloy electrodes, there are various phenomena ranging from the formation of oxides, (oxy)hydroxides and the associated segregation of metal atoms. In this work, we study various NiFe electrodes as model systems for the OER. We have developed the procedure for the quantification of chemical depth-profiling by XPS/HAXPES measurement, showing a marked Fe segregation

and dissolution. The results explain the electrochemical performance of NiFe electrodes for OER. All the electrodes studied suffer from segregation of iron and subsequent formation of FeO_x on the surface, with only minor influence from morphology, porosity and total Fe content.

- [1] S. W. Sharshir et al., *International Journal of Hydrogen Energy* (2023).[2] Z.-Y. Yu et al., *Advanced Materials* **33**, 2007100 (2021).[3] A. Wang et al., *Mater. Chem. Front.* **7**, 5187 (2023).[4] F. Dionigi and P. Strasser, *Advanced Energy Materials* **6**, 1600621 (2016).

SS-ThP-12 Surface Modification of Titanium Dioxide Nanomaterials via Functionalization with Triol Compounds, Asishana Onivefu, A. Teplyakov, University of Delaware

Surface modification of titanium dioxide (TiO₂) nanoparticles with trimethylolpropane (TMP) and dimethylolpropionic acid (DMPA) holds significant promise for advancing various technological applications. This research explores the functionalization of TiO₂ nanomaterials and compares with pigmentary TiO₂ surface coatings technologies used at industrial scale. Through a combination of experimental techniques including FTIR spectroscopy, X-ray photoelectron spectroscopy (XPS) and density functional theory (DFT) calculations, the interactions between surface modifiers and TiO₂ are elucidated, revealing the formation of specific surface adsorbates. The results obtained from these studies demonstrated the displacement of surface impurities by adsorption of functionalized small molecules and evaluated the displacement processes among these surface modifiers. Hexafluoroacetylacetone (Hfac) was used as a test compound in displacement investigations utilizing fluorine as a spectroscopic label to precisely trace the displacement chemistry with XPS. This work provides fundamental understanding and offers novel strategies and valuable insights for enhancing the performance of TiO₂-based materials.

SS-ThP-13 Model Studies of Single-Atom Alloy (SAA) Catalysts, F. Zaera, Ravi Ranjan, University of California - Riverside

Single-atom alloy (SAA) catalysts have become a prominent way to enhance selectivity in a number of catalytic processes. The mechanism by which these alloys attain their improved performance is still being debated, however, especially when considering the effect of the reaction environment on their structure and chemical composition. We have embarked on a project to emulate those catalysts using model systems where the metals are dispersed as nanoparticles (NPs) onto a flat oxide surface under controlled ultra-high vacuum (UHV) conditions, characterized using a combination of surface-sensitive techniques, and tested for their catalytic behavior using a so-called high-pressure cell. This work focuses on the characterization of the nature of surfaces of SAA catalysts made out of Pt (minority) and Cu (majority) metals and their performance for the promotion of the hydrogenation of unsaturated aldehydes. Cu/Ta_xO_y/Ta surfaces have been prepared via the oxidation of a Ta crystal followed by the vapor deposition of controlled amounts of Cu and characterized using reflection-absorption infrared spectroscopy (RAIRS) and temperature-programmed desorption (TPD) together with carbon monoxide (CO) as a probe molecule. A series of changes in the RAIRS data has been observed as a function of the Cu deposition time, an indication of the development of the Cu NPs from small clusters of atoms with multiple low-coordination sites to larger NPs with more basal planes exposed. These Cu NPs were found to form stable in the temperature range from 300 K to 600 K, but to change beyond 600 K. Like Cu, Pt and Cu-Pt NPs can be grown and characterized via CO titrations using RAIRS and TPD, following a similar approach. Kinetic measurements under catalytic conditions can then be performed to test the efficacy of the Cu, Pt, or Cu-Pt NPs catalysts supported on the tantalum oxide surface and to identify the appropriate structure-reactivity correlations.

SS-ThP-14 Enhancing Gas-Evolving Electrocatalysis by Tuning the Wetting Properties of Catalyst Microenvironment, Kaige Shi, X. Feng, University of Central Florida

Electrocatalysis plays a critical role in the conversion between electricity and chemical fuels. In addition to the development of electrocatalysts, efforts are made to understand and control their local environment during operations, which may influence the mass transport and kinetics of the reactions. Particularly, when gas-phase reactants or products are involved, the wetting properties of the microenvironment around catalytic sites can determine the distribution and diffusion of gas and liquid near the catalyst, and thus impact the catalytic performance. Here we present a study of catalyst microenvironment by controlling the wetting properties of carbon black, which is widely used as a catalyst support in electrocatalysis. We chose the electro-oxidation of hydrazine (N₂H₄) on carbon-supported Pt

nanocatalyst and tuned the wetting properties of carbon support by doping of fluorine (F) or oxygen (O). Interestingly, the electrode with F-doped carbon (more hydrophobic) exhibited a higher activity than that with pristine carbon black. This is attributed to the accelerated removal of N₂ gas generated from the catalyst, which would otherwise block the catalyst surface from liquid reactant. Furthermore, the electrode with O-doped carbon (more hydrophilic) showed an even higher activity, benefiting from the increased exposure of catalytic sites to liquid reactant. Our work demonstrates that controlling the catalyst microenvironment by doping of carbon black as catalyst support can be a powerful approach to enhance gas-evolving electrocatalysis. This work is supported by the National Science Foundation (NSF) Chemical Catalysis Program under Grant No. 1943732.

SS-ThP-15 Advanced Evaluation of Sub-nm Surface Roughness using Electron Diffraction, Rivaldo Marsel Tumbelaka, K. Hattori, Nara Institute of Science and Technology, Japan

Achieving precise control over surface roughness at the sub-nanometer scale is paramount for enhancing the physical properties of semiconductor materials, particularly their electrical transport characteristics. Current methodologies, predominantly scanning probe microscopy, facilitate quantitative roughness assessment but face challenges when applied to surfaces with intricate structures such as vertical and facet faces of three-dimensional (3D) structures, owing to steric hindrance. Our prior research effectively utilized reflection high-energy electron diffraction (RHEED) to observe atomic ordering on various structure surfaces in different directions, overcoming the challenge of steric hindrance [1-3]. In this study, we explore the potential of RHEED as an alternative avenue for evaluating surface roughness. Kinematic diffraction theory introducing diffraction spots from atomic positions, we explore the correlation between RHEED spot profile and surface roughness. Our approach involves systematically analyzing RHEED intensity profiles alongside surface roughness measurements of Highly Ordered Pyrolytic Graphite (HOPG), serving as a prototype sample.

HOPG samples with varying degrees of surface roughness were prepared via Ar sputtering, and their roughness was assessed using atomic force microscopy (AFM). Figure 1(a) shows a typical RHEED pattern for the HOPG whose roughness was 0.163 nm. Through the analysis of RHEED spot profiles, we discerned distinct intensity components, and , corresponding to sharpened and broadened spot intensities, respectively (Fig 1(b)). Our findings reveal an excellent correlation between increased surface roughness and the ratio of broadened spot intensity to total intensity (Fig 1(c)), indicating RHEED's adaptability for quantitative evaluation of surface roughness. This study not only shows how effective RHEED can be in measuring surface roughness but also demonstrates its usefulness in analyzing complex 3D surfaces in small-scale research and making semiconductor devices. The details will be discussed in the presentation.

References:

- [1] A. N. Hattori, K. Hattori, *et al.*, Surf. Sci. 644 (2016) 86.
- [2] A. N. Hattori, K. Hattori, *et al.*, Appl. Phys. Exp. 9 (2016) 085501.
- [3] K. Hattori, *et al.*, Jap. J. Appl. Phys. 51 (2012) 055801.

SS-ThP-16 Post-Synthesis Characterization of PtNi Nanowires for Enhanced Durability and Efficiency, Cesar Saucedo, J. Mann, S. Zaccarine, Physical Electronics USA

Polymer electrolyte membrane fuel cells (PEMFCs) offer a promising avenue for sustainable electricity production with minimal environmental impact. However, their widespread adoption faces challenges due to durability concerns and the sluggish kinetics of the oxygen reduction reaction (ORR) at the cathode. Consequently, to advance PEMFCs, there is a pressing need for the advancement of catalyst technologies to overcome these limitations. Previous works have looked at the synthesis of extended-surface platinum-nickel (PtNi) nanowires (NWs) via atomic layer deposition (ALD) and their durability. Here we show how the composition and chemical states of the nanowires evolve after a series of post-synthetic modifications designed to maximize the longevity of these nanowires as catalysts. By combining complementary surface analytical techniques (X-ray photoelectron spectroscopy, hard X-ray photoelectron spectroscopy, and nanoscale Auger electron spectroscopy) we develop a more complete model of the complex chemical nature of these catalysts than any single technique could by itself, accelerating the development of more durable and efficient PEMFC catalysts.

SS-ThP-17 Temperature Dependence of Surface-Catalyzed Ullmann Coupling via Activation of Highly Labile C-I, Chamath Siribaddana, N. Jiang, University of Illinois Chicago

The surface-catalyzed Ullmann-coupling via activation of highly labile C-I was studied on Au(111) using metal β -diketonato molecules with scanning tunneling microscopy. Unexpectedly the C-I bonds do not dissociate upon deposition of the molecule on the Au(111) surface held at room temperature which is known to catalyze the C-I dissociation reaction under such conditions. Rather the molecules form self-assembled monolayers stabilized by halogen bonds on Au(111). Annealing this sample to 100° C or direct deposition of the molecules on a Au(111) substrate held at 100° C triggers C-I bond cleavage. However, at 100° C intact C-I bonds can be observed, as only a portion of the molecules undergo C-I dissociation. Annealing to 200° C results in complete dehalogenation of the molecules and forming two types of COFs with triangle and cross-shaped connections. The dissociated Iodine atoms are incorporated within the COF. The two kinds of COFs exhibit only short-range network order due to the irreversible nature of the C-C bond formation. This trend is observed up to annealing temperatures of 370° C and no preference is observed towards one type of COF throughout this temperature range. Annealing temperatures beyond 400° C results in the decomposition of the molecules into its ligands which form a COF different from the COFs formed by the molecule.

SS-ThP-18 Accurate SIMS Characterization of Indium Implant in Silicon, Xuefeng Lin, S. York, N. Kaushik, Micron Technology

Secondary ion mass spectrometry (SIMS) is an ideal technique to provide indium (In) implant depth profiles in Si. However, this approach faces a critical challenge for overcoming the Si molecular mass interferences (MIs). These MIs can create high backgrounds during profiling and create an ambiguous determination of true In depth distributions. This phenomenon is especially true for SIMS analysis of lower dosed In implants <1E15 (at/cm²). The challenge is that the combination of three Si isotopes creates significant MIs with a high mass resolution (MR) > ~45370 needed for separation from In. This is far beyond the magnetic sector dynamic SIMS mass separation capability <10000MR. A special SIMS analysis method of energy filtering by applying an offset voltage has been often used to minimize or remove the Si MIs for In implant analysis. However, applying the different voltage offsets produces different In tailing profiles and background levels. Fig. 1 shows seven SIMS depth profiles acquired on In30KeV7.85E13 implanted in Si, acquired by applying seven voltage offsets from -10 to -30eV, which create different In background levels and tailing profile shapes below 1E18 (at/cm³). Increasing the voltage offset values from -10 to -30eV reduces the In background levels and shrinks the tailing profiles (Fig. 2, as determined at 100nm depth scale). Some previous SIMS studies used the background subtraction rather than applied voltage offset to characterize and obtain the precise In implant profiles, but determination of the specific subtraction value might be an issue since different subtractions would also affect the measured In implant doses and shapes. Fig. 3 shows the same SIMS In implant depth profiles with no subtraction and no voltage offset in green, and light and heavy subtractions in red and blue. To obtain more accurate In implant profiles in Si to overcome random background subtraction issues, we have used SIMS analysis combined with TCAD simulation. This combined method uses an appropriate voltage offset to obtain the SIMS profiles and then it is compared with the TCAD simulation, as shown in Fig. 4. Although several different voltage offsets have to be used to obtain the SIMS depth profiles to match the TCAD simulations to determine the applied voltage offsets at the beginning, once the SIMS analysis protocol is established, the analysis recipes would be used for analyzing the similar In implants in Si. In addition, we present the first study of using secondary ion energy distribution to determine the voltage offsets for analyzing In implants (Fig. 5) and that data will be shown in a full paper.

SS-ThP-19 Monitoring the Dynamics of Carbon-Carbon Bond Formation in Solid-Gas Heterogeneous Photoinduced Reactions, Aakash Gupta, K. Blackman, A. Rodriguez, Department of Physics, University of Central Florida; *M. Vaida,* Department of Physics and Renewable Energy and Chemical Transformations Cluster, University of Central Florida

Carbon-carbon (C-C) bond formation is paramount for a large variety of man-made chemicals such as commodity chemicals, synthetic materials, and pharmaceuticals. Monitoring the dynamics of the C-C bond formation in real time at surfaces and how this is influenced by the surface properties could be a game changer in improving the efficiency of various heterogeneous reactions. To study the dynamics of C-C bond formation, an experimental technique is employed that combines time-of-flight mass spectrometry with pump-probe spectroscopy and fast surface preparation

with molecules. CH_3I and CO are used as precursor molecules. These molecules are dosed on metal oxides such as titanium dioxide and cerium oxide, on which the reactions are monitored.

The reaction is triggered by the pump laser pulse at a central wavelength of 266 nm which excites CH_3I into the dissociative A-band, which leads to the formation of CH_3 and I fragments. Subsequently, the probe laser pulse in ultraviolet spectral domain will ionize the reaction intermediates and final products, which are immediately removed from the surface by a static electric field and detected by the time-of-flight mass spectrometer. By varying the pump-probe time delay, the formation dynamics of CH_3 intermediate, as well as the reaction of CH_3 with CO , which leads to the formation CH_3CO (acetyl) and finally to CH_3COCH_3 (acetone) will be monitored. Details on CO and CH_3I partial pressure dependence as well as the influence of the surface composition and temperature will be presented.

SS-ThP-20 Transient Kinetics Study of CO Adsorption and Dissociation on a Ru (001) Surface Crystal, *Eliseo Perez Gomez*, Stony Brook University; *A. Boscoboinik*, Center for Functional Nanomaterials, BNL; *S. Sikder*, Stony Brook University

The adsorption and dissociation of carbon monoxide (CO) on metal surfaces is a fundamental reaction with many applications in the field of surface chemistry. Particularly, this research studied the reaction between CO and a Ru (0001) single crystal. The adsorption and dissociation of the gas were investigated through the use of techniques such as infrared spectroscopy (IR) and mass spectroscopy (MS). We also employed a pulsing valve system, where controlled pulses of CO (and other reactant gases) influence the surface reaction. The effects of temperature and pressure on the adsorption kinetics and subsequent dissociation were explored in detail, to reach a broad understanding in the transient kinetics of the reaction. By modifying various parameters, the intention is to optimize the dynamic reaction conditions. Through this comprehensive approach, we sought to contribute valuable insights into the mechanisms driving CO adsorption and dissociation, with implications for catalysis and surface science applications.

SS-ThP-21 Bimetallic Pt-Sn and Ni-Cu Catalysts for Dehydrogenation Reactions Designed for Hydrogen Storage and Transportation, *Mengxiang Qiao*, *F. Li*, University of South Carolina; *A. Ahsen*, Gebze Technical University, Turkey; *D. Chen*, University of South Carolina

The use of liquid organic hydrogen carriers (LOHC) for the safe transport and storage of hydrogen requires the development of more selective catalysts for the dehydrogenation step. For example, the methylcyclohexane (MCH)-toluene pair is an attractive choice for a LOHC system, but a more selective dehydrogenation catalyst that is less prone to deactivation by fouling is needed. The bimetallic Pt-Sn and Cu-Ni systems are promising candidates for selective dehydrogenation catalysts; the addition of Sn to Pt catalysts is known to improve stability and decrease deactivation, and the addition of Cu to Ni catalysts may serve to break up the Ni ensembles that are responsible for nonselective decomposition. Model catalyst surfaces are prepared in ultrahigh vacuum (UHV) by deposition of thin films of Sn and Cu on Pt(111) and Ni(111) respectively, as well as by sequential vapor deposition of the two metals on a rutile $\text{TiO}_2(110)$ support. The surface compositions and bimetallic cluster sizes are investigated with low energy ion scattering, temperature programmed desorption with CO as a probe molecule, X-ray photoelectron spectroscopy, and scanning tunneling microscopy. Our studies have shown that Sn on Pt clusters tend to be rich in Sn due to the higher surface free energy of Pt compared to Sn, but cluster surfaces with a low concentration of Sn can also be prepared by deposition of small coverages of Sn on existing Pt clusters. In contrast, Cu on Ni clusters exhibit low Cu concentrations due to the diffusion of Cu into Ni, which is consistent with the facile alloying of Ni and Cu. A high-sensitivity recirculating loop microreactor system has been constructed for investigating the activity for MCH dehydrogenation on the bimetallic model surfaces under catalytically relevant atmospheric pressures; the microreactor is coupled directly to the UHV chamber so that the model catalysts can be transferred between the microreactor and UHV chamber without exposure to air.

SS-ThP-22 Coverage-Dependent Adsorption and Reactivity of Formic Acid on $\text{Fe}_3\text{O}_4(001)$, *Jose Ortiz-Garcia*, Pacific Northwest National Laboratory; *M. Sharp*, Washington State University; *Z. Novotny*, *B. Kay*, *Z. Dohnalek*, Pacific Northwest National Laboratory

Formic acid (FA) is a crucial intermediate in important catalytic reactions such as Fischer-Tropsch synthesis and water-gas shift. On oxide surfaces, FA generally undergoes decomposition to CO or CO_2 through decarbonylation or decarboxylation mechanisms. We study the adsorption of FA on the

reconstructed $\text{Fe}_3\text{O}_4(001)$ surface, followed by stepwise annealing using a combination of scanning tunneling microscopy (STM), x-ray photoelectron spectroscopy, low-energy electron diffraction, and temperature programmed desorption (TPD). Dissociative adsorption of formic acid leads to the adsorbed formate and hydroxyl species on the surface. At low coverages, isolated formates and hydroxyls are observed. At intermediate coverages, local clustering of formate is observed, giving rise to both (1×1) and (2×1) surface periodicities. A fully saturated surface shows formates arranging predominately in the (1×1) periodicity but retains some formates in the (2×1) periodicity in agreement with prior studies.¹ Annealing the surface to 450 K induces the formation of a well-ordered surface with a (1×1) periodicity, which results in the lifting of the surface reconstruction. Stepwise annealing enables monitoring of formate reactivity and surface structure changes. Two major peaks are observed via TPD at 525 and 565 K, indicating that the formate undergoes decarbonylation to CO and H_2O , with decarboxylation to CO_2 as a minor reaction pathway. STM reveals that annealing to 550 K leads to a partial recovery of the surface reconstruction and a possible formation of single oxygen vacancy defects. Further annealing to 650 K, which leads to the conversion of all formate species, reveals the formation of pits extended along the Fe rows. This is consistent with the non-stoichiometric formic acid decarboxylation accompanied by water formation proceeding via the Mars van Krevelen mechanism. We are currently focusing on understanding the initial stages of pit formation and the role of hydroxyls in reaction mechanisms. This work underscores the significance of fundamental studies to unravel the effect of structural changes on reaction mechanisms and dynamics.

SS-ThP-23 Using Single-Layered COFs to Stabilize Single-Atom Catalysts on Model Surfaces, *Yufei Bai*, *D. Wisman*, *S. Tait*, Indiana University Bloomington

Single-atom catalysts (SACs) combine the advantages of homogeneous and heterogeneous catalysts by limiting the reaction sites to isolated single metal atoms with well-defined chemical properties. A metal-ligand coordination method to stabilize SACs has been developed by the Tait group, in which 1,10-phenanthroline-5,6-dione (PDO) was used as ligand to coordinate with metal such as Pt, Fe, and Cr. To further improve the stability of SACs and increase the metal loading, we have synthesized single-layered covalent organic frameworks (sCOFs) on model surfaces under ultra-high vacuum (UHV) conditions or under ambient conditions. These networks with high porosity and stability were used to confine single Pt atoms coordinated with ligands into sCOF pores. Under UHV conditions, the successful formation of sCOF with regular hexagonal pores on the Au(111) surface was achieved by surface-mediated Ullmann radical coupling of 1,3,5-tris-(4-bromophenyl)benzene (TBB). Further sequential deposition of PDO ligand and Pt on the TBB-sCOF surface allowed the formation of single-site Pt catalysts by coordination interaction. The scanning tunneling microscopy (STM) images show the confinement of PDO in the sCOF pores, while X-ray photoelectron spectroscopy (XPS) has proven the existence of oxidation state of Pt, which is an indication of the single atom character. Under ambient conditions, an imine-linked sCOF was formed on the highly oriented pyrolytic graphite (HOPG) surface by a solid-vapor interface mechanism which allows for a high quality sCOF with long-range order. STM characterization has shown that regular sCOF networks with few defects were formed on the HOPG surface. This sCOF is facile to prepare and can be stored stably under ambient conditions for several weeks. These systems which combine the COF and metal-ligand coordination strategy to stabilize SACs offer the possibility to achieve higher stability and greater loading in SACs.

SS-ThP-24 N-doped Graphene Synthesis through N_2^+ Irradiation, *Buddhika Alupotho Gedara*, *P. Evans*, *Z. Dohnalek*, *Z. Novotny*, Pacific Northwest National Laboratory

Hydrogen (H_2) is one of the most promising clean and renewable energy sources. Nevertheless, the storage of hydrogen shows poor performance due to the low gravimetric and volumetric densities. Nitrogen-doped graphene (Gr) has been identified as a potential material for H_2 storage. Here, we study the growth of Gr on a Ru(0001) surface by chemical vapor deposition (CVD) of pyridine and N-doping through N_2^+ beam irradiation using scanning tunneling microscopy (STM) and x-ray photoelectron spectroscopy (XPS). A high-quality Gr film with low N densities was obtained by pyridine CVD on Ru(0001) at 1063 K. Higher concentrations of N-dopants were introduced on the Gr/Ru(0001) through low-energy N_2^+ irradiation at 100 eV. Nitrogen can be embedded in the Gr lattice preferentially in two configurations, namely graphitic N (N substituted in the C lattice) and pyridinic N (substitutional N next to a C vacancy). Atomically resolved STM images of graphitic and pyridinic-N defects

demonstrate their preferential locations within the Gr Moiré. XPS shows that coverage of up to 3.9% of pyridinic-N and 2.3% of graphitic N can be embedded into the high-quality Gr film using N₂ irradiation at room temperature, indicating a preferential formation of pyridinic N over graphitic N. Only graphitic N was observed upon annealing the ion-irradiated Gr/Ru(0001) to 1063 K, revealing higher thermal stability of graphitic N over pyridinic N. Our current efforts center on the adsorption studies of atomic hydrogen, its interactions with N dopants, and thermally induced diffusion.

SS-ThP-25 Coverage Dependent Interaction of N-Methylaniline with Pt (111) Surface, Bushra Ashraf, D. Austin, University of Central Florida; N. Brinkmann, K. Al Shamery, Carl von Ossietzky University Oldenburg, Germany; T. Rahman, University of Central Florida

The study of N-methylaniline (NMA) coverage dependent adsorption and reaction on the Pt(111) surface has gained attention because of the alkyl and aromatic amine interaction with transition metal surface. In this work, we use Density functional theory (DFT) simulations and experiment to study the structural and electronic properties of coverage dependent adsorption of NMA on Pt(111) surface. Firstly, we found that the molecule adheres to the surface by forming bonds with both the phenyl ring and the nitrogen (N) atom at the lower coverage. However, as coverage increases, a fascinating phenomenon unfolds: the phenyl ring undergoes a distinctive tilting motion away from the surface. This tilting is accompanied by a change in the incline angle, transitioning from a mere 2° at low coverage (approximately 0.02 ML) to a substantial 33° at higher coverage (around 0.17 ML). This structural transformation also brings about a variation in the adsorption energy, shifting from -2.9 eV at low coverage to -1.5 eV at high coverage. Secondly, Bader charge analysis provided further insights into these interactions. At low coverage, the charge is shared between the N atom and the surface Pt atom and from the surface to the carbon (C) atoms within the phenyl ring. In contrast, at higher coverage, charge sharing primarily takes place through the N atom to the surface. This shift towards a more robust and bi-centered bonding with the surface at lower coverage indicates an increased propensity for molecular dissociation under these conditions. Finally, the analysis of the projected density of states shed more light on revealing the hybridization of the N p_z orbital with the Pt d_{z²} orbital at higher coverage. Conversely, at low coverage, hybridization of the carbon p_z orbital with the Pt d_{z²} orbital was observed, alongside Pt-N hybridization. These observations regarding molecular adsorption at different coverages indicated that, at high coverage, the molecule easily lifts off intact from the surface, while at low coverage, it tends to break into smaller fragments, consistent with experimental findings.

SS-ThP-26 Effect of an Electric Field on the Co Adsorption on Pt, Steven Arias, D. Stacchiola, J. Boscoboinik, Brookhaven National Laboratory

The adsorption of carbon monoxide (CO) on platinum (Pt) has been widely studied in the literature. Pt is one of the most frequently used active metals in catalysis, with CO playing an important role in many reactions, including hydrogenation, oxidation, and car emission controls. Here, we present our preliminary progress on the study of the effect of an electric field on CO adsorption on Pt. To do this, we designed a device that can apply a direct electric field to the surface of our Pt catalyst. A layer of porous alumina was synthesized on a Pt film, to allow CO molecules to diffuse through, making the underlying Pt accessible. A layer of graphene is added on top of the porous layer to complete the device. The bottom Pt and the top layer of graphene are biased to apply an electric field that directly interacts with the Pt surface where the CO is being adsorbed. Using infrared reflective adsorption spectroscopy (IRRAS) we study the effect of such fields on CO adsorption.

SS-ThP-27 Generating Defects in Semiconductor Monolayers on Metal Surface, Sayantan Mahapatra, J. Guest, Argonne National Laboratory, USA

Nanoscale observation and deliberate engineering of atomic defects within semiconductor transition metal dichalcogenides (TMDs) hold significant importance for their utilization in cutting-edge quantum optics and nano-electronic devices. Here, we demonstrate a versatile approach in generating single defects on TMDs monolayers using a photon source. The newly generated defects were visualized via scanning tunneling microscopy (STM) at room temperature at the atomic level. These defects can act as single-photon emitters (SPE) and their performance remains excellent in high vacuum conditions. Furthermore, our simulations provide insights into the defect formation energies on metal surfaces compared to an insulating surface. The charge transfer between the metal and monolayer TMDs plays a significant role in generating the defects. Furthermore, simulation also

sheds light on the mono- or di-chalcogen vacancies as the potential candidates for these defects, thereby providing a direct match between theory and experiment.

SS-ThP-28 Characterization of Oxygen on Rh-Based Model Catalysts, Maxwell Gillum, A. Gonzalez, E. Serna-Sanchez, A. Kerr, S. Danahey, D. Killelea, Loyola University Chicago

The studies presented investigate the influence that surface and defect geometry have on the kinetics and reactivity of oxygen on various Rh-based model catalysts. The experiments focus on gaining structural information about the oxygen species present on the surface under various oxidative conditions utilizing scanning tunneling microscopy (STM) and low energy electron diffraction (LEED). These techniques are used in unison with temperature programmed desorption (TPD) and Meitner-auger electron spectroscopy (MAES) to identify optimal conditions for further study

SS-ThP-30 Kinetic Monte Carlo Modelling of Hydrogen Oxidation on Pt/Pd Surfaces, Alexander Kandratsenka, MPI for Multidisciplinary Sciences, Germany

Recent velocity-resolved kinetics measurements of water production from gas-phase H₂ and O₂ at Pt and Pd surfaces revealed the complex dependence of reaction rates on the oxygen coverage and step density. We aim to clarify the detailed mechanisms of these oxidation reactions by means of Kinetic Monte Carlo approach with adsorption energies, reaction barriers and transition state geometries determined from *ab initio* calculations, and rate constants derived from the Transition State Theory.

SS-ThP-31 Epoxidation of Styrene on Ag(111) Surface, Rasika E. A. Dissanayake, Institute of Physical Chemistry, University of Göttingen, Germany; A. Dorst, K. Benfreha, Institute For Physical Chemistry, University Of Goettingen, Germany; D. Killelea, Loyola University Chicago; T. Schaefer, Institute For Physical Chemistry, University Of Goettingen, Germany

Epoxidation of olefins on catalytic surfaces is considered to play a major role in chemical industries where Ag-based catalysts are prominently used due to the surface chemistry of the alkene/silver system. However, the fundamentals of olefin oxidation on metal surfaces are still not well understood. Therefore, in this research, we use controlled ultra-high vacuum conditions to understand the fundamentals of the styrene oxidation on an Ag(111) surface.

For this purpose, we initially formed an atomic oxygen layer on the Ag(111) surface by dosing 10% NO₂ seeded in He at 510 K surface temperature using a supersonic molecular beam. Subsequently, we dosed styrene onto the oxidized silver surface. Desorbing products from the surface were ionized using focused laser radiation and ionized molecules were detected using an ion imaging system equipped with micro-channel plates, a phosphor screen, and a CMOS camera.

We systematically form nucleophilic and electrophilic oxygen at the silver surface using two different preparation methods. When the surface was sputtered with Ar⁺ ions and annealed to 700 K we predominantly formed nucleophilic oxygen, which led to the complete combustion of the styrene. When we only annealed the surface to 700 K, the surface predominantly formed electrophilic oxygen, which led to the formation of styrene oxide. We identified electrophilic oxygen being accompanied by the formation of subsurface oxygen, which seems to amplify the production of styrene oxide.

Keywords: Epoxidation, Ion imaging, Molecular beam, Silver, Styrene

SS-ThP-32 Weakly and Strongly Adsorbed H₂O Layers on Hydroxylated SiO₂ Surfaces: Dependence on H₂O Pressure at Various Temperatures, Samantha Rau, R. Hirsch, M. Junige, University of Colorado Boulder; A. Rotondaro, H. Paddubrouskaya, K. Abel, Tokyo Electron America, Inc.; S. George, University of Colorado Boulder

Although H₂O adsorption on SiO₂ surfaces has been studied extensively, there are still many questions about the nature of the H₂O adsorbed layer. In this work, the H₂O layer thickness on flat hydroxylated SiO₂ surfaces was examined in a vacuum environment using in situ spectroscopic ellipsometry (SE). The H₂O water layer thickness was measured versus H₂O pressure at various temperatures. Complementary Fourier transform infrared (FTIR) analysis was also performed on SiO₂ powders.

Flat SiO₂ surfaces were hydroxylated using H₂O₂ plasma exposure to produce a hydrophilic surface with a water contact angle of < 10°. The in situ SE measurements were then conducted in a warm-wall vacuum chamber designed with a temperature-controlled sample stage. The H₂O layer thickness was measured versus pressure at various temperatures

Thursday Evening, November 7, 2024

(Figure 1). The H₂O pressures were varied up to the saturation H₂O vapor pressure corresponding to the sample temperature. The H₂O layer thickness versus relative humidity was consistent with general expectations from the BET adsorption isotherm model.

The SE measurements showed that there were two distinct types of H₂O layers: a weakly adsorbed layer and a strongly adsorbed layer (Figure 2). The weakly adsorbed layer could be added or subtracted by increasing or removing the H₂O pressure. The strongly adsorbed layer was not lost by removing the H₂O pressure. However, the strongly adsorbed layer could be desorbed by heating the sample stage to 120°C. The SE measurements characterized the layer thicknesses for the weakly and strongly adsorbed layers versus H₂O pressure at various sample temperatures.

Using repeating H₂O exposures, the strongly adsorbed layer reached an approximate plateau at ~1 Å at various temperatures. In contrast, the weakly adsorbed layer obtained higher thicknesses at larger H₂O pressures. For example, the weakly adsorbed layer thickness was 7 Å at 92% relative humidity at 30.4°C (30 Torr). The FTIR investigations on SiO₂ powders were in qualitative agreement with the SE studies. These studies confirm the existence of a strongly adsorbed vicinal layer and a weakly adsorbed layer explained by the BET model on hydroxylated SiO₂.

Surface Science

Room 120 - Session SS+AMS+AS+CA+LS-FrM

Advanced Surface Characterization Techniques & Mort Traum Presentation

Moderators: Donna Chen, University of South Carolina, Charles Sykes, Tufts University

8:15am **SS+AMS+AS+CA+LS-FrM-1 Infrared Spectroscopy as a Surface Science Technique**, *Michael Trenary*, University of Illinois - Chicago **INVITED**
Infrared spectroscopy is widely used to probe the vibrational properties of molecules in the gas, liquid, and solid phases. On the other hand, precise information on the structure and chemistry of solid surfaces, and of molecular adsorbates on solid surfaces, is best gained through use of surface science methods. These methods generally entail the use of single crystals, ultrahigh vacuum conditions, and surface sensitive techniques. Reflection absorption infrared spectroscopy (RAIRS) is a surface sensitive technique that can be used in ultrahigh vacuum to study molecular adsorption on well characterized metal single crystal samples. Unlike many other surface science methods, it can also be used under elevated gas pressures. The spectra obtained display features that are quite distinct from those of other phases of matter. For example, in the gas phase, rotational fine structure greatly complicates the appearance of the spectra but is absent in the spectra of adsorbed molecules. In the liquid phase, spectra are broadened by both static and dynamic effects often making it difficult to resolve vibrational peaks due to different chemical species. In polycrystalline molecular solids, molecules are randomly oriented relative to the electric field directions of the infrared radiation, limiting the value of the spectra as a structural probe. In contrast, when molecules adsorb on metal surfaces, they often adopt a definite orientation with respect to the surface normal. This orientation can be deduced through the surface dipole selection rule, which states that only normal modes with a component of the dynamic dipole moment oriented along the surface normal will be allowed. While IR spectroscopy in several forms has long been used to study molecular adsorption on supported transition metal catalysts, the high degree of heterogeneity of the catalyst surfaces leads to very broad peaks, with full width at half maxima (FWHM) of 10-50 cm^{-1} . In contrast, the FWHM of peaks measured with RAIRS on well-ordered metal surfaces can be quite narrow, in some cases even less than 1 cm^{-1} . When a polyatomic molecule exhibits sharp peaks throughout the mid-IR range, the advantages of performing RAIRS with a Fourier transform infrared spectrometer are most pronounced. This talk will cover the speaker's forty years of research using the technique of RAIRS to study molecular adsorbates on metal surfaces.

8:45am **SS+AMS+AS+CA+LS-FrM-3 Modeling Pipeline Surface Chemistry: Reaction of Monochloramine on Iron Surfaces**, *Kathryn Perrine, S. Pandey, O. Agbelusi*, Michigan Technological University

Monochloramine (NH_2Cl), a secondary disinfectant, is utilized to treat pathogens in the municipal water system, producing fewer halogenated disinfection by-products and lasting longer than free chlorine (hypochlorite). Although a weaker oxidant, NH_2Cl has the potential to corrode the surface of pipeline materials resulting in the dissolution of unwanted species. Copper and lead pipelines have been shown to corrode in chloramine solutions, however on iron materials the surface chemistry is unexplored. Complex chemistry occurs on the surface of pipelines at solution/metal interfaces, thus providing catalytic sites for dissociation, decomposition, and degradation. Iron comprises distribution pipelines and also exists as oxides in soils in the natural environment. Redox reactions occur on the surface of iron materials, thus initiating surface corrosion. Here, various active sites on iron are produced and known for high reactivity with nitrogen compounds. Our group employs a surface science approach to uncovering mechanisms at complex interfaces.

In this study, the reaction of monochloramine (NH_2Cl) was investigated on single crystal Fe(111) in ultra-high vacuum at the gas/solid interface using *in situ* infrared reflection absorption spectroscopy and Auger electron spectroscopy. At -160 °C, NH_2Cl molecularly adsorbs to the surface while the annealing leads to the loss of key vibrational modes, suggesting that either molecular desorption or dissociation occurs. These observations are contrasted with our findings at the solution/iron interface, where polarized modulated infrared reflection absorption spectroscopy (PM-IRRAS), ATR-FTIR, XPS, and XRD were used to assess the various regions after corrosion and their film growth. In solution, localized heterogeneous corrosion

products were observed and identified, suggesting different reaction pathways exist in strongly oxidizing solutions. These findings are important for understanding the mechanism of chloramines and water disinfectants on iron interfaces relevant for water quality, material degradation, and other complex environmental processes.

9:00am **SS+AMS+AS+CA+LS-FrM-4 Development of Tip-Enhanced Raman Spectroscopy for Solid-Liquid Interfaces**, *Naihao Chiang*, University of Houston

Tip-enhanced Raman spectroscopy (TERS) combines the spatial resolution of scanning probe microscopy (SPM) with the chemical sensitivity of Raman spectroscopy. TERS with sub-nanometer resolution has been demonstrated under ultrahigh vacuum conditions. We aim to extend this unprecedented chemical mapping capability to interfacial studies under the solution phase. Specifically, we have developed a scanning ion-conductance microscope for TERS (SICM-TERS) capable of interrogating soft samples. In this presentation, the instrumental design will be discussed first. SICM-TERS probe fabrication and evaluation will be followed. Then, a distance-dependent SICM-TERS measurement on two-dimensional MoS_2 sheets will be used to assess the strain created by the SICM probe in close proximity. Our results demonstrate the potential of combining TERS with SICM for obtaining chemical information at interfaces, thus setting the stage for future investigation into soft materials in electrolytic environments.

9:15am **SS+AMS+AS+CA+LS-FrM-5 Ion Based Pump-Probe: Probing the Dynamics Following an Ion Impact**, *Lars Breuer, L. Kalkhoff, A. Meyer, N. Junker, L. Lasnik*, Universität Duisburg-Essen, Germany; *Y. Yao, A. Schleife*, University of Illinois at Urbana Champaign; *K. Sokolowski-Tinten, A. Wucher, M. Schleberger*, Universität Duisburg-Essen, Germany

The study of ion-surface interactions is crucial for understanding material properties and their atomic-level dynamic responses. The transient nature of these interactions, occurring on ultrafast time scales, has so far limited direct experimental observation and has left the field reliant on computer simulations. Existing experimental methods, such as pump-probe techniques, have faced challenges in generating and precisely timing short, monoenergetic ion pulses essential for capturing these ultrafast phenomena.

Our group has pioneered a novel approach that overcomes these limitations by generating the world's shortest monoenergetic ion pulses in the keV regime, with a current duration of approximately 5 ps. These pulses are produced using femtosecond photoionization of a geometrically cooled gas jet, coupled with miniaturization of the ionization section.

In our experiments, we conduct ion-based pump-probe experiments observing the emission of hot electrons post-ion impact, similar to processes studied in two-photon photoemission (2PPE) experiments. Our findings not only demonstrate the feasibility of our approach and provide direct measurements of the ion pulse characteristics but also offer insights into the non-equilibrium dynamics of electronic excitation in solids following an ion impact. We can track the electronic excitation and determine the temporal evolution of a pseudo electron temperature.

This research opens new avenues for understanding the fundamental processes underlying ion-solid interactions, with significant implications for semiconductor manufacturing and materials science. Our work sets a new standard for temporal resolution in the study of ion-induced phenomena and lays the groundwork for future innovations in the field.

9:30am **SS+AMS+AS+CA+LS-FrM-6 How Hot Plasmonic Heating Can Be: Phase Transition and Melting of P25 TiO_2 from Plasmonic Heating of Au Nanoparticles**, *W. Lu, R. Kayastha, B. Birmingham, B. Zechmann, Zhenrong Zhang*, Baylor University

Plasmonic heating has been utilized in many applications including photocatalysis, photothermal therapy, and photocuring. However, how high the temperature can be reached for the surrounding media due to the collective heating of the plasmonic nanoparticles (NPs) and the impact of the heat dissipation on the surrounding media is not clear. Herein we studied the impact of plasmonic heat generated by resonantly excited gold (Au) NPs on P25 TiO_2 nanoparticle film. Under 532 nm continuous laser irradiation at the surface of the Au- TiO_2 , the surface evaporation of Au nanoparticles and phase transition of TiO_2 were observed at moderate laser power. More importantly, as high as the melting point of TiO_2 of 1830°C is confirmed from the molten TiO_2 rutile phase. When Au/ TiO_2 was irradiated with an off-resonance laser at 638 nm, no phase transformation or melting of TiO_2 was observed. The temperature calculation shows that the heating generated by Au nanoparticles is not localized. The collective heating from an ensemble of Au nanoparticles in the irradiated area produces a global

Friday Morning, November 8, 2024

temperature rise that melts TiO₂. Our results suggest that the photothermal effect could be a major mechanism in the plasmon-assisted photocatalytic reactions. The experimental observation of the high temperature of the supporting media suggests new applications for utilizing plasmonic heating, for example, additive manufacturing.

9:45am **SS+AMS+AS+CA+LS-FrM-7 Kinetics and Dynamics of Recombinative Desorption of Oxygen from Silver and Rhodium Surfaces, Dan Killelea**, Loyola University Chicago

The ability to obtain velocity distributions of molecules desorbing from surfaces with both high temporal precision and angular resolution provide newfound insight into both the kinetics and the dynamics of recombinative desorption and subsurface emergence.

I will discuss our observations of subsurface oxygen emerging from beneath Rh(111) and how the velocity distribution shifts in comparison to the thermally-dominated desorption pathways found for surface-adsorbed oxygen. In addition, it was recently discovered that decomposition of oxygenaceous surface phases on Ag(111) also exhibit pronounced shifts in the energetics of the desorbing oxygen molecules. I will discuss these observations and their potential impacts in oxidation reactions in heterogeneously catalyzed reactions over transition metal surfaces.

10:00am **SS+AMS+AS+CA+LS-FrM-8 Mort Trau Award Announcement**,

10:30am **SS+AMS+AS+CA+LS-FrM-10 Unveiling Surface Mysteries with XPS Lab from Scienta Omicron, Tamara Sloboda**, Scienta Omicron, Sweden; *P. Amann*, Scienta Omicron, Germany; *B. Gerace, F. Henn, A. Yost, X. Zhang*, Scienta Omicron; *M. Lundwall*, Scienta Omicron, Sweden

Surface analysis is paramount for understanding material properties, and Scienta Omicron's XPS Lab system excels in this realm. Featuring a compression unit for superior count rates and sensitivity, it offers unparalleled quantitative XPS enabled by a true counting multi-anode detector inside the Argus CU analyser. This unique detector employs 128 individual counters connected to a striped-anode array. With a linear response extending to the highest count rates and an exceptional dynamic range, it ensures high resolution precise measurements across various sample types.

The versatility of XPS Lab is evident through its scanning, imaging, snapshot, and dynamic measurement modes (see Figure 1), enabling researchers to tailor their experiments to specific needs. The chemical state mapping capability of the XPS Lab provides comprehensive insights into surface chemistry, empowering researchers to unravel complex phenomena.

Illustrating its prowess, case studies span catalysis, energy storage, semiconductor technology, and biomaterials, showcasing its ability to address diverse research challenges. Recent enhancements further strengthen its capabilities, solidifying XPS Lab as the premier choice for XPS analysis.

In summary, Scienta Omicron's XPS Lab system offers unmatched precision, sensitivity, and versatility, driving advancements in surface science and materials research.

10:45am **SS+AMS+AS+CA+LS-FrM-11 Investigation of Stannane (SnH₄) Decomposition and Sticking Coefficient on Varied Metal Surfaces in EUV Lithography Environments, Emily Greene, N. Barlett, D. Qerimi, D. Ruzic**, University of Illinois at Urbana-Champaign

In the context of extreme ultraviolet (EUV) lithography, the evaporation of tin droplets frequently leads to the deposition of tin on various chamber surfaces, including collector mirrors. A prevalent method to remove this tin deposition involves hydrogen plasma etching, which transforms the deposited tin into stannane (SnH₄). This compound, existing in a gaseous state under operational conditions, can be evacuated from the chamber using a vacuum pump. However, stannane is characterized by its instability, tending to decompose and adhere to various surfaces within the chamber.

To systematically study the decomposition behavior of stannane, a specialized experimental chamber has been designed. This chamber integrates a load-lock mechanism for inserting a test tube containing liquid stannane into a loading section, which is isolated from the main vacuum chamber by a valve. Within the main chamber, a quartz crystal microbalance (QCM), regulated by a cartridge heater, measures the mass of stannane deposits. The QCM will be set to temperatures between 30-300 °C. Upon opening the valve, the stannane vaporizes and interacts with the temperature-controlled QCM, facilitating the quantitative

determination of the sticking coefficient as a function of both the surface material and the temperature.

Stannane is synthesized through the reaction of LiAlH₄, SnCl₄, C₈H₁₈O, and C₄H₁₀O₂. The four chemicals are mixed in a 3-neck flask while under vacuum. The reaction produces SnH₄ which flows through three U-tubes traps. The first trap is held at -96 °C to trap precursors, the second two traps are held at -196 °C and trap the stannane. The stannane is increasingly pure the more traps are used.

This investigation aims to understand and quantify the mechanisms of stannane deposition and decomposition, enhancing the maintenance and efficiency of EUV lithographic systems by optimizing the cleaning protocols for tin contamination.

11:00am **SS+AMS+AS+CA+LS-FrM-12 First Principles Methods for Predicting Surface Reaction Mechanisms for Chemical Functionalization of Semiconductor Surfaces, Roberto Longo, S. Sridhar, P. Ventzek**, Tokyo Electron America Inc.,

The density of semiconductor devices continues to increase, accompanied by the subsequent scaling down of the critical dimension (CD) size, which is now on the order of a few nanometers. This results in device structure changes, from two-dimensional (2D) to three-dimensional (3D) structures, because the CD size has reached its limit of reduction. To accomplish this, precise chemical modification of the required surfaces with atomic scale precision is key to obtain the desired geometric control. Precise modification implies being able to leverage knowledge of individual plasma born species and surface interactions. Unfortunately, species specific chemical interaction mechanisms in the context of reactive ions and chemical etching are still poorly understood for the full range of chemical environments at play. Once dissociated in plasma radicals, there might be a wide array of compositions. For similar atomic compositions, variations in the molecular structure of the chemical precursor can also result in significant differences as to the surface modifications and subsequent etching characteristics. The chemical nature of the surface including coverage and chemical activity add significant dimensionality to the problem of controlling plasma surface interactions in general. We divide the problem of elucidating plasma surface interactions into two major categories for practical purposes: hydrofluorocarbon driven for oxide etch and halogen driven for silicon etch. We present here semiconductor surface modeling with general characteristics and investigate the reaction mechanisms undergone by a large variety of hydrofluorocarbon molecular precursors using density-functional theory (DFT), with a focus on reactive halogen adsorption. Given the large parameter space of this problem, we describe computational approaches that efficiently and accurately generate fundamental data. Physical and chemical surface reactions and the corresponding byproducts are identified, obtaining self-limitation thresholds for each specific functionalizing chemistry. Therefore, our computational results provide valuable insights on the complex physical, chemical, and dynamic molecular and ion interactions with functionalized semiconductor surfaces, paving the road for designing tailored strategies with the desired outcome for each specific system.

Bold page numbers indicate presenter

— A —

Abel, K.: SS-ThP-32, 30
 Adachi, Y.: SS+2D+AMS-WeA-2, 19
 Agbelusi, O.: SS+AMS+AS+CA+LS-FrM-3, 32
 Ahmad, M.: SS+2D+AMS-WeA-1, **19**
 Ahmed, A.: 2D+AP+EM+QS+SS+TF-TuM-6, 8
 Ahsen, A.: SS-ThM-1, 22; SS-ThP-21, 29
 Al Shamery, K.: SS-ThP-25, 30
 Alanwoko, O.: 2D+AP+EM+QS+SS+TF-TuM-14, 9
 Alfonso, D.: SS+CA+LS-TuM-3, 10
 Alupothe Gedara, B.: SS-ThP-24, **29**
 Amann, P.: SS+AMS+AS+CA+LS-FrM-10, 33; SS+CA+LS-TuA-3, **13**
 Arias, S.: SS-ThP-26, **30**
 Ariga-Miwa, H.: SS+AMS-MoM-4, 1
 Árnadóttir, L.: SS-ThM-7, **22**
 Arsyad, R.: SS+CA+LS-TuA-13, 15
 Asakura, K.: SS+AMS-MoM-4, 1
 Ashraf, B.: SS-ThP-25, **30**
 Asscher, M.: SS-ThP-1, 25
 Asthagiri, A.: SS+AMS-MoA-12, 6; SS+AMS-MoA-3, 4; SS+AMS-MoA-9, 5
 Austin, D.: SS+AMS-MoA-2, **4**; SS-ThP-25, 30
 Auwärter, W.: SS+2D+AMS-WeM-5, **16**
 Ayoade, O.: SS+CA+LS-TuA-5, **14**

— B —

Baber, A.: SS+AMS-MoA-11, 5
 Bae, D.: SS+AMS-MoA-9, 5
 Bai, Y.: SS-ThP-23, **29**
 Balajka, J.: SS+2D+AMS-WeA-5, 19; SS+AMS-MoM-12, 2
 Balasubramanian, G.: SS+2D+AMS-WeA-12, 20
 Banerjee, P.: SS+AMS-MoM-5, 1
 Bara, J.: SS+2D+AMS-WeM-17, 17
 Barba-Nieto, I.: SS-ThP-9, **26**
 Barlett, N.: SS+AMS+AS+CA+LS-FrM-11, 33
 Batzill, M.: 2D+AP+EM+QS+SS+TF-TuM-13, **8**; 2D+AP+EM+QS+SS+TF-TuM-14, 9
 Benfreha, K.: SS-ThP-31, 30
 Bergsman, D.: SS+2D+AMS-WeM-13, **17**
 Berriel, N.: SS+AMS-MoM-5, 1
 Bilal, L.: 2D+LS+NS+SS-TuA-12, **13**
 Birmingham, B.: SS+AMS+AS+CA+LS-FrM-6, 32
 Blackman, K.: SS+AMS-MoM-5, 1; SS+CA+LS-TuA-12, 15; SS-ThP-19, 28
 Blades, W.: SS+2D+AMS-WeA-11, 20
 Bliem, R.: SS+AMS-MoA-1, 4; SS+AMS-MoM-6, **2**
 Boden, D.: SS-ThP-10, 27
 Boehm, A.: 2D+LS+NS+SS-TuA-11, 12
 Borgschulte, A.: SS-ThP-11, 27
 Boscoboinik, A.: 2D+LS+NS+SS-TuA-12, 13; SS-ThP-20, 29
 Boscoboinik, J.: SS+2D+AMS-WeA-1, 19; SS+2D+AMS-WeM-16, **17**; SS-ThP-26, 30
 Bostwick, A.: 2D+LS+NS+SS-TuA-1, **12**; 2D+LS+NS+SS-TuA-3, 12
 Breuer, L.: SS+AMS+AS+CA+LS-FrM-5, **32**
 Brinkmann, N.: SS-ThP-25, 30
 Brohet, M.: SS+2D+AMS-WeA-10, 20
 Bruce, J.: SS+CA+LS-TuM-14, **11**
 Butler, A.: 2D+AP+EM+QS+SS+TF-TuM-6, 8
 — C —
 Cabanillas, A.: 2D+AP+EM+QS+SS+TF-TuM-6, 8
 Campbell, C.: SS+AMS-MoM-15, 3; SS-ThA-3, **24**
 Campi, G.: SS+2D+AMS-WeA-15, 21
 Campos Jara, S.: SS+2D+AMS-WeA-10, 20
 Carreño, V.: SS+2D+AMS-WeA-15, 21
 Carreño-Díaz, V.: SS+2D+AMS-WeM-3, 16

Ceccatto, A.: SS+2D+AMS-WeA-15, **21**; SS+2D+AMS-WeM-3, 16
 Cechal, J.: SS+2D+AMS-WeM-4, 16
 Chakravarty, A.: 2D+AP+EM+QS+SS+TF-TuM-6, 8
 Chan, M.: SS+2D+AMS-WeA-14, 21
 Chen, C.: 2D+AP+EM+QS+SS+TF-TuM-6, **8**
 Chen, D.: SS-ThM-1, **22**; SS-ThP-21, 29
 Chiang, N.: SS+AMS+AS+CA+LS-FrM-4, **32**
 Chien, T.: SS+2D+AMS-WeA-12, 20
 Christopher, P.: SS+AMS-MoM-3, 1; SS-ThP-2, 25
 Corkery, P.: SS+2D+AMS-WeA-1, 19
 Counsell, J.: 2D+LS+NS+SS-TuA-4, **12**
 Coye, S.: 2D+AP+EM+QS+SS+TF-TuM-7, 8
 Cramer, L.: SS+AMS-MoM-3, 1

— D —

Danahey, S.: SS-ThP-28, 30
 Daniels, A.: SS+2D+AMS-WeM-7, **16**
 de Siervo, A.: SS+2D+AMS-WeA-15, 21; SS+2D+AMS-WeM-3, **16**
 Debenedetti, W.: SS+AMS-MoA-8, 5
 Deng, X.: SS+CA+LS-TuM-3, **10**
 Dhas, J.: SS+2D+AMS-WeM-17, 17
 Diebold, U.: SS+2D+AMS-WeA-5, 19; SS+AMS-MoA-1, 4
 Dissanayake, N.: SS+2D+AMS-WeM-8, 17; SS-ThP-5, 25
 Dissanayake, R.: SS+AMS-MoM-7, 2; SS-ThP-31, **30**
 Dohnalek, Z.: SS+AMS-MoA-8, 5; SS-ThP-22, 29; SS-ThP-24, 29
 Dorst, A.: SS+AMS-MoM-7, 2; SS-ThP-31, 30
 Dowben, P.: SS+2D+AMS-WeA-6, 20
 Dunuwila, S.: SS-ThP-8, **26**
 Dürr, M.: SS+2D+AMS-WeM-15, **17**; SS-ThP-7, **26**

— E —

Eder, M.: SS+AMS-MoA-1, 4; SS+AMS-MoM-12, 2
 Eres, G.: 2D+AP+EM+QS+SS+TF-TuM-8, 8
 Esposito, D.: SS+CA+LS-TuA-10, 14
 Evans, P.: SS-ThP-24, 29

— F —

Farber, R.: SS+2D+AMS-WeM-8, **17**; SS-ThP-5, 25
 Faussett, S.: SS+CA+LS-TuM-14, 11
 Feng, X.: SS+CA+LS-TuA-4, 14; SS+CA+LS-TuM-13, 11; SS+CA+LS-TuM-4, 10; SS+CA+LS-TuM-5, 10; SS-ThP-14, 27
 Ferreira, E.: SS+2D+AMS-WeA-15, 21; SS+2D+AMS-WeM-3, 16
 Fonseca Vega, J.: 2D+LS+NS+SS-TuA-11, 12
 Franceschini, E.: SS+CA+LS-TuM-6, 10
 Franchini, C.: SS+AMS-MoA-1, 4
 Freiburger, E.: SS+2D+AMS-WeA-15, 21
 Freund, L.: SS-ThP-7, 26
 Fritz, T.: 2D+AP+EM+QS+SS+TF-TuM-5, 7
 Fu, Y.: 2D+AP+EM+QS+SS+TF-TuM-6, 8
 Fukazawa, A.: 2D+AP+EM+QS+SS+TF-TuM-3, 7
 Fukutani, K.: SS+AMS-MoM-4, 1
 Furche, F.: SS+CA+LS-TuM-14, 11

— G —

Gao, M.: SS+AMS-MoM-4, 1
 Geohagan, D.: 2D+AP+EM+QS+SS+TF-TuM-4, 7; 2D+AP+EM+QS+SS+TF-TuM-8, 8
 George, A.: 2D+AP+EM+QS+SS+TF-TuM-5, 7
 George, S.: SS-ThP-32, 30
 Gerace, B.: SS+AMS+AS+CA+LS-FrM-10, 33
 Gerrits, N.: SS+AMS-MoM-1, 1
 Ghorbani-Asl, M.: 2D+AP+EM+QS+SS+TF-TuM-5, 7
 Gillum, M.: SS-ThP-28, **30**

Gil-Rostra, J.: SS-ThP-11, 27
 Glaser, T.: SS+2D+AMS-WeM-15, 17; SS-ThP-7, 26
 Gonzalez, A.: SS-ThP-28, 30
 González-Elípe, A.: SS-ThP-11, 27
 Greene, E.: SS+AMS+AS+CA+LS-FrM-11, **33**
 Groot, I.: SS+2D+AMS-WeA-10, **20**; SS-ThP-10, 27
 Groothuis, C.: SS+CA+LS-TuA-11, 15
 Gruenewald, M.: 2D+AP+EM+QS+SS+TF-TuM-5, 7
 Guest, J.: SS-ThP-27, 30
 Guisinger, N.: SS+2D+AMS-WeA-14, **21**
 Gupta, A.: SS+AMS-MoM-5, 1; SS+CA+LS-TuA-12, 15; SS-ThP-19, **28**

— H —

Hachtel, J.: 2D+AP+EM+QS+SS+TF-TuM-4, 7
 Haines, A.: SS+CA+LS-TuM-14, 11
 Hajzuz, J.: 2D+AP+EM+QS+SS+TF-TuM-16, **9**
 Happel, E.: SS+AMS-MoM-3, **1**; SS-ThP-2, **25**
 Harris, S.: 2D+AP+EM+QS+SS+TF-TuM-8, 8
 Hasegawa, J.: SS+AMS-MoM-4, 1
 Hattori, K.: SS-ThP-15, 28
 Hayashida, K.: SS+CA+LS-TuM-8, **10**
 Hazeldine, E.: SS+AMS-MoM-13, **2**
 Hedevar, M.: SS+AMS-MoM-13, 2
 Heldebrant, D.: SS+2D+AMS-WeM-17, 17
 Hemminger, J.: SS+CA+LS-TuM-14, 11
 Henn, F.: SS+AMS+AS+CA+LS-FrM-10, 33
 Hetti Arachchige, H.: SS-ThP-5, 25
 Hibbitts, D.: SS+AMS-MoA-6, 5
 High, E.: SS-ThM-13, 23
 Hirsch, R.: SS-ThP-32, 30
 Hirushan, H.: SS+2D+AMS-WeM-8, 17
 Hossain, M.: SS-ThP-4, **25**
 Hruza, D.: SS+2D+AMS-WeM-4, 16
 Huang, Y.: 2D+AP+EM+QS+SS+TF-TuM-3, 7
 Hui, H.: 2D+AP+EM+QS+SS+TF-TuM-6, 8
 Hurst, K.: SS+CA+LS-TuA-10, 14
 Hütner, J.: SS+2D+AMS-WeA-5, **19**; SS+AMS-MoM-12, 2

— I —

Ilevlev, A.: 2D+AP+EM+QS+SS+TF-TuM-4, 7
 Irisawa, T.: 2D+AP+EM+QS+SS+TF-TuM-3, 7
 Isegawa, M.: SS+CA+LS-TuM-8, 10
 Ishigami, M.: 2D+LS+NS+SS-TuA-10, 12
 Islam, A.: SS+AMS-MoA-5, 4

— J —

Jaekel, S.: SS+2D+AMS-WeA-15, 21
 Jakub, Z.: SS+2D+AMS-WeM-4, **16**; SS+AMS-MoA-1, 4
 Jalil, A.: SS+AMS-MoM-3, 1
 Jamir, J.: SS+AMS-MoA-12, 6; SS+AMS-MoA-3, 4
 Janulaitis, N.: SS+AMS-MoM-15, **3**
 Jessup, D.: SS+2D+AMS-WeA-11, 20
 Jiang, N.: SS-ThP-17, 28; SS-ThP-6, 26
 Jimenez, J.: SS+CA+LS-TuM-6, 10
 Johnson, K.: 2D+AP+EM+QS+SS+TF-TuM-7, 8
 Jonker, B.: 2D+LS+NS+SS-TuA-3, 12
 Jozwiak, C.: 2D+LS+NS+SS-TuA-3, 12
 Junige, M.: SS-ThP-32, 30
 Junker, N.: SS+AMS+AS+CA+LS-FrM-5, 32

— K —

Kalkhoff, L.: SS+AMS+AS+CA+LS-FrM-5, 32
 Kandratsenka, A.: SS-ThP-30, **30**
 Kasala, P.: SS+AMS-MoA-13, 6
 Katoch, J.: 2D+LS+NS+SS-TuA-3, **12**
 Kauffman, D.: SS+CA+LS-TuM-3, 10
 Kaushik, N.: SS-ThP-18, 28
 Kay, B.: SS-ThP-22, 29
 Kayastha, R.: SS+AMS+AS+CA+LS-FrM-6, 32
 Kerr, A.: SS-ThP-28, 30
 Khatun, S.: 2D+AP+EM+QS+SS+TF-TuM-14, **9**

Author Index

- Killelea, D.: SS+AMS+AS+CA+LS-FrM-7, **33**;
SS+AMS-MoM-7, 2; SS-ThP-28, 30; SS-ThP-31, 30
- Kim, A.: 2D+LS+NS+SS-TuA-11, 12
- Kim, L.: SS+2D+AMS-WeA-12, **20**
- Kim, M.: SS+AMS-MoA-12, 6; SS+AMS-MoA-3, 4; SS+AMS-MoA-9, 5
- Kim, T.: SS-ThM-13, 23
- Kimmel, G.: SS+AMS-MoA-8, 5
- Klimek, J.: SS+CA+LS-TuA-11, 15
- Koch, R.: 2D+LS+NS+SS-TuA-3, 12
- Koert, U.: SS+2D+AMS-WeM-15, 17; SS-ThP-7, 26
- Kraetz, A.: SS+2D+AMS-WeA-1, 19
- Krashennikov, A.: 2D+AP+EM+QS+SS+TF-TuM-5, 7
- Kretschmer, S.: 2D+AP+EM+QS+SS+TF-TuM-5, 7
- Kruse, N.: SS+CA+LS-TuA-11, 15
- Kugler, D.: SS+2D+AMS-WeA-5, 19
- Kühnle, A.: SS+2D+AMS-WeA-5, 19
- L —
- Lang, J.: SS+2D+AMS-WeA-9, 20
- Länger, C.: SS-ThP-7, 26
- Lasnik, L.: SS+AMS+AS+CA+LS-FrM-5, 32
- Law, S.: 2D+AP+EM+QS+SS+TF-TuM-15, 9
- Le, D.: SS+AMS-MoA-2, 4; SS+AMS-MoM-14, 3; SS+CA+LS-TuM-4, 10; SS+CA+LS-TuM-5, 10
- Lee, C.: SS+AMS-MoA-6, 5
- Lewis, F.: SS+AMS-MoM-12, 2
- Li, F.: SS-ThM-1, 22; SS-ThP-21, 29
- Li, H.: 2D+AP+EM+QS+SS+TF-TuM-6, 8
- Li, X.: SS+CA+LS-TuA-12, 15
- Libuda, J.: SS+CA+LS-TuA-8, **14**
- Lilley, C.: SS+2D+AMS-WeA-14, 21
- Lin, X.: SS-ThP-18, **28**
- Liu, C.: SS+AMS-MoM-4, 1
- Liu, F.: SS+AMS-MoM-14, 3
- Liu, Y.: SS+2D+AMS-WeA-9, 20
- Lloreda Jurado, P.: SS-ThP-11, 27
- Longo, F.: SS-ThP-11, **27**
- Longo, R.: SS+AMS+AS+CA+LS-FrM-12, **33**
- Lough, S.: 2D+LS+NS+SS-TuA-10, **12**
- Lu, B.: SS+AMS-MoM-4, 1
- Lu, W.: SS+AMS+AS+CA+LS-FrM-6, 32; SS+CA+LS-TuA-5, 14
- Lundgren, E.: SS+CA+LS-TuA-1, **13**
- Lundwall, M.: SS+AMS+AS+CA+LS-FrM-10, **33**
- M —
- Machamer, K.: SS+AMS-MoM-5, 1
- Mack, S.: 2D+AP+EM+QS+SS+TF-TuM-16, 9
- Maehara, H.: 2D+AP+EM+QS+SS+TF-TuM-3, 7
- Mahapatra, S.: SS-ThP-27, **30**
- Mann, J.: SS-ThP-16, 28
- Mariscal, M.: SS+CA+LS-TuM-6, **10**
- McCreary, K.: 2D+LS+NS+SS-TuA-3, 12
- McNeary, W.: SS+CA+LS-TuA-10, **14**
- Meier, M.: SS+AMS-MoA-1, 4
- Meinecke, J.: SS-ThP-7, 26
- Meißner, O.: 2D+AP+EM+QS+SS+TF-TuM-5, 7
- Meng, Z.: SS+CA+LS-TuA-4, 14; SS+CA+LS-TuM-13, **11**
- Meyer, A.: SS+AMS+AS+CA+LS-FrM-5, 32
- Meyer, J.: SS+AMS-MoM-1, 1; SS-ThP-10, **27**
- Miura, H.: 2D+AP+EM+QS+SS+TF-TuM-3, 7
- Miwa, J.: 2D+LS+NS+SS-TuA-3, 12
- Moffitt, C.: 2D+LS+NS+SS-TuA-4, 12
- Mohrhusen, L.: SS+AMS-MoM-13, 2; SS+CA+LS-TuA-11, **15**
- Montemore, M.: SS+AMS-MoM-3, 1; SS-ThP-2, 25
- Mowbray, D.: SS+2D+AMS-WeA-15, 21
- Myers-Ward, R.: 2D+AP+EM+QS+SS+TF-TuM-16, 9
- N —
- Nakamura, J.: SS+CA+LS-TuA-13, 15; SS+CA+LS-TuM-8, 10
- Namari, N.: SS+CA+LS-TuA-13, 15
- Nawaz, A.: SS-ThP-1, **25**
- Neumann, C.: 2D+AP+EM+QS+SS+TF-TuM-5, 7
- Nguyen-Phan, T.: SS+CA+LS-TuM-3, 10
- Niu, Y.: SS+2D+AMS-WeA-11, 20; SS+AMS-MoA-14, 6
- Novotny, Z.: SS-ThP-22, 29; SS-ThP-24, 29
- Nykypanchuk, D.: SS+2D+AMS-WeA-1, 19
- O —
- O'Connor, C.: SS+AMS-MoA-8, 5; SS-ThM-13, 23
- Ogaki, T.: SS+2D+AMS-WeA-2, 19
- Ogura, S.: SS+AMS-MoM-4, 1
- Ohta, T.: 2D+LS+NS+SS-TuA-11, **12**
- Okada, N.: 2D+AP+EM+QS+SS+TF-TuM-3, 7
- Ologun, A.: SS-ThP-3, **25**
- ones, A.: 2D+LS+NS+SS-TuA-3, 12
- Onivefu, A.: SS-ThP-12, **27**
- Orson, K.: SS+2D+AMS-WeA-11, **20**
- Ortiz-Garcia, J.: SS-ThP-22, **29**
- Otto, F.: 2D+AP+EM+QS+SS+TF-TuM-5, 7
- P —
- Paddubrouskaya, H.: SS-ThP-32, 30
- Pan, X.: SS+CA+LS-TuA-10, 14
- Panagiotakopoulos, T.: SS+CA+LS-TuM-4, **10**; SS+CA+LS-TuM-5, 10
- Pandey, S.: SS+AMS+AS+CA+LS-FrM-3, 32
- Papp, C.: SS+2D+AMS-WeA-15, 21
- Park, N.: SS+AMS-MoA-9, 5
- Parkinson, G.: SS+AMS-MoA-1, 4; SS+AMS-MoM-12, 2
- Patel, R.: SS+2D+AMS-WeA-1, 19
- Pathan, M.: SS+AMS-MoM-5, 1
- Pathirage, V.: 2D+AP+EM+QS+SS+TF-TuM-14, 9
- Pavelec, J.: SS+AMS-MoA-1, 4; SS+AMS-MoM-12, 2
- Penland, L.: SS+2D+AMS-WeM-8, 17; SS-ThP-5, **25**
- Pennachio, D.: 2D+AP+EM+QS+SS+TF-TuM-16, 9
- Perez Gomez, E.: SS-ThP-20, **29**
- Perrine, K.: SS+AMS+AS+CA+LS-FrM-3, **32**
- Peters, J.: SS+2D+AMS-WeM-15, 17
- Picker, J.: 2D+AP+EM+QS+SS+TF-TuM-5, 7
- Plaisance, C.: SS+AMS-MoA-6, 5
- Planer, J.: SS+2D+AMS-WeM-4, 16
- Pookpanratana, S.: SS+2D+AMS-WeA-3, **19**
- Pope, C.: SS+AMS-MoA-12, 6; SS+AMS-MoA-3, 4
- Prabhu, M.: SS-ThP-10, 27
- Prerna, P.: SS+2D+AMS-WeA-1, 19
- Prochazka, P.: SS+2D+AMS-WeM-4, 16
- Puntscher, L.: SS+AMS-MoA-1, 4
- Puretzky, A.: 2D+AP+EM+QS+SS+TF-TuM-4, 7; 2D+AP+EM+QS+SS+TF-TuM-8, 8
- Q —
- Qerimi, D.: SS+AMS+AS+CA+LS-FrM-11, 33
- Qiao, M.: SS-ThM-1, 22; SS-ThP-21, **29**
- Qin, T.: SS+2D+AMS-WeM-1, 16
- R —
- Rahman, T.: SS+AMS-MoA-2, 4; SS+AMS-MoM-10, 2; SS+AMS-MoM-14, 3; SS+CA+LS-TuM-4, 10; SS+CA+LS-TuM-5, 10; SS-ThP-25, 30
- Rajak, S.: SS-ThP-6, **26**
- Ramasubramanian, S.: SS+AMS-MoA-3, 4; SS+AMS-MoA-6, 5
- Ranjana, R.: SS-ThP-13, **27**
- Rath, D.: SS+AMS-MoM-12, 2
- Rau, S.: SS-ThP-32, **30**
- Ravula, S.: SS+2D+AMS-WeM-17, 17
- Reddy, K.: SS+AMS-MoA-5, 4
- Reddy, R.: SS+AMS-MoA-12, 6
- Reece, C.: SS-ThM-13, **23**
- Reinke, P.: SS+2D+AMS-WeA-11, 20
- Ren, Z.: SS+CA+LS-TuA-4, **14**; SS+CA+LS-TuM-13, 11
- Reutt-Robey, J.: SS+AMS-MoA-14, 6
- Robinson, J.: 2D+LS+NS+SS-TuA-11, 12; 2D+LS+NS+SS-TuA-3, 12
- Rodriguez, A.: SS-ThP-10, 28
- Rodriguez, J.: SS+AMS-MoA-13, 6; SS+AMS-MoA-5, 4; SS-ThP-9, 26
- Roldan Cuenya, B.: SS+CA+LS-TuM-1, **9**
- Roorda, T.: SS+2D+AMS-WeA-10, 20
- Rosner, M.: 2D+LS+NS+SS-TuA-3, 12
- Rost, M.: SS-ThP-10, 27
- Rotenberg, E.: 2D+LS+NS+SS-TuA-3, 12
- Rotondaro, A.: SS-ThP-32, 30
- Rouleau, C.: 2D+AP+EM+QS+SS+TF-TuM-4, 7
- Ruzic, D.: SS+AMS+AS+CA+LS-FrM-11, 33
- S —
- Sabath, F.: SS+2D+AMS-WeA-5, 19
- Sadowski, J.: SS+2D+AMS-WeA-11, 20
- Sakaguchi, I.: SS+2D+AMS-WeA-2, 19
- Saucedo, C.: SS-ThP-16, **28**
- Schaal, M.: 2D+AP+EM+QS+SS+TF-TuM-5, 7
- Schaefer, T.: SS-ThP-31, 30
- Schäfer, T.: SS+AMS-MoM-7, **2**
- Scharf, D.: SS+2D+AMS-WeM-15, 17
- Schleberger, M.: SS+AMS+AS+CA+LS-FrM-5, 32
- Schleife, A.: SS+AMS+AS+CA+LS-FrM-5, 32
- Schmid, M.: SS+2D+AMS-WeA-5, 19; SS+AMS-MoA-1, 4
- Segrest, E.: SS+AMS-MoM-5, 1
- Seidel, R.: SS+CA+LS-TuM-14, 11
- Senevirathna, M.: 2D+AP+EM+QS+SS+TF-TuM-7, 8
- Serna-Sanchez, E.: SS-ThP-28, 30
- Shahsavari, A.: SS+2D+AMS-WeM-4, 16
- Shang, A.: SS+2D+AMS-WeA-13, 21
- Shang, Z.: SS+2D+AMS-WeA-13, 21
- Sharma, P.: SS+2D+AMS-WeA-12, 20
- Sharp, M.: SS-ThP-22, 29
- Sheng, X.: SS+2D+AMS-WeA-13, **21**
- Sherazi, S.: SS+AMS-MoM-14, **3**
- Shi, K.: SS+CA+LS-TuA-4, 14; SS+CA+LS-TuM-13, 11; SS+CA+LS-TuM-4, 10; SS+CA+LS-TuM-5, **10**; SS-ThP-14, **27**
- Shimizu, K.: SS+AMS-MoM-4, 1
- Shimizu, R.: SS+CA+LS-TuM-8, 10
- Shin, J.: SS+AMS-MoA-6, 5
- Siepmann, J.: SS+2D+AMS-WeA-1, 19
- Sikder, S.: SS-ThP-20, 29
- Singh, S.: 2D+LS+NS+SS-TuA-3, 12
- Siribaddana, C.: SS-ThP-17, **28**
- Sloboda, T.: SS+AMS+AS+CA+LS-FrM-10, **33**
- Smith, C.: SS+CA+LS-TuA-12, 15
- Sokolowski-Tinten, K.: SS+AMS+AS+CA+LS-FrM-5, 32
- Soldano, G.: SS+CA+LS-TuM-6, 10
- Sombut, P.: SS+AMS-MoA-1, 4
- Soomary, L.: 2D+LS+NS+SS-TuA-4, 12
- Spataru, C.: 2D+LS+NS+SS-TuA-11, 12
- Sridhar, S.: SS+AMS+AS+CA+LS-FrM-12, 33
- Stacchiola, D.: SS+AMS-MoA-7, **5**; SS-ThP-26, 30
- Steinrück, H.: SS+2D+AMS-WeA-15, 21
- Stinson, W.: SS+CA+LS-TuA-10, 14
- Strange, L.: SS+2D+AMS-WeM-17, 17
- Stratton, S.: SS+AMS-MoM-3, 1
- Subedi, A.: SS+2D+AMS-WeA-6, **20**

Author Index

- Sudarshan, C.: SS+AMS-MoA-6, 5
Sugar, J.: 2D+LS+NS+SS-TuA-11, 12
Surman, D.: 2D+LS+NS+SS-TuA-4, 12
Suzuki, H.: SS+CA+LS-TuA-13, 15
Suzuki, T.: SS+2D+AMS-WeA-2, **19**
Sykes, C.: SS+2D+AMS-WeM-7, 16; SS-ThM-15, **23**
Sykes, E.: SS+AMS-MoM-3, 1; SS-ThP-2, 25
— **T** —
T. Lee, D.: SS+2D+AMS-WeA-1, 19
Tait, S.: SS-ThP-23, 29
Takakusagi, S.: SS+AMS-MoM-4, **1**
Takyasu, K.: SS+CA+LS-TuA-13, **15**;
SS+CA+LS-TuM-8, 10
Tanabe, S.: 2D+AP+EM+QS+SS+TF-TuM-3, **7**
Tenney, S.: SS+2D+AMS-WeA-1, 19
Teplyakov, A.: SS-ThP-12, 27; SS-ThP-8, 26
Thuermer, K.: 2D+LS+NS+SS-TuA-11, 12
Tian, Y.: SS+AMS-MoA-5, 4
Tong, X.: SS+2D+AMS-WeA-1, 19
Trenary, M.: SS+AMS+AS+CA+LS-FrM-1, **32**;
SS-ThM-3, **22**; SS-ThP-3, 25; SS-ThP-4, 25
Tsapatsis, M.: SS+2D+AMS-WeA-1, 19
Tumbelaka, R.: SS-ThP-15, **28**
Turchanin, A.: 2D+AP+EM+QS+SS+TF-TuM-1,
7; 2D+AP+EM+QS+SS+TF-TuM-5, 7
Turkowski, V.: 2D+AP+EM+QS+SS+TF-TuM-4,
7
Turner, G.: SS+AMS-MoM-5, 1
— **U** —
Ulstrup, S.: 2D+LS+NS+SS-TuA-3, 12
Utz, A.: SS-ThM-5, **22**
— **V** —
Vaida, M.: SS+AMS-MoM-5, 1; SS+CA+LS-
TuA-12, **15**; SS-ThP-19, 28
van den Bosch, F.: SS+AMS-MoM-1, 1
Vang Lauritsen, J.: SS+AMS-MoM-13, 2
Veld, Y.: 2D+LS+NS+SS-TuA-3, 12
Ventzek, P.: SS+AMS+AS+CA+LS-FrM-12, 33
Vlassioux, I.: 2D+AP+EM+QS+SS+TF-TuM-8, 8
Vovk, E.: SS+2D+AMS-WeA-9, 20
— **W** —
Waleska-Wellenhofer, N.: SS+2D+AMS-WeA-
15, 21
Wang, C.: SS+AMS-MoA-1, 4
Wang, D.: SS+2D+AMS-WeA-9, 20
Wang, H.: SS+2D+AMS-WeA-13, 21
Wang, T.: SS+CA+LS-TuA-12, 15
Wang, X.: SS+AMS-MoA-8, **5**
Waqar, M.: SS+CA+LS-TuA-10, 14
Warashina, H.: 2D+AP+EM+QS+SS+TF-TuM-
3, 7
Weaver, J.: SS+AMS-MoA-12, 6; SS+AMS-
MoA-3, **4**; SS+AMS-MoA-6, 5; SS+AMS-
MoA-9, 5; SS-ThA-1, **24**
Williams, M.: 2D+AP+EM+QS+SS+TF-TuM-7,
8
Winter, B.: SS+CA+LS-TuM-14, 11
Wisman, D.: SS-ThP-23, 29
Wong, K.: 2D+AP+EM+QS+SS+TF-TuM-6, 8
Woods, R.: SS+CA+LS-TuM-14, 11
Wright, E.: 2D+AP+EM+QS+SS+TF-TuM-7, **8**
Wucher, A.: SS+AMS+AS+CA+LS-FrM-5, 32
— **X** —
Xiao, K.: 2D+AP+EM+QS+SS+TF-TuM-4, **7**;
2D+AP+EM+QS+SS+TF-TuM-8, 8
Xie, S.: SS+AMS-MoM-14, 3
Xu, X.: SS+2D+AMS-WeA-6, 20
— **Y** —
Yadav, A.: 2D+AP+EM+QS+SS+TF-TuM-6, 8
Yan, M.: SS+CA+LS-TuA-13, 15
Yang, D.: SS+2D+AMS-WeA-6, 20
Yang, Y.: SS+2D+AMS-WeA-9, **20**
Yao, F.: 2D+AP+EM+QS+SS+TF-TuM-6, 8
Yao, J.: SS+2D+AMS-WeM-17, **17**
Yao, Y.: SS+AMS+AS+CA+LS-FrM-5, 32
Ye, K.: SS+AMS-MoM-14, 3
Yimam, D.: 2D+AP+EM+QS+SS+TF-TuM-8, **8**
York, S.: SS-ThP-18, 28
Yost, A.: SS+AMS+AS+CA+LS-FrM-10, 33
Yu, M.: 2D+AP+EM+QS+SS+TF-TuM-15, **9**
Yu, Y.: 2D+AP+EM+QS+SS+TF-TuM-4, 7
Yubero, F.: SS-ThP-11, 27
Yun, J.: SS+AMS-MoA-12, 6; SS+AMS-MoA-3,
4; SS+AMS-MoA-9, **5**
— **Z** —
Zaccarine, S.: SS-ThP-16, 28
Zaera, F.: SS-ThP-13, 27
Zahra, K.: 2D+LS+NS+SS-TuA-4, 12
Zakharov, A.: SS+2D+AMS-WeA-11, 20
Zang, W.: SS+CA+LS-TuA-10, 14
Zechmann, B.: SS+AMS+AS+CA+LS-FrM-6, 32
Zeng, H.: 2D+AP+EM+QS+SS+TF-TuM-6, 8
Zhang, K.: SS+CA+LS-TuM-14, 11
Zhang, X.: SS+2D+AMS-WeA-13, 21;
SS+AMS+AS+CA+LS-FrM-10, 33
Zhang, Z.: SS+AMS+AS+CA+LS-FrM-6, **32**;
SS+CA+LS-TuA-5, 14
Zhao, K.: SS+AMS-MoM-15, 3
Zhu, H.: SS+CA+LS-TuA-5, 14
Zhu, J.: SS+2D+AMS-WeM-1, **16**
Zhu, T.: 2D+LS+NS+SS-TuA-8, **12**
Zhu, Z.: SS+2D+AMS-WeM-17, 17